INFORMATION TO USERS

This manuscript has been reproduced from the microfilm master. UMI films the text directly from the original or copy submitted. Thus, some thesis and dissertation copies are in typewriter face, while others may be from any type of computer printer.

The quality of this reproduction is dependent upon the quality of the copy submitted. Broken or indistinct print, colored or poor quality illustrations and photographs, print bleedthrough, substandard margins, and improper alignment can adversely affect reproduction.

In the unlikely event that the author did not send UMI a complete manuscript and there are missing pages, these will be noted. Also, if unauthorized copyright material had to be removed, a note will indicate the deletion.

Oversize materials (e.g., maps, drawings, charts) are reproduced by sectioning the original, beginning at the upper left-hand corner and continuing from left to right in equal sections with small overlaps.

ProQuest Information and Learning
300 North Zeeb Road, Ann Arbor, MI 48106-1346 USA
800-521-0600

Université d'Ottawa · University of Ottawa

Design of Sialyl Lewis^x Glycomimetics: A Novel Approach Towards the Synthesis of Sugar-Coated Anti-Inflammatory Drugs

Cindy Jane Smith

Thesis submitted to the School of Graduate Studies and Research in partial fulfillment of the degree of Master of Science in Chemistry

Ottawa-Carleton Chemistry Institute

Department of Chemistry

University of Ottawa

Ottawa, Ontario CANADA

Abstract

The tetrasaccharide sialyl Lewis^x (SLe^x) is the smallest recognizable ligand for selectins. The binding of SLe^x to the selectins triggers the inflammatory cascade and recruits leukocytes to the injured cells. Chronic and acute inflammatory diseases result from the over-recruitment of leukocytes leading to damage of normal cells. Carbohydrate-based mimetics, maintaining functionality while improving stability, binding affinity and structural simplicity, are ideal candidates for anti-inflammatory drugs.

Sialyl Lewis^x glycomimetics were synthesized using two different convergent approaches. Each synthesis used an enzyme-resistant α-carbon-linked fucosyl moiety (C-glycoside) to replace the unstable anomeric oxygen linkage of the natural ligand.

One synthetic route coupled a rigid proline ring to the fucosyl carboxylic acid derivative made from L-fucose to form one branch of the mimetic. The second branch was synthesized by coupling modified amines to form functionalized peptide chains of various lengths. The chiral centre of the proline ring was exploited to devise two analogue series (L and D) for convergence with diversified peptide chains.

NMR experimental data imply that a synthesized novel glycomimetic of the D-proline series has a similar solution conformation to that of the bioactive conformation of SLe^x. Preliminary molecular modelling studies confirm that the

peptide chain length of the D-proline β-alaninyl derivative is comparable to the backbone chain length of the natural ligand.

The second convergent approach used novel olefin metathesis chemistry in the preparation to orchestrate a stereoselective *cis*-alkene bond formation extending from the fucosyl branch of the synthetic pathway. A challenging alkenic seven-membered ring connected to the fucosyl residue was the precursor required for the stereoselective conjugate reaction. The ruthenium Grubbs' catalysts bis (tricyclohexylphosphine)benzylidine ruthenium (IV) dichloride and tricyclohexylphosphine[1,3-bis(2,4,6-trimethylphenyl)-4,5-dihydroimidazol-2-ylidene][benzylidine] ruthenium (IV) dichloride were examined in this study. The latter was found to be more active than the former and able to catalyze electron deficient, sterically hindered alkenes. It was also the only catalyst capable of forming the difficult intramolecular ring closing metathesis to provide the desired *cis*-alkene derivative precursor.

Acknowledgements

By the grace of God and the combined efforts of my supervisor, professors, lab mates, technical support, friends and family I am finally finished!!!

I would first like to thank my supervisor, Dr. René Roy for giving me the opportunity to work with him and whose ideas prompted this interesting and challenging research project. His guidance and patience throughout the duration of my graduate studies were truly appreciated.

I would also like to thank Dr. Tony Durst whose kindness, support, encouragement and long friendly chats helped me through the rough times (and there were many). He gave me the incentive and structure I needed to finally tackle the difficult parts of this project.

My lab mates, past and present, were extremely supportive over the course of my project and especially in the last few months. Romyr Dominque, Brad Schmor, Mary King, Bingcan Liu, and Heba Abourahma were always willing to help me if I had any experimental difficulties. Romyr was always encouraging and motivating, Brad helped me with difficult synthetic steps and entertained me with many stories and Mary was a genius at editing the final copy of my thesis. Mary's efforts to help me finish have astounded me and are greatly appreciated. I would also like to thank Dr. Sanjoy Das who was an inspiring mentor and renewed my interest in chemistry.

I am also very grateful to the fast and efficient technical support staff of the chemistry department. I would like to thank Dr. Glen Facey and Raj Capoor who

helped me at the beginning of my project as well as Dr. Clem Kazakoff who was always willing to answer my many questions about mass spectrometry analysis. Especially helpful was Kim Yach with her dedication to obtaining high quality spectral data in a timely manner. She played a pivotal role in the outcome of my thesis.

I would like to thank my friends for their support and assistance through this project, especially the one from Scotland who did what he could to cheer me up and help me out over the Christmas holidays.

Finally, I would like to thank my parents, Jean and Rusty Smith for their financial and emotional support. I would also like to thank my sisters Jenny and Robin and especially Julie and Sarah who wanted an honourable mention for being my lab assistants for one whole day. My family's continued support was essential for the completion of this thesis project.

I am finally finished and ready to take on the next challenge – joining the real world!!

Table of Contents

List of Figures

List of Schemes

List of Tables

List of Abbreviations

Ac	acetate
Ala	alanine
Ac_2O	acetic anhydride
AcOH	acetic acid
b	broad
Boc	tert-butoxycarbonyl
BOP	benzotriazole-1-yl-oxy-tris-(dimethylamino)-phosphoniumhexafluorophosphate
bm	broad multiplet
bs	broad singlet
tBu	tert-butyl
cat	catalytic
CI	chemical ionization
COSY	shift correlation spectroscopy
d	doublet
DCC	dicyclohexylcarbodiimide
dd	doublet of doublet
ddd	doublet of doublet of doublet
DEPT	distortionless enhanced polarization transfer
DIPEA	diisopropylethylamine
DMF	N,N-dimethylformamide
DMS	dimethylsulfide

DMSO	dimethylsulfoxide
EDC	1-(3-dimethlyaminopropyl)-3-ethylcarbodiimide hydrochloride
eq	equivalent(s)
ES	electrospray
Et_3N	triethylamime
EtOAc	ethyl acetate
EtOH	ethanol
FAB	fast atom bombardment
Fmoc	9-fluorenylmethoxycarbonyl
Grubbs' **2**	bis (tricyclohexylphosphine)benzylidine ruthenium (IV) dichloride
Grubbs' **3**	tricyclohexylphosphine[1,3-bis(2,4,6-trimethylphenyl)-4,5-dihydroimidazol-2-ylidene][benzylidine] ruthenium (IV) dichloride
hr	hour(s)
HATU	O-(7-azabenzotriazol-1-yl)-N,N,N',N'-tetramethyluroniumhexafluorophosphate
HMQC	heteronuclear multiple quantum coherence
HOBt	1-hydroxybenzotriazole
Hz	hertz
HRMS	high resolution mass spectra
IR	infrared
Lit.	literature
m	multiplet
M	molar

M+	parent molecular ion
MeOH	methanol
Me	methyl
MHz	megahertz
min	minute(s)
mmol	millimole(s)
mol	mole(s)
mp	melting point
MS	mass spectrometry
MW	molecular weight
m/z	mass to charge ratio
NaOMe	sodium methoxide
NMM	4-methylmorpholine
NMR	nuclear magnetic resonance
ppm	parts per million
PyBOP	benzotriazole-1-yl-oxy-tris-pyrrolidino-phosphonium hexafluorophosphate
Rf	retention factor
rt	room temperature
rxn	reaction
s	singlet
TBTU	2-(1H-benzotriazole-1-yl)-1,1,3,3-tetramethyluronium tetrafluoroborate
TFA	trifluoroacetic acid

THF	tetrahydrofuran
TLC	thin layer chromatography
TMSOMeTf	trimethylsilylmethyl trifluoromethanesulfonate

Chapter 1. Introduction

1.1. Biological Significance of Carbohydrates

Carbohydrates are an important chemical and biological group of compounds. They constitute the majority of naturally occurring products found in plants and animals, serving as energy sources for cells and structural building blocks for living organisms.[1]

Amongst the four major classes of biological macromolecules: nucleic acids, proteins, lipids and carbohydrates; carbohydrates are the most diverse Nucleic acids and proteins are mainly linear molecules that are linked through 3'-5' phosphodiester and amide bonds respectively. Whereas, carbohydrates can be linked at several different sites and through varying linkages that can lead to highly branched molecules. For example, three different amino acids can combine to form 6 separate tripeptides, while the same number of monosaccharides can produce 1 056 trimers.[2] Although proteins and nucleic acids are responsible for encoding important genetic information, the complex and diverse structures of carbohydrates have the greatest potential for carrying the most biological information per unit weight.[3]

The immense capacity of carbohydrates to mediate biological information makes them fundamental for a myriad of biological functions. These biological functions begin at the surface of the cell. The outer membrane of a cell: the glycocalyx is densely covered with carbohydrates bound to protein (glycoproteins), lipids (glycolipids) and/or polysaccharide proteoglycans.[4] These

glycomimetics are responsible for cell surface interactions such as fertilization, hormonal activities, cell growth, proliferation and differentiation, embryogenesis, neuron development, cellular trafficking, viral and bacterial infection, cancer metastasis, inflammation and cell-cell recognition[5] (Figure 1.1.1.).[6]

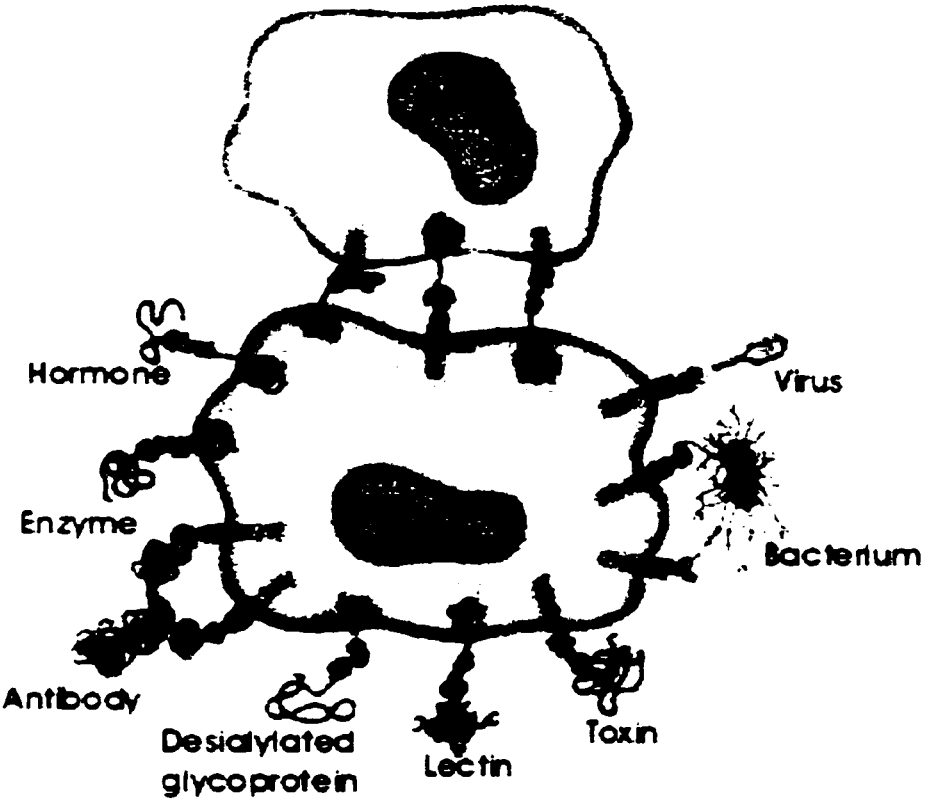

Figure 1.1.1. Cell surface carbohydrate interactions.[6]

Cell-cell recognition is mediated by complimentary receptor proteins on cell surfaces called lectins. The high specificity of their interaction can be exploited to design alternative approaches in the treatment of infectious diseases.

1.2. Carbohydrates in Drug Design

The growth of infectious diseases, combined with the alarming increase of antibiotic resistance are constant reminders of the desperate urgency for novel therapeutic interventions.

Carbohydrates are ideal arsenal possibilities for present and future drug design. These are molecules that occur naturally in the body (e.g. fluids, cell surfaces) and may be considered gentle and mild in comparison to the harsh conditions of current chemotherapy treatment. The structures of carbohydrate ligands are constant and not bactericidal and thus not likely to encourage the mutation and spread of anti-bacterial resistant strains.[7]

As mentioned, carbohydrates are involved in cell differentiation. Tumour cells exhibit incomplete and unusual glycosylation patterns which distinguish them from healthy cells. These unique carbohydrates aid in the survival and spread of the cancer cells by metastasis.[8] The metastatic cells interact with lectins on the lining of blood vessels granting them ability to circulate throughout the body. The glycosylation differences in tumour cells are useful markers that can be exploited in designing immunotherapies such as vaccines.

A vaccine can be synthesized by attaching the appropriate surface carbohydrates to a protein carrier. The body would elicit an immune response to the antigen and build up antibodies. These antibodies would then be capable of selectively destroying cancer cells that exhibit the distinct glycosylation pattern or inhibit metathesis.

Current research is presently investigating the prospect of anti-cancer vaccines. Encouraging results have been reported by Danishefsky *et al.*[9] in mouse studies using the globo-H antigen, which is a carbohydrate located on the surface of pancreatic, prostatic, breast and colon tumour cells. The mice treated with the protein linked antigen developed immense amounts of antibodies that in turn recognized tumour cells. The clinical trial of this carbohydrate-based vaccine also gave favourable results in a small patient group study. In 1987, the first carbohydrate vaccine was approved for use in the preventative treatment of invasive diseases associated with *Haemophilus influenza* type b in children.[10] The vast significance and attractive qualities of possible glycoconjugate-based vaccines have inspired many more research groups to undertake this challenge.[11]

Another employer of carbohydrates as recognition agents are pathogenic bacteria. The adhesion of bacterial lectins to host cell surface carbohydrates is a prerequisite for infection. Infection can occur when the body's natural cleansing mechanisms fail to dislodge adhered pathogens. One approach to disease prevention would be to selectively block the host-guest interaction by designing drugs that mimic the cell-surface carbohydrates. These drugs would act as molecular decoys and competitively bind with the natural carbohydrate cell surface ligand for the bacteria receptors.[3]

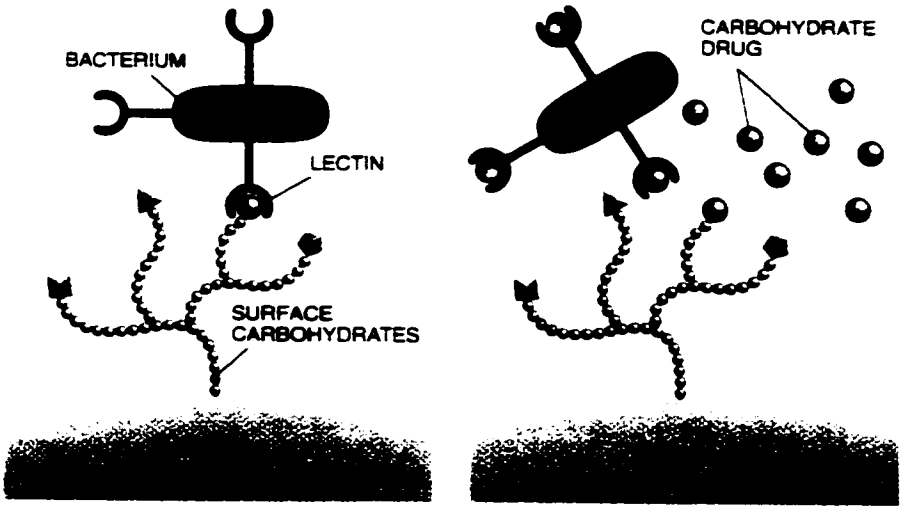

Figure 1.1.2. Carbohydrate drugs in anti-adhesion treatment of bacterial pathogens.[3]

The presence of many inhibitory oligosaccharides in human milk implies that nature uses this mechanism in protecting breast-fed babies from infections.[12]

Several glycoconjugate-based drugs are currently on the pharmaceutical market. Some examples are Streptozocin (treatment of Hodgkin's disease), Topiramate (prototype of anti-epileptic drug)[13] and AZT and 3TC (AIDS treatment),[14] while many others are beginning clinical trials.[15] Possible future applications of carbohydrates as drugs that are under present investigation include their potential as drug delivery systems,[16] contraceptives,[17] and novel inhibitors.[18]

The combination of cell-cell recognition and the application of anti-adhesive (infective) models will undoubtedly be potent weapons in the arsenal of drugs for the therapy of infectious diseases. Thus, therapeutic agents based on

carbohydrates and their biological pathways are extremely important and meaningful pharmaceutical targets. Lectins are important biological molecules that recognize carbohydrates and thus this relationship can be exploited in the attainment of anti-adhesive drugs.

1.3. Lectins

A general definition of a lectin is a protein of non-immune origin which specifically binds or crosslinks with carbohydrates. Lectins bind with mono- and oligosaccharides rapidly, selectively and reversibly.[19] There are several classes of lectins based on their saccharide specificity. The main class of lectins is the C-type lectin family that requires Ca^{+2} for binding and is found on the plasma membrane. All members of this family have a highly conserved carbohydrate recognition domain (CRD) which regulates its carbohydrate-binding activity. C-type lectins are of animal origin and have at least two carbohydrate binding sites. There are two categories of C-type lectins: soluble and transmembrane. Transmembrane lectins are involved in recognition between cells, cell-cell adhesion and molecular uptake. Selectins are a member of transmembrane C-type lectins.[20]

1.3.1. Selectins

Selectins are cell-cell recognition molecules that are involved in initial leukocyte and vascular endothelial cell adhesive interactions at the site of tissue injury.[21] There are three different selectins, P-, L- and E-selectin, each named

after the cell type on which they were initially found (i.e. platelets, leukocytes endothelium). They consist of an extracellularly exposed calcium-dependent CRD at the amino terminus (L) connected through an epidermal growth factor (EGF) domain (E) to a varying number (2-9) of repeated compliment regulatory (CR) protein units (C) in tandem. These protein-like units are attached to a hydrophobic transmembrane cystolic tail that anchors the selectin in the cell membrane.[22] A simplistic view of each selectin is represented in Figure 1.1.3.

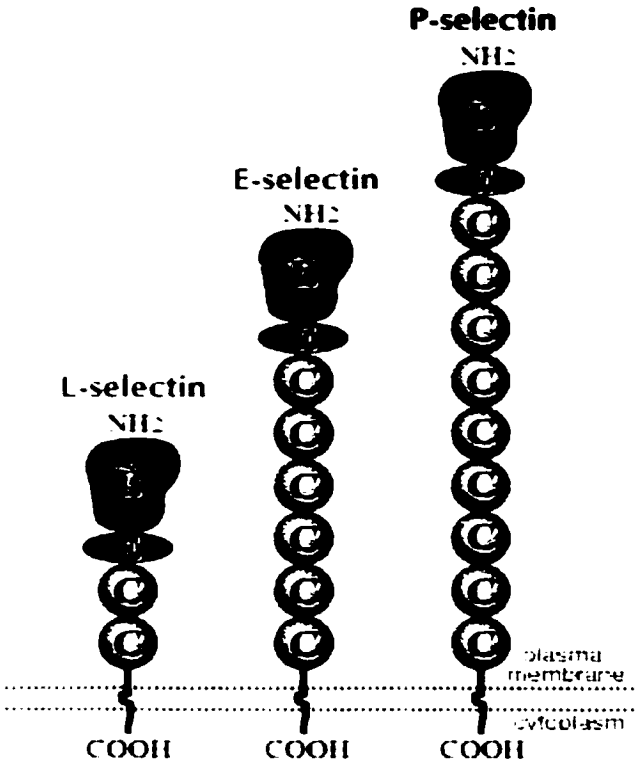

Figure 1.1.3. L-, E- and P-selectins. (adapted from www.glycoforum.gr.jp.com, 1998)

All three selectins recognize sialylated, sulfated and fucosylated glycoproteins of the leukocyte membrane. The smallest distinguishable epitopes of these are sialyl Lewis^x (SLe^x), sialyl Lewis^a (its isomer) and sulfo-Lewis^x (Figure 1.1.4.).[23]

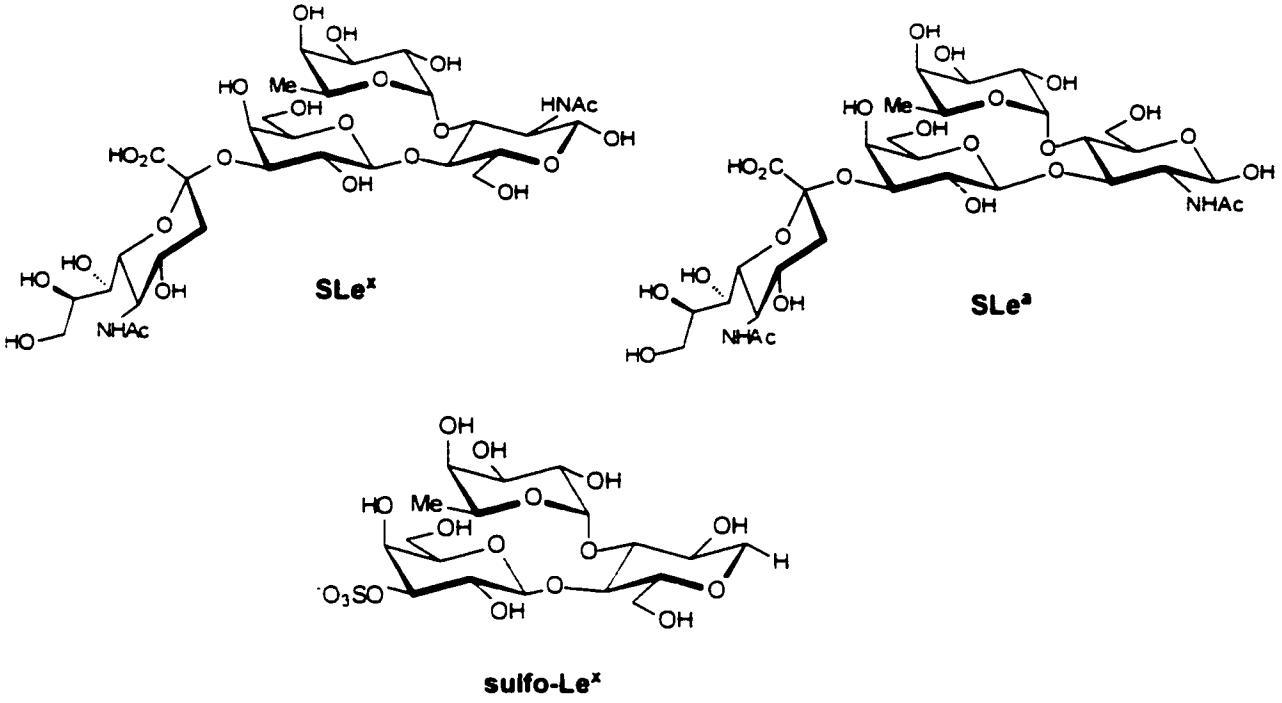

Figure 1.1.4. Smallest recognizable epitopes for selectins.[23]

1.3.2. P-Selectin

P-selectin is the largest of the known selectins containing 9 CR units and extending approximately 40 nm from the endothelial surface (Figure 1.1.3.). P-selectins were initially found in alpha granules of activated platelets and are also stored in endothelial cells. The presence of P-selectin on the endothelial surface is detected within minutes after stimulation by inflammatory molecules (e.g.

thrombin, histidine, phorbol esters). Initial leukocyte rolling on the vascular is mediated by this selectin. The expression of the selectin peaks after 10 minutes. Additional synthesis of P-selectin is stimulated by cytokines two hours after initial leukocyte recruitment. The primary natural ligand for P-selectin is P-selectin glycoprotein ligand 1 (PSGL-1). It is a mucin-like homodimer rich in O-linked oligosaccharides found on all leukocytes.[24] The other possible ligand is CD24. The sulfated Lewis structures do not bind to P-selectin.[25] However, sulfation of at least one of the three clustered tyrosines and an adjacent O-glycan expressing SLe^x of PSGL-1 is required for high avidity binding to P-selectin.[26] These recent reports suggest a possible two-site model for the binding of P-selectin to PSGL-1. One site interacts with anionic tyrosine and the other site recognizes SLe^x on the adjacent oligosaccharide.[27]

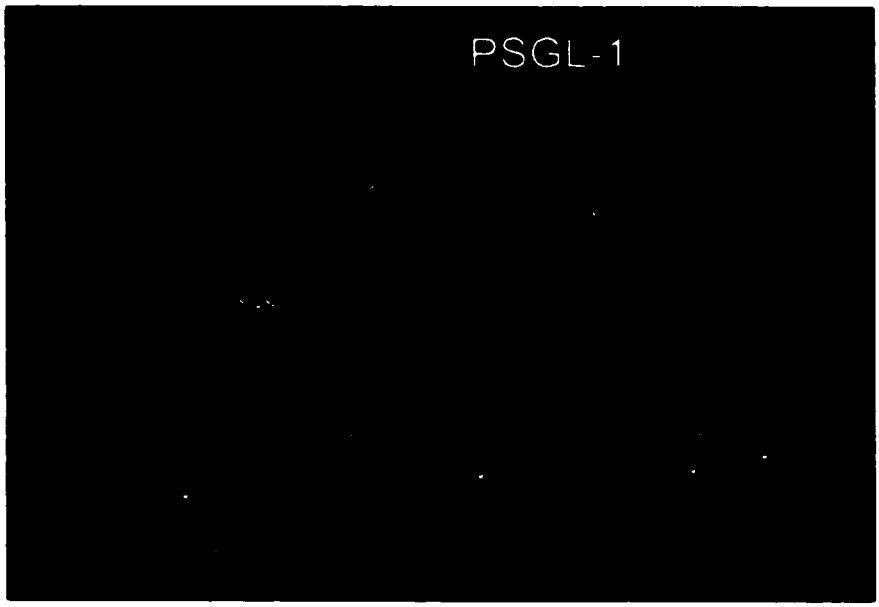

Figure 1.1.5. Generalized schematic of P-selectin glycoprotein ligand 1 (PSGL-1) (adapted from www.med.virginia.edu).

1.3.3. L-Selectin

L-selectin is the smallest of the three selectins having only 2 CR and is found on circulating lymphocytes (Figure 1.1.3.). L-selectin participates in the emigration of leukocytes into peripheral lymph nodes. This selectin is key in the capture of leukocytes during the early phases of recruitment and rolling. Once P-selectin diminishes (initially), L-selectin becomes the primary mediator of leukocyte rolling.

There are four carbohydrate presenting molecules (ligands) recognized by L-selectin: GlyCAM-1, CD34, MAdCAM-1 and PSGL-1. L-selectin recognizes all three forms of the sialyl Lewis structure present on these glycoproteins. L- and P-selectins are necessary to capture leukocytes as without them, rolling and eventually extravasion cannot occur.[28]

1.3.4. E-Selectin

Pro-inflammatory cytokines induce the expression of E-selectins on inflamed vascular endothelial cells. E-selectins are the last to appear on the endothethial surface (approximately 2 hours after the other selectins). Unlike P-selectin which is stored in the endothelial cells, E-selectin must first be synthesized. There is an apparent redundancy between E- and P-selectins in mediating leukocyte rolling. Although, it is thought that E-selectin and subsequently integrins play a major role in the transition of rolling to firm adhesion. Firm adhesion is characterized by stronger interactions between the endothelial cell and the leukocyte which leads to extravasion. All three forms of

SLe^x were recognized by E-selectin. These sialylated saccharides were identified on the glycoprotein receptor ESL-1.[29] It is also thought that PSGL-1 is another possible ligand of E-selectin.[30]

The crystal structure of E-selectin has been recently examined and is seen in Figure 1.1.6.

Figure 1.1.6. X-ray structure of E-selectin (adapted from www.med.virginai.edu).

The inter-relationships between selectins and their ligands are key to understanding the dynamics behind certain immunological responses. A summary of these interactions is seen below (Figure 1.1.7.).

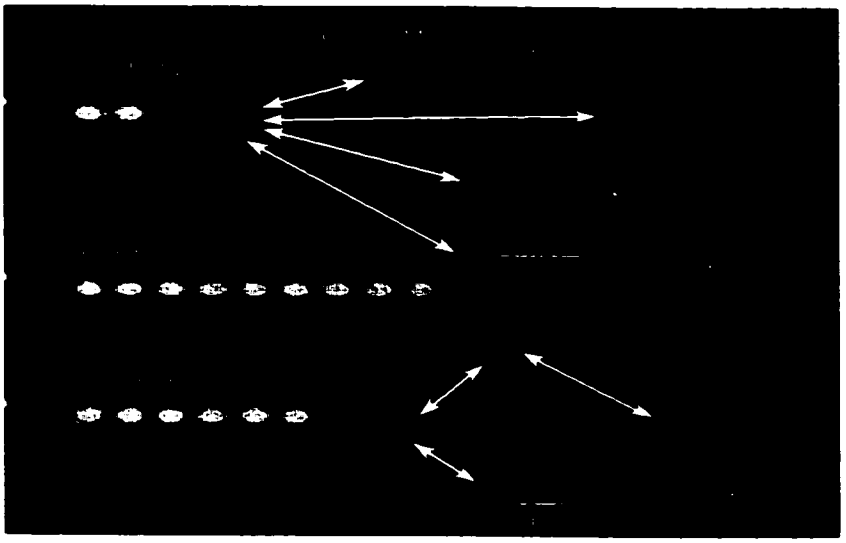

Figure 1.1.7. Selectins and their corresponding ligands (adapted from www.med.virginia.edu).

There are still many unresolved questions regarding the true ligands for selectins. E-, P- and L- selectins all recognize SLe^x; however, their binding affinities are rather weak (K_D in mmol range). This discovery has inspired great efforts in the search for analogues with higher selectin binding affinity as potential new anti-inflammatory agents.

1.4. Sialyl Lewis^x

Sialyl Lewis^x was originally identified as a human tumour-associated antigen.[31] As previously mentioned, there is a dramatic change in the glycocalyx of malignant cancer cells. Patients expressing this abnormality have significantly reduced survival times as compared to other types of tumours.

Sialyl Lewis^x is a tetrasaccharide comprised of a fucose, galactose, N-acetylglucosamine and sialic acid residue (NeuAcα-(2,3)-Galβ(1,4)-[Fucα(1,3)]-

GlcNAcβ-(1-OR)) (Figure 1.1.4.). Some sialyl Lewis^x structures are classified as gangliosides since they are part of complex glycolipids containing at least one sialic acid residue. SLe^x is the smallest recognizable ligand for selectins and plays an important role in the recruitment of leukocytes to the site of injury.

1.4.1. The Inflammation Cascade

In the case of tissue damage or bacterial infection, white blood cells are recruited by means of cell-cell recognition, followed by intercellular adhesion to the site of injury. This is a vital function of our immune system that is responsible for repair and protection of affected cells. This process consists of three main steps: dilation of capillaries, structural microvascular changes and leukocyte extravasion to the site of injury.

The inflammatory cascade (Figure 1.1.8.) is initiated by damaged tissues releasing cytokines that stimulates the expression of P- and E-selectins on the surface of the endothelium. P-selectin is the first to be expressed and recognizes its corresponding ligand PSGL-1 containing SLe^x on the surface of leukocytes. At the same time, L-selectin on the surface of leukocytes recognizes SLe^x in one of its many ligands (GlyCAM-1, CD34, PSGL-1, MAdCAM-1) on the endothelial lining. The combined efforts of these selectins (mostly mediated by P-selectin) capture or tether the leukocyte providing the first contact with the activated endothelium. Rolling by the leukocytes along the vascular endothelium is also primarily mediated by P-selectin. During this process, the endothelium expresses E-selectin that recognizes SLe^x on its corresponding ESL-1 leukocyte

ligand. Concurrently, immunoglobin superfamily proteins such as ICAM-1 on the endothelial surface interact with integrins on the leukocyte. These stronger interactions lead to slow rolling and firm adhesion. The presence of chemoattractants and proteolytic cleavage of L-selectin leads to the transmigration (extravasion) of the leukocytes through to the site of injury.[32] The details of the last step are not fully understood, although it is postulated that the mechanism of signal transduction may be mediated by an integrin pathway.[33]

a)

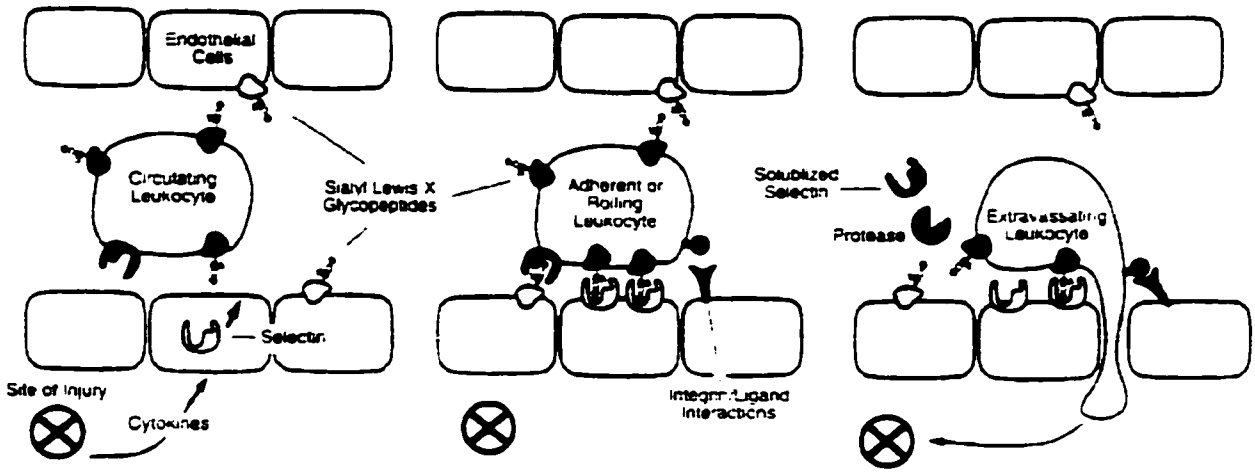

b)

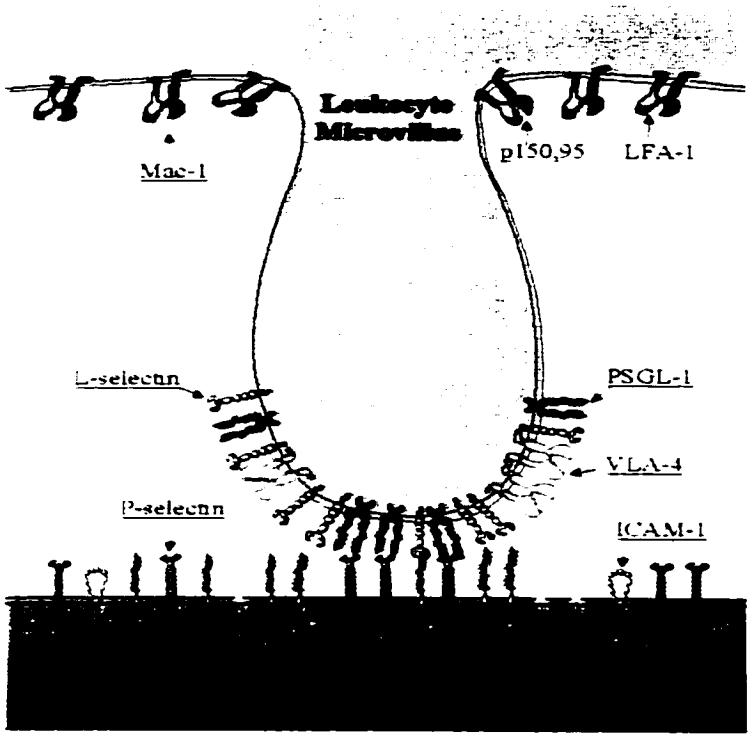

Figure 1.1.8. (a) Inflammation Cascade[32] (b) Magnified interpretation of surface interactions between leukocyte and activated endothelium (adapted from www.med.virginia.edu).

1.4.2. The Problem

The defense mechanism of the inflammation cascade is indispensable in damaged or injured cells. However, if too many leukocytes are recruited to an injury, healthy cells can be damaged resulting in redness, heat, swelling and pain. These are symptoms of chronic and/or acute inflammatory diseases such as rheumatoid arthritis, myocardial shock (reperfusion injury), psoriasis, stroke, thrombosis, encephalitis, dermatitis, asthma and even metastasis.[34] Inhibition of any of the steps of the inflammation cascade will dramatically reduce the over

recruitment of leukocytes resulting in a potentially broad spectral treatment of both acute and chronic inflammatory diseases.

1.4.3. Solution and Bound Conformations of SLe^x

Several studies using NMR techniques, computational calculations and ultimately X-ray crystallography have been performed to further analyze the important selectin- SLe^x interactions of the inflammatory cascade.

The solution conformation of SLe^x was determined by Wong and colleagues using 2D NMR (nOe) experiments and MM2 calculations (Figure 1.1.9.).[35]

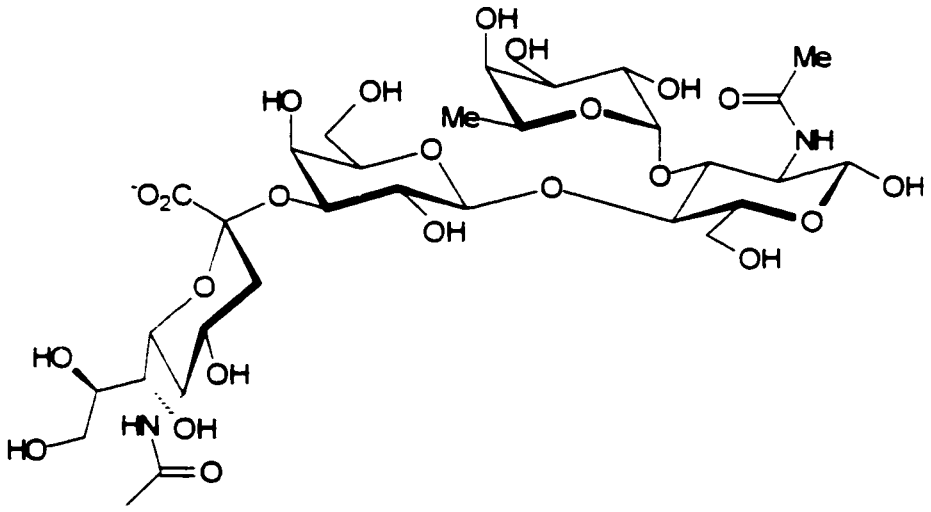

Figure 1.1.9. Solution-bound conformation of SLe^x to E-selectin.[35]

Wong *et al.*[36] have also proposed the bound conformation of SLe^x with E-selectin (Figure 1.1.10.).

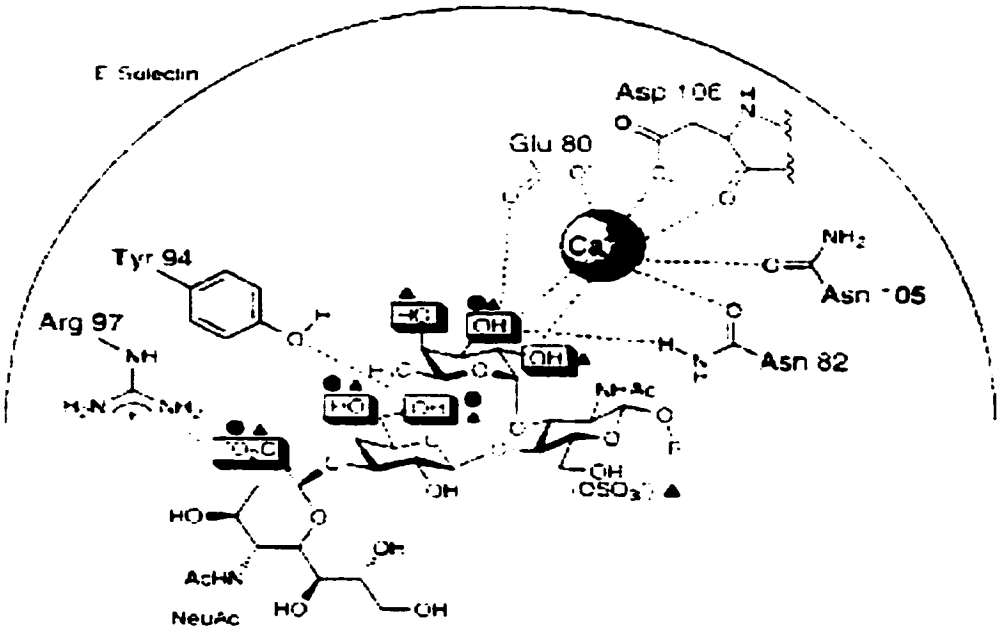

Figure 1.1.10. Model depicting structure of SLe^x bound to E-selectin and the functional groups involved in E- (□), P- (●) and L-selectin (▲) interactions.[36]

Recent crystal structures of P- and E-selectin bound domains complexed with SLe^x (Figure 1.1.11.) have revealed that the interactions are mostly electrostatic and only a small surface area of SLe^x is buried in the selectin. Another surprising result was that the selectin bound calcium ion is ligated by the 3- and 4-hydroxyl groups of the fucose residue and not the 2-,3-hydroxyl groups as previously thought. as shown in Figure 1.1.10.[37]

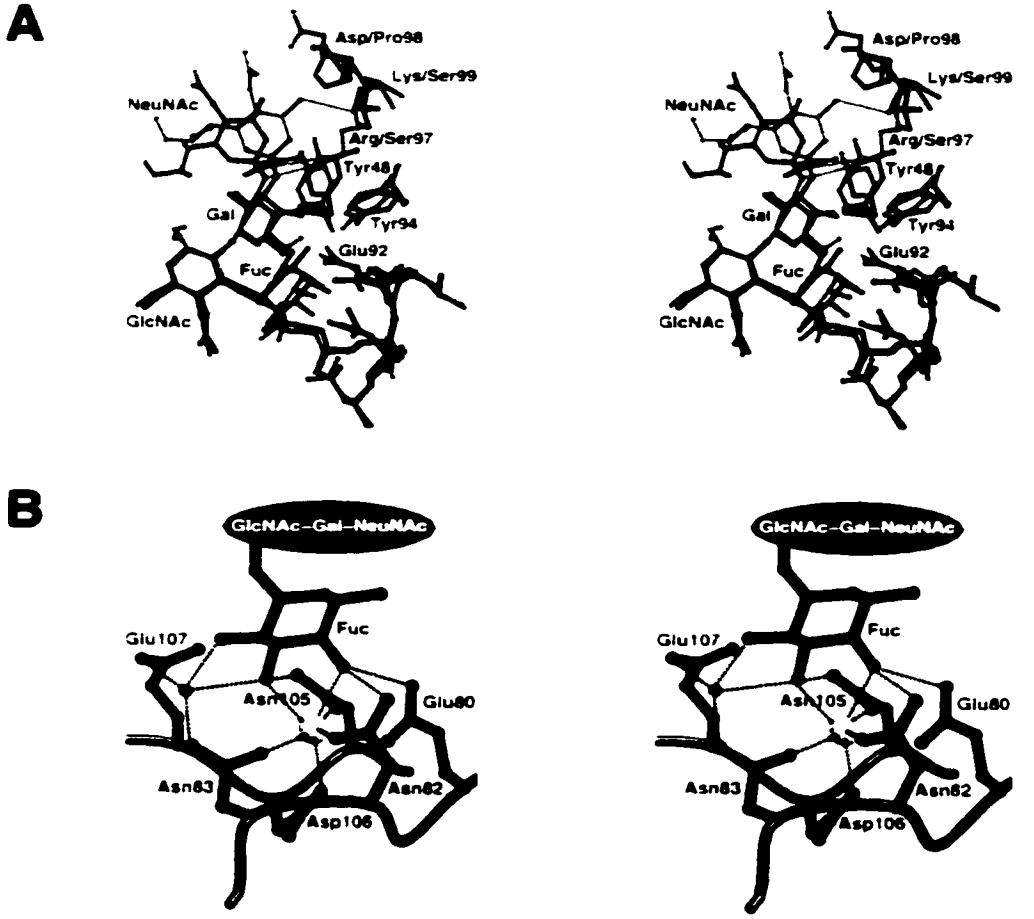

Figure 1.1.11. (a) Stereo view of superposition of SLe^x bound to P- and E-selectins showing similarities to binding conformation. P-selectin residues are blue, E-selectin residues are green, SLe^x bound to P-selectin is orange and SLe^x bound to E-selectin is purple. (b) Stereo view of SLe^x bound to E-selectin residues highlighting fucosly interactions. E-selectin residues are green and the SLe^x residue is purple.[37]

1.4.4. Interventions of SLe^x-Selectin Binding

Intervention of the selectin mediated leukocyte recruitment can be achieved using several strategies involving the inhibition of: selectin expression,

carbohydrate ligand biosynthesis, anti-selectin antibodies, binding with peptides and antibodies against SLe^x and binding by selectin ligands.[34] The latter is most attractive since the target molecule (SLe^x) is well known and has weak binding affinities to the selectins. As well, the high specificity of the tetrasaccharide selectin interaction makes this an ideal candidate for anti-adhesive therapy (Figure 1.1.2.). For example, increased binding affinities of SLe^x glycomimetic would block the leukocytes from entering the joints, but the high specificity would ensure that the carbohydrate-based drug would not interfere in other parts of the body; thus, achieving two seemingly incompatible goals.

1.4.5. Glycoside/Glycoconjugate Synthesis

It is clear that tetrasaccharide SLe^x and its analogues are key target molecules in the design of anti-adhesive ant-inflammatory drugs. Unfortunately the synthesis of carbohydrates and glycoconjugates is very difficult and complex in comparison to other biomolecules such as proteins. There is no automated template-driven system for glycan synthesis as glycosylation is a post-translational modification. Therefore, it can not be controlled by direct transcription and is influenced by environmental factors (e.g. enzyme competition, enzyme-substrate specificity and variant glycosylation).[38] The selective formation of each glycosidic bond presents many challenges as each sugar is highly functionalized. Many protection and deprotection steps are needed to avoid complicated mixtures of products and low yields. The synthesis

of this extremely functionalized tetrasaccharide represents a daunting task for any synthetic research group.

1.4.6. Synthesis of Sialyl Lewis^x

Advanced methods in oligosaccharide synthesis have enabled several groups to successfully synthesize SLe^x via chemical,[39] chemoenzymatic,[40] and enzymatic[41] strategies. An example of chemical and chemoenzymatic synthesis is depicted in Scheme 1.1.1.

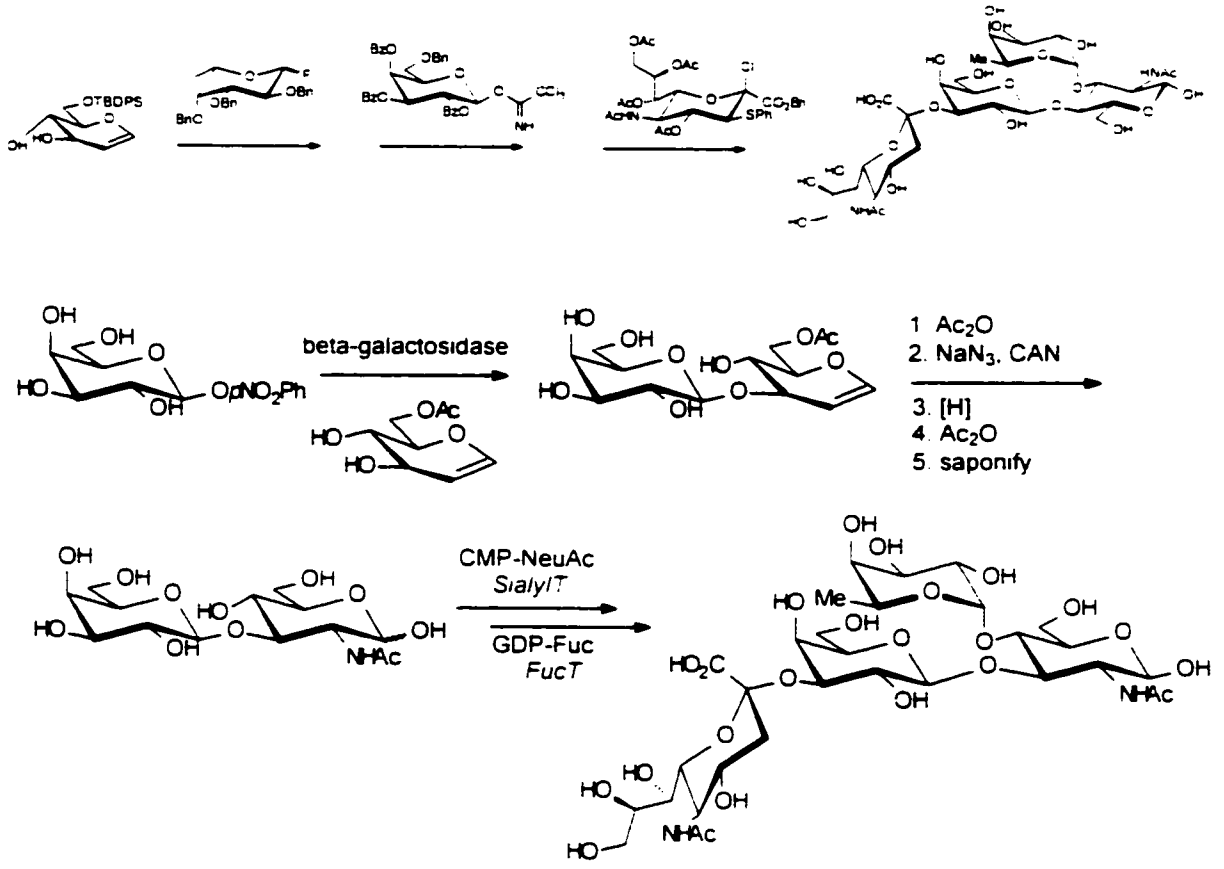

Scheme 1.1.1. (a) Chemical synthesis of SLe^x by Danishefsky *et al.*[42] (b) Chemoenzymatic synthesis of SLe^x by Wong *et al.*[40]

The yields of chemical syntheses range from 2% (Danisefsky *et al.*).[42] to 26% (Hasagawa *et al.*).[39] The enzymatic synthesis was a one pot reaction producing SLe^x in high yields. Although chemoenzymatic and enzymatic methods present high yielding routes to SLe^x, they are limited to SLe^x itself and not suitable for synthesis of varying glycomimetics.

1.4.7. SLe^x as an Anti-Inflammatory Drug

Although, enzymatic and chemoenzymatic synthesis have provided a relatively easy route to the synthetic target of SLe^x, it is cost prohibitive to use this method to produce the quantities of SLe^x necessary for treatment. Also, SLe^x is an O-linked saccharide that is readily cleaved by enzymes or hydrolyzed. This renders the natural ligand orally inactive and unstable in the bloodstream. Injection of SLe^x would be necessary for acute symptoms. The poor binding affinity of SLe^x to the selectins (mmol range) would require high doses to compensate for its low potency.[43, 44] The expense and/or difficulty of synthesis and instability of SLe^x disqualifies the natural ligand as a viable pharmaceutical. However, using SLe^x as a model, the structural elements can be determined and incorporated into a glycomimetic that has a simple structure, increased stability and a higher binding affinity to all three selectins.

1.5. Glycomimetics

As a consequence of the problems associated with SLe^x, SLe^x is not a drug candidate itself but serves as a lead structure for numerous industrial and

academic research groups. The main objective has been to design SLe^x mimetics with simplified structures, improved bioavailability and increased inhibitory potency.

1.5.1. Structural Simplicity

In order to pinpoint the SLe^x groups that are important for binding of different selectins, a large number of SLe^x analogues have been synthesized and examined. The lack of a universal assay for selectin-mimetic binding makes direct comparison of binding affinities difficult. The most prominent assay was ELISA which uses colour to quantitate the resultant IC_{50} value (the concentration of the inhibitor that gives a 50% inhibition of the selectin-SLe^x complex). The results are usually compared to the binding capacity of unmodified SLe^x, but can only be considered as crude measurements given the degree of variation of biological assays.

As mentioned, sialyl Lewis^x is comprised of four different carbohydrate moieties: sialic acid, galactose, glucosamine and fucose (Figure 1.1.12.).

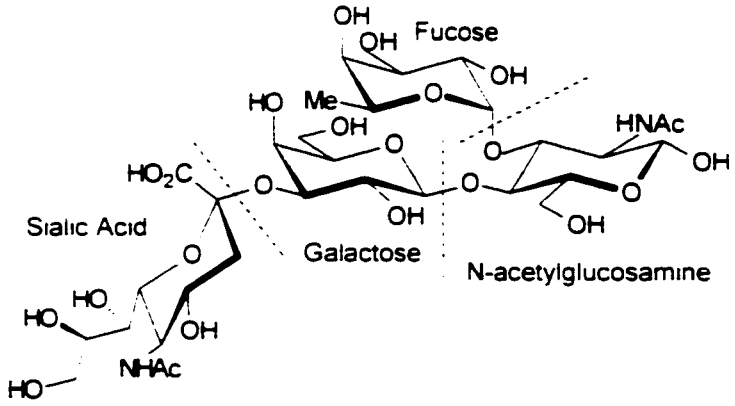

Figure 1.1.12. Basic components of SLe^x

This is a very complex and synthetically challenging molecule. Each of the four carbohydrate residues were modified and/or deleted to determine their role in the bioactivity of SLe^x.

One modification of SLe^x was that of the glycerol side chain of the sialic acid residue. All analogues bound E-, P- and L-selectin to the same extent as SLe^x indicating that this side chain was not necessary for selectin binding. The acetamido group was also modified and determined not to play an important role in selectin recognition.[45] Deletion of the sialic acid and replacement with anionic groups such as phosphate,[46] sulfate,[47] and carboxylate[48] on the 3 position of galactose retained the binding affinity to the selectins. This indicates that the complete sialic acid residue is not necessary in the minimized SLe^x structure. In fact, by replacing sialic acid with an acetic moiety demonstrated an increased inhibition against all three selectins.[48]

A number of deoxy-analogues of the galactose residue were synthesized. The analogues containing 4-deoxy residues were only recognized by P-selectin, whereas the 6-deoxy analogues were not recognized by any of the selectins.[49] The analogues synthesized by Bartnik *et al.*[50] showed the tightest binding molecules had at least one hydroxyl group in approximately the same position as the natural ligand. Thus the galactose backbone serves as a linker to N-acetylglucosamine residue and more importantly, it provides the necessary hydroxyl groups for selectin recognition and binding.

Modification of the N-acetylglucosamine residue by substitution of deoxy analogues[46] and changing the acetamido group[51] confirmed that the GlcNAc

moiety functions mainly as a scaffold to connect galactosyl and fucosyl residues. Positions 1 and 2 can be deoxygenated without any loss of activity. Cyclohexyl groups appear to best mimic the shape and rigidity provided by the N-acetylglucosamine residue of SLe^x.[52]

The fucose residue is very important to the SLe^x-selectin binding. Deletion of the fucosyl residue moiety results in no activity in an E-selectin assay.[53] Crystal structures have proven that hydroxyl groups of the fucose residue are involved in the calcium ion ligation of the SLe^x-selectin complex (Figure 1.1.11.). A systematic search of the necessary fucosyl functional groups was performed by Hasegawa *et al.*[45] In order to examine the relative contribution of the groups, each was sequentially replaced with a hydrogen to assess the effect on the analogues binding affinity to the selectins. It was determined that the presence and configuration of all hydroxyl groups in the fucose moiety were important for the binding of E- and L-selectins, however, only the 3-hydroxyl group is critical for the binding to P-selectin. The absence of the 6-methyl group decreases the activity 5 fold as it is necessary for E-selectin recognition.

Table 1.1.1. Systematic search for fucosyl functional groups necessary for SLe^x-E-selectin recognition.[45]

SLe^x	R_1	R_2	R_3	R_4	Activity
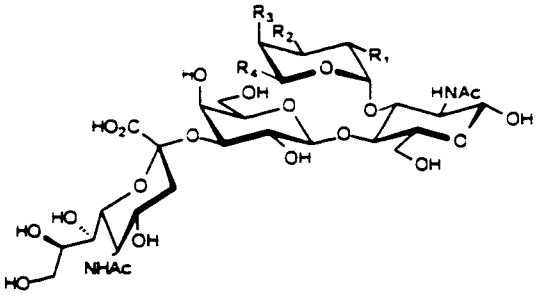	OH	OH	OH	CH_3	-
	H	OH	OH	CH_3	Inactive
	OH	H	OH	CH_3	Inactive
	OH	OH	H	CH_3	Inactive
	OH	OH	OH	H	5x less active

The modifications and deletions of a structure-activity reductionist approach have revealed the four essential groups necessary for selectin recognition. These groups include the fucose moiety, 4- and 6-hydroxyl groups of the galactose moiety and an anionic group (preferentially carboxylic acid) to replace the sialic acid moiety (Figure 1.1.13.).

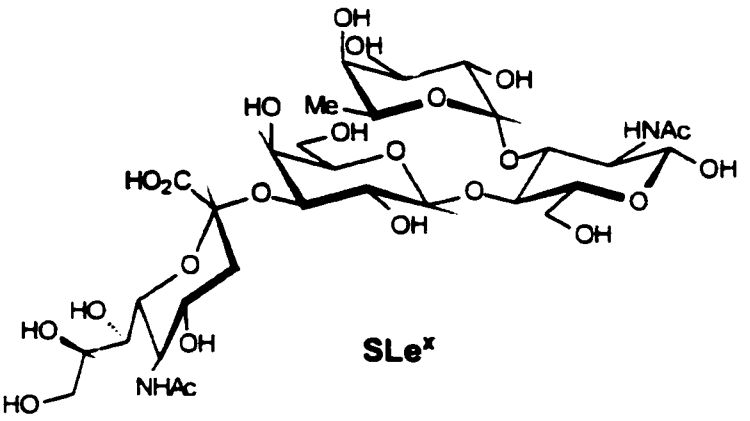

Figure 1.1.13. Functional group map (highlighted) indicating the active topography of SLe^x with the selectins.

1.5.2. Structural Stability

Identification of the important features of the tetrasaccharide is instrumental in developing a mimic that has increased stability in the bloodstream. The O-linked fucose residue is susceptible to fucosidase and will quickly be metabolized by the body.[42] However, studies have proven that the exocyclic, anomeric oxygen of the fucosyl residue is not necessary for selectin recognition[46] (section 1.5.1.) and thus can be replaced by other atoms such as sulfur, nitrogen or carbon.

Substitution of sulfur for the anomeric O yields a more stable compound as thioglycosides are resistant to glycosidase enzymes.[54] However, conformational analysis showed that thio analogues had a slightly altered conformation compared to the parent compound SLe^x. The C-S bond is longer than the C-O bond and the C-S-C angle differs by 16° from the C-O-C angle. These differences resulted in loss of biological activity.[55]

Nitrogen linked analogues are also resistant to enzymatic cleavage and have a longer lifetime in the blood stream. These analogues would be advantageous as the additional bonding potential of the nitrogen could lead to new and interesting mimetics. However, the synthesis of these N-linked fucosyl SLe^x mimetics is extremely difficult as there are currently no published papers on this topic.[56]

The other possible substitution for the fucosyl anomeric oxygen is carbon. There are many stability advantages gained by this replacement as C-linked glycosides are resistant to both chemical and enzymatic hydrolysis. As well, they

do not differ markedly from O-glycosides in solution conformation or in selectin binding affinities.[42] Additional bonds of the carbon (in comparison to O) also creates an opportunity for a broader range of structural diversity. The only disadvantage might be that C-linked SLe^x mimetics could be too stable and unable to be metabolized by the body.

1.5.3. Increased Binding Affinity

A large number of analogues have been reported in literature. The best mimetics produced to date have eliminated labile glycosidic bonds (e.g. O-linked) and replaced them with enzyme and hydrolysis resistant bonds such as C-linked glycomimetics which is the focus of this study. As discussed, the fucose moiety was found to be imperative for selectin recognition and most reported mimics contain this or the structurally similar mannose moiety.

An example of a natural product mimetic of SLe^x is the triterpene glycyrrhizin that was found using a 3-D database computational search.[57] Glycyrrhizin is detected in licorice and is currently used as an anti-inflammatory drug in Chinese herbal medicine. The modified α-C-fucopyranoside derivative **1** (Figure 1.1.14.) was found to have IC_{50} values lower than SLe^x for each selectin (Table 1.1.2.).

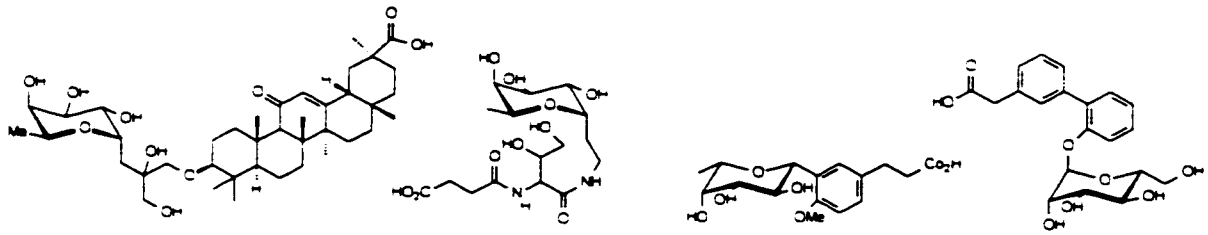

1 2 3 4

Figure 1.1.14. Examples of C-linked SLe^x mimetics with increased binding affinities.

Table 1.1.2. Relative binding affinities of selected SLe^x mimetics.

Compound	IC_{50} (mM)			Reference
	L-selectin	P-selectin	E-selectin	
SLe^x	2.5	2.5	0.75-2.5	**34**
1	0.005	0.005	0.5	**57**
2	-	-	3	**44**
3	0.003	0.001	>1.0	**58**
4	4.1	2.6	3.1	**59**

Many of the glycomimetics synthesized were glycopeptidomimetics[32]. These are easily synthesized and can be achieved using a combinatorial approach. Compound **2** was synthesized via a Ugi reaction which is a rapid and flexible strategy which can generate many diversified compounds.[44] Aryl C-glycosides have also been synthesized by Satoh *et al.*[58] The most potent was compound **3**

in spite of the C-β-configuration which is different from the anomeric α-O configuration of SLe^x. Although, this is not too surprising as there are several examples of β- linked compounds with nearly the same affinities as SLe^x known.[32] Significant inhibitory effects were observed with P- and L-selectin, however, none of the C-aryl glycosides exhibited significant binding affinity with E-selectin. An example of an anti-inflammatory SLe^x mimetic that has made it to the first stage of clinical trial with Texas Biotechnology Corporation is TBC 265 (**4**). It is a D-mannopyranosyloxybiphenyl substituted carboxylic acid. The conformation of the molecule displays the required functional groups in the essential orientation. It has a comparable in *vitro* potency and improved bioavailability over SLe^x.[59]

Secondary binding groups can be added to further enhance the binding affinity of potential glycomimetics to the selectins. In the case of carbohydrates, their function is dependent on their polyvalent presentation. The binding affinity of proteins to carbohydrates is often weak and yet the required specificity and strength is high in cell-cell interactions. Carbohydrate-binding proteins (e.g. selectins) tend to have multiple copies of their carbohydrate domain at the cell surface. This allows for simultaneous multiple binding events between the protein and the carbohydrate epitope which amplifies affinity.[60] This amplification has been demonstrated using secondary binding groups such as glycopolymers, anionic groups, liposomes and macrocylizations that are able to increase the binding affinity by factors as high as thousands. Enthalpy and entropy play roles in determining the binding affinity between the SLe^x mimetic and E-, L- and P-

selectins. Enthalpy depends directly on the number and strength of the interactions while binding entropy depends on the rigidity of the SLe^x mimetic and its ability to adopt the bioactive form.[61]

Simple dendrimers and tetramers of SLe^x reported to have IC_{50} values of less than 50 nM and 0.15 mM towards L-selectin respectively which is a 60-fold increase of the tetramer over its corresponding monomer.[62]

Copies of the glycomimetic can be substituted on polymers. These multivalent glycoconjugates show increased binding affinities as they mimic nature's own strategy. An interesting example of a glycopolymer, synthesized by Kiessling *et al.*[63] was decorated with galactose-3-sulfate and showed an IC_{50} value of >20 mM against P-selectin. The additive effect of a second anionic group (SO_3^-) is evident by the significant decrease in the IC_{50} value to 0.167 mM (500 fold better than SLe^x). The chemistry used to synthesize this polymer was that of the novel olefin metathesis (ROMP) which will be discussed in further detail in chapter 3. Since the polymer was only recognized by P-selectin, it has the potential to serve as an instrument in deciphering the specificities of each selectin.[17]

Anionic groups also enhance inhibitory potencies as seen with polyanionic mimics such as fucoidin (sulfated fucose) or the hexaphosphate cyclitol which is very active against L-selectin (Figure 1.1.15.).[64]

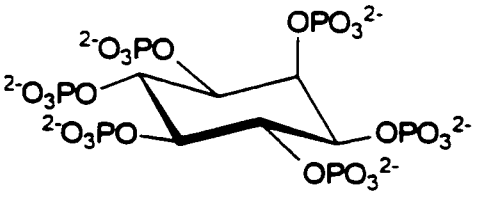

5

Figure 1.1.15. Cyclitol derivative.[64]

Overall, the polyanions showed the highest affinity for P-selectin which could be interacting with the highly positive charged residues of P-selectin and related to the requirement of tyrosine sulfation on PSGL-1.[32]

Another secondary binding group is liposomes. Liposomes are alkyl chains that can form self-assembled dendrimers due to the hydrophobic effect. Hydrophobic tails added to the reducing end of a sugar can increase the binding from 3-10-fold.[32] Defrees *et al.*[65] prepared liposomes containing 0.5-5mol% of an SLe^x analogue and reported a 5000-fold in *vitro* and 40-fold in *vivo* improved binding affinity towards E-selectins. Wong *et al.*[66] also used liposomes to improve IC_{50} values of the parent compound **2** by synthesizing the glycopeptide **6** (Figure 1.1.16.). The addition of the hydrophobic tail increased the potency of **6** by 15-fold in comparison to SLe^x (IC_{50} (μM) E=37, P=7, L=190).

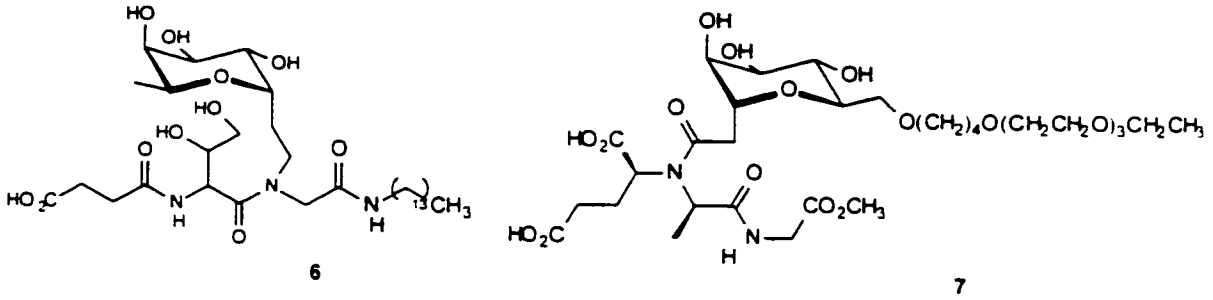

Figure 1.1.16. Wong *et al.*[66] incorporation of liposomes improved binding affinity of parent compound **2**.

However, addition of a hydrophobic tail to the sugar (compound **7**) resulted in even stronger binding affinities to the selectins by 20-fold. (IC_{50} P-selectin = 5 μM). Another approach by Wong *et al.* used a glycopeptidomimetic template similar to compound **2** and cross-metathesis (chapter 3) to generate a series of aryl-substituted mimetics that exhibited 3x better binding to E-selectin and 1000x better activity to P-selectin.[67] It is obvious that liposomes have the ability to increase the potency of SLe^x mimetics and it was assumed that the enhancement was due to the formation of micelles. However, recent studies by Hasegawa *et al.*[68] indicate that these hydrophobic chains appear to fit into a hydrophobic pocket near the binding site of the selectins.

Macrocyclizations can further improve the potency of SLe^x mimetics by having all the necessary elements pre-organized in a defined structure that will ultimately lower entropic costs upon binding to the selectin. Kunz *et al.*[69] prepared two trivalent SLe^x analogues based on cyclic peptides and were found to be 2-3x as active as SLe^x monomer. An example of one of these macrocyclizations is shown in Figure 1.1.17. Wong *et al.*[66] synthesized the

macrolactone ring **8** that defined the structure so that all the required points of contact were aligned. The increased inhibitory effect was 1000-fold greater than that of SLe^x. This enhanced potency is comparable to the hydrophobic effect exhibited in **7**.

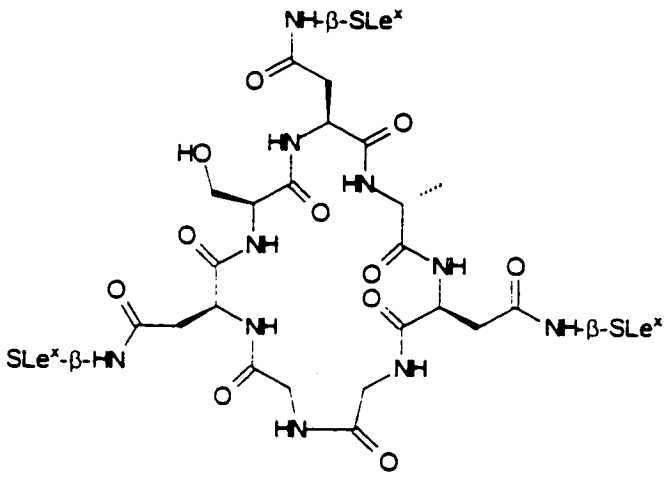

8

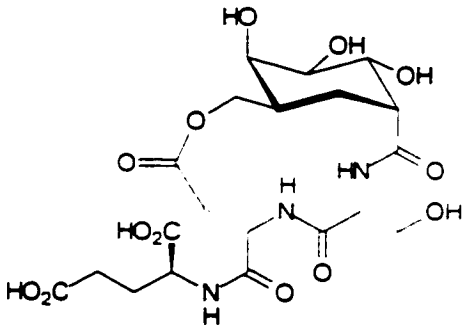

9

Figure 1.1.17. Macrocyclizations of Kunz (**8**)[69] and Wong (**9**).[66]

Bertozzi *et al.*[70] have synthesized a "mega"- SLe^x mimetic by incorporating carbohydrate multimerization on a polymerized liposome surface with anionic groups (Figure 1.1.18.). The most potent compounds had the anionic CO_2^- and SO_3^- having IC_{50} values in the nM range for both L- and P-selectins. These results appear to support the proposed two-site model for P-selectin and suggest the same model for L-selectin.

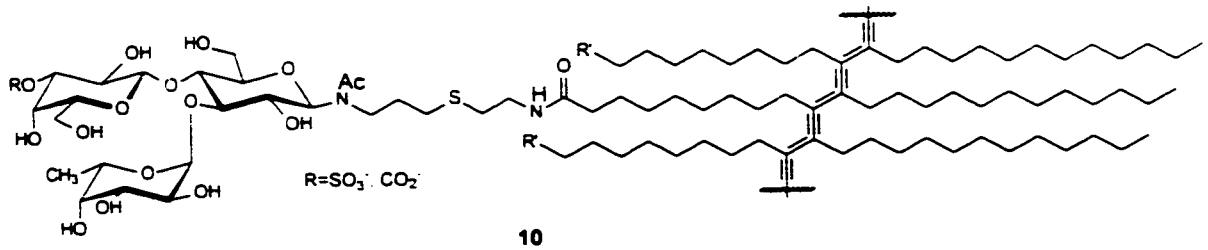

10

Figure 1.1.18. SLe^x of Bertozzi *et al.*[70] incorporating multi-secondary binding groups.

The recent findings of multivalent amplification of SLe^x mimetic-selectin interaction encouraged Texas Biotechnology Corporation. to add an additional binding group to their original SLe^x mimetic **4** (TBC 265) as seen in Figure 1.1.19.[58]

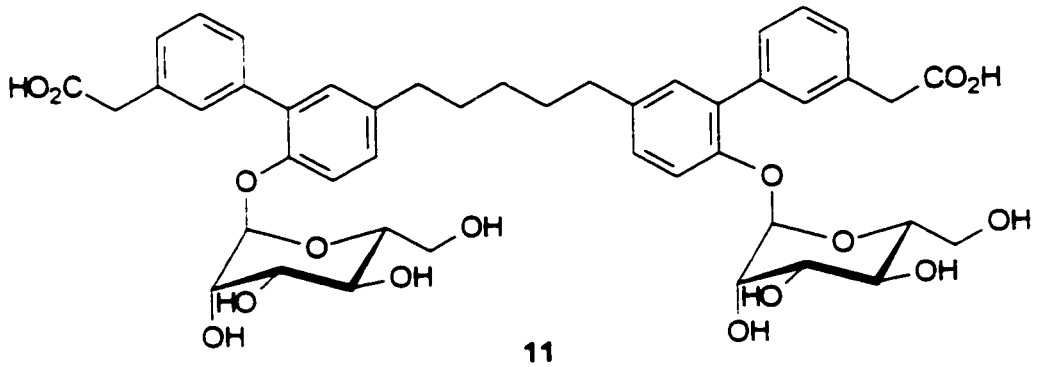

11

Figure 1.1.19. Modified TBC 265 (**4**) to TBC 1269 (**11**).

Compound **11** has stronger binding affinity to all three selectins than its parent compound **4** (IC_{50} (μM) E=0.5, P=0.07, L=0.56). This SLe^x mimetic is currently

under research for treatment of psoriasis and phase IIA clinical trials for treatment of pediatric asthma. However, this compound and others in its series have a very short life time in the blood stream due to the instability of the O-glycoside towards enzymatic cleavage.

This brief review of key glycomimetics has demonstrated the need for continued research into the glycobiology and glycochemistry governing the SLe^x-selectin interactions to provide the missing clues to solve this complex cellular event. Future work will need to incorporate simplicity, stability and strong binding affinities in the quest for the ultimate selectin glycomimetic inhibitor.

References

(1) Boons, G. J. In *Organic Synthesis with Carbohydrates;* Boons, G. J., Hale, K. J., Eds.; Sheffield Academic Press: Sheffield, 2000; p 1.

(2) Laine, R. A. In *Glycosciences;* Gabius, H.J., Gabius, S., Eds.; Chapman & Hall: Weinham, 1997; p 1.

(3) Sharon, N.; Lis, H. *Sci. Amer.* **1993**, 82.

(4) Dwek, R. A. *Chem. Rev.* **1996,** 96, 683.

(5) Boons, G. J. In *Carbohydrate Chemistry*; Boons, G. J. Ed.; Blackie Academic & Professional: London, 1998; p 1.

(6) Zanini, D. In *Quantitative Multivalent Carbohydrate-Protein Interactions from Novel Glycodendrimers (Ph.D. Thesis)*; University of Ottawa: Ottawa, 1997; p 2.

(7) Sharon, N.; Ofek, I. *Glycoconjugate J.* **2000**, 17, 659.

(8) Toyokuni, T.; Singhal, A. K. *Chem. Soc. Rev.* **1995**, 231.

(9) Ragupath, G.; Slovin, S. F.; Adluri, S.; Sames, D.; Kim, I. J.; Kim, H. M.; Spassova, M.; Bornmann, W.G.; Lloyd, K. O.; Scher, H. I.; Livingston, P. O.; Danishefsky, S. J. *Agnew. Chem. Int. Ed. Engl.* **1999**, 38, 563.

(10) Jennings, H. J.; Snood, R. K. In *Neoglyconjugates, Preparation and Application*; Lee, V. C.; Lee R. T., Eds.; Academic: San Diego, 1999; p 325.

(11) Hakomori, S.; Zhang, Y. *Chem. Biol.* **1997**, 4, 97.

(12) Coppa, G. V.; Pierani, P.; Zampini, L.; Carloni, I. *Acta. Paediatr. Suppl.* **1999**, 88, 89.

(13) Witczak, Z. J. *Curr. Med. Chem.* **1995**, 392

(14) (a) Stevens, R. L.; Faull, K. F.; Conklin, K. A.; Green, B. N.; Fluharty, A. L. *Biochem.* **1993**, 32, 4051. (b) Swapna, G. T.; Jaganadh, B.; Gurjar, M. K.; Kunwar, A. C. *Biochem. Biophys. Res. Commun.* **1989**, 164, 1086.

(15) (a) Wessel, H. P. In *Glycoscience*; Driguez, H.; Thiem, J., Eds.; Springer-Verlag: Berlin, 1997, 215. (b) Fukuda, M. N.; Sasaki, H.; Lopez, L.; Fukud, M. *Blood* **1989**, 73, 84. (c) Smythe, H. H.: White, S. W.; Colman, P. M. *Nature* **1993**, 363, 418.

(16) (a) Bertozzi, C. R.; Bednarski, M. D. *J. Am. Chem. Soc.* **1992**, 114, 2242 (b) Stahn, R.; Grither, C.; Zeisig, R.; Karsten, U.; Felix, S. B.; Wenzel, K. *Cell Mol. Life Sci.* **2001**, 58, 147.

(17) Spyker, N. M.; Westerduin, P.; van Boeckel, C. A. A. *Tetrahedron*, **1992**, 48, 6297.

(18) (a) Verheul, A. M.; Boons, G. H.; van der Marel, G. A.; van Boom, J. H.; Jennings, H. J.; Snippe, H.; Verhoet, J.; Hoogerhout, P.; Poolman, J. T. *Infect. and Immun.* **1991**, 59, 3566. (b) Yarema, K. J.; Bertozzi, C. R. *Curr. Bio.* **1998**, 2, 49.

(19) Halina, L.; Sharon, N. *Chem. Rev.* **1998**, 98, 637.

(20) Drickamer, K. J. *Biol. Chem.* **1998**, 263, 9557.

(21) Lawrence, M. B.; Springes, T. A. *Cell* **1991**, 65, 859.

(22) Falguni, D. *Bio. Med. Chem.* **2000**, 123.

(23) Paulson, J. C. In *Adhesion: It's role in inflammatory diseases*; Harlan, J. M.; Liu, D. Y., Eds.; W. H. Freeman & Co.: New York, 1992; p. 19.

(24) Pouyani, T.; Seed, B. *Cell* **1995**, 83, 333.

(25) Polley, M. J.; Philips, M. L.; Waynes, E.; Nudelman, E.; Singhal, A. K.; Hakomori, S. I.; Paulson, J. C. *Proc. Natl. Acad. Sci.* **1991**, 88, 6224.

(26) Leppanen, A.; Whites, S. P.; Helin, J; McEver, P; Cummings, R. D. *J. Bio. Chem.* **2000**, 275, 39569.

(27) Wittmann, V.; Shuich, T.; Gong, K. W.; Weitz-Schmidt, G.; Wong, C. H. *J. Org. Chem.* **1998**, 63, 5137.

(28) Varki, A. In *Essentials of Glycobiology:* Cummings, R.; Esko, J.; Varki, A.; Freeze, H.; Hart, G.; Mauth, J., Eds.; Cold Spring Harbour Laboratory Press: New York, 1999; p. 393.

(29) Yuen, C. T.; Bezouska, K.; O'Brien, J.; Stoll, M.; Lemoine, R.; Lubineau, A.; Kiso, M.; Hasegawa, A.; Bockovich, N. J.; Nicolaou, K. C.; Feizi, T. *J. Biol. Chem.* **1994**, 269, 1595.

(30) Moore, K. L.; Stutts, N. L.; Diaz, S.; Smith, D. F.; Cummings, R. D.; Varki, A.; McEver, R. P. *J. Cell. Biol.* **1992**, 118, 445.

(31) Kim, Y. J.; Varki, A. *Glycoconjugate J.* **1997**, 14, 569.

(32) Simanek, E. E.; McGarvey, G. J.; Jablonowski, J. A.; Wong, C. H. *Chem. Rev.* **1998**, 98, 833.

(33) Schlaepfer, D. D.; Hanks, S. K.; Hunter, T.; van der Geer, P. *Nature* **1994**, 372, 786.

(34) Roy, R. In *Carbohydrates in Drug Design*, Witczak, Z.; Nieforth, K. A., Eds.; Marcel Dekker Inc.: New York, 1997, p. 83.

(35) Lin, C. Y.; Hummel, C. W.; Huang, D. H.; Ichikawa, Y.; Nicolaou, K. C.; Wong, C. H. *J. Am. Chem.Soc.* **1992**, 114, 5452.

(36) Wong, C. H.; Moris-Varas, F.; Hung, S. C.; Marron, T. G.; Lin, C. C.; Gong, K. W.; Weitz-Schmidt, G. *J. Am. Chem. Soc.* ***1997, 119, 8152.***

(37) Somens, W. S.; Tang, J.; Shaw, G. D.; Camphausen, R. T. *Cell* **2000**, 103, 467.

(38) Koeller, K. M.; Wong, C. H. *Chem. Rev.* **2000**, 100, 4465.

(39) Kameyama, A; Ishida, H.; Kiso, M.; Hasegawa, A. *J. Carbohydr. Chem.* **1991**, 10, 549.

(40) Cook, G. C.; Wong, C. H. *Tetrahedron Lett.* **1992**, 33, 4253.

(41) Ichikawa, Y.; Lin, Y. C.; Dumas, D. P.; Shen, G. J.; Garcia-Juneda, E.; Williams, M. A.; Bayer, R.; Ketchum, C.; Walker, L. E.; Paulson, J. C.; Wong, C. H. *J. Am. Chem. Soc.* **1992**, 114, 9283.

(42) Danishefsky, S. J.; Gervay, J.; Peterson, J. M.; McDonald, F. G.; Koseki, K.; Griffith, D. A.; Oriyama, T.; Marsden, S. P. *J. Am. Chem. Soc.* **1995**, 117, 1940.

(43) Uchiyama, I.; Vassilev, V. P.; Kajimoto, T.; Wong, W.; Huang, H.; Lin, C. C.; Wong, C. H. *J. Am. Chem. Soc.* **1995**, 117, 5395.

(44) Sutherlin, D. P.; Stark, T. M. ; Hughes, R.; Armstrong, R. W. *J. Org. Chem.* **1996**, 61, 8350.

(45) Brandley, B. K.; Kiso, M.; Abbas, S.; Nikrad, P.; Srivasatava, O.; Foxall, C.; Oda, Y.; Hasegawa, A. *Glycobiology* **1993**, 3, 633

(46) Onmoto, H.; Nakanura, K.; Inoue, T.; Kondo, N.; Inoue, Y.; Yoshino, K.; Kondo, H.; Ishida, H.; Kiso, M.; Hasegawa, A. *J. Med. Chem.* **1996**, 39, 1339

(47) Manning, D. D.; Bertozzi, C. R.; Pohl, N. L.; Rosen, S. D.; Keissling, L. L. *J. Org. Chem.* **1995**, 60, 6254.

(48) Yoshida, M.; Kawakami, Y.; Ishida, H.; Kiso, M.; Hassegawa, A. *J. Carbohydr. Chem.* **1996**, 15, 399.

(49) (a) Stahl, W.; Spiengard, U.; Kretzschmar, G.; Kunz, H. *Agnew. Chem. Int. Ed. Engl.* **1994**, 33, 2096. (b) Komba, S.; Ishida, H.; Kiso, M.; Hasegawa, A. *Glycoconjugate J.* **1996**, 13, 241.

(50) Toeter, A. G.; Kretschemar, G.; Bartnik, E. *Tetrahedron Lett.* **1995**, 36, 1961.

(51) Nikrud, P. V.; Kashem, M. A.; Wlasichuk, K. B.; Alton, G.; Venot, A. P. *Carbohydr. Res.* **1993**, 250, 145.

(52) Bamford, M. J.; Bird, M.; Gore, P. M.; Holmes, D. S.; Priest, R.; Prodger, J. C.; Saez, V. *Bioorg. Med. Chem. Lett.* **1996**, 6, 239.

(53) Nelson, R. M.; Dolich, S.; Aruffo, A.; Cecconi, O.; Bevilacqua, M. P. *J. Clin. Invest.* **1993**, 91, 1157.

(54) Defaye, J.; Gebis, J. In *Studies in Natural Products Chemistry;* Rahman, A., Ed.; Elsevier: Amsterdam, 1991, 315.

(55) Nilsson, U.; Johansson, R; Magnusson, G. *Chem. Eur. J.* **1996**, 2, 295.

(56) Schmor, B; Roy, R. *Anomeric Selectivity in Coupling of Fucosylamines with Protected Amino Acids* manuscript in preparation.

(57) Rao, B. N.; Anderson, M. B.; Musser, J. H.; Gilbert, J. H.; Schaeter, M. E.; Foxall, C.; Brandley, B. K. *J. Biol. Chem.* **1994**, 269, 19663.

(58) Kuribayashi, T.; Ohkawa, N.; Satoh, S. *Bioorg. Med. Chem.* **1998**, 8, 3307.

(59) Kogan, T. P.; Dupré, B.; Bui, H.; McAbee K. C.; Kassir, J. M.; Scot, I. L.; Hu, X.; Vanderslice, P.; Beck, P. J.; Dixon, R. F. *J. Med. Chem.* **1998**, 41, 1099.

(60) Roy, R. In *Carbohydrate Chemistry*; Boons, G. J. Ed.; Blackie Academic & Professional: London, 1998; p 243.

(61) Ernst, B.; Dragic, Z.; Marti, S.; Muller, C.; Wagner, B.; Jahnek, W.; Magnani, T. L.; Norman, K. E.; Dehrlein, R.; Peters, T.; Kollo, H. C. *Chimia* **2001,** 55, 268.

(62) Roy, R. In *Glycochemistry*; Wang, P. G.; Bertozzi, C. R. Eds.; Marcel Dekker Inc.: New York, 2001, 277.

(63) Manning, D. D.; Hui, C.; Beck, P.; Kiessling, L. L. *J. Am. Chem. Soc.* **1997**, 119, 3161.

(64) Cecconi, O.; Nelson, R. M.; Roberts, W. G.; Hanasaki, K.; Mannori, G.; Schultz, C.; Ulrich, T. R.; Aruffo, A.; Bevilacqua, M. P. *J. Biol. Chem.* **1994**, 269, 15060.

(65) DeFrees, S. A.; Phillips, L.; Zalipsky, S; Guo, L. *J. Am. Chem.* **1996**, 118, 6101.

(66) Tsai, C. Y.; Xuefei, H.; Wong, C. H. *Tetrahedron Lett.* **2000**, 41, 9499.

(67) Huwe, C. M.; Woltering, T. J.; Jiricek, J.; Weitz-Schmidt, G.; Wong, C. H. *Bioorg. Med. Chem.* **1999**, 7, 773.

(68) Tsujishita, M.; Hiramatsu, Y.; Kondo, N.; Ohmoto, H.; Kondo, H.; Kiso, M.; Hasegawa, A. *J. Med. Chem.* **1997**, 40, 362.

(69) Sprengard, U.; Schudok, M.; Scmidt, W.; Kretzschmoer, G.; Kunz, H. *Angew. Chem. Int. Ed. Engl.* **1996**, 35, 321.

(70) Bruehl, R. E.; Dasgupta, F.; Katsumoto, T. R.; Tan, J. H.; Bertozzi, C. R.; Spevak, W.; Ahn, D. J.; Rosen, S. D.; Nagy, J. O. *Biochem.* **2001**, 40, 5964.

Chapter 2. Synthesis of Sialyl Lewis^x Mimetics

2.1. Introduction

As mentioned in chapter 1, glycomimetics are logical and practical substitutions for the natural ligand sialyl Lewis^x in the treatment of inflammatory diseases. The potential of generating diverse glycomimetics through solution chemistry has fuelled an interest in developing chemical tools that would interfere with SLe^x-selectin recognition. SLe^x is a complicated molecule that carries unnecessary groups and the instability of SLe^x, for the most part, is due to the ease of hydrolysis of O-glycosides. As a result, our main objective was to synthesize simplistic SLe^x mimetic structures containing the key pharmacophores necessary for selectin recognition that were linked through an enzyme resistant anomeric carbon providing the necessary stability for bioavailability.

2.2. Results and Discussion

2.2.1. Strategies

The numerous SLe^x mimetics of Wong *et. al.*[1] provided a knowledgeable starting point in devising target mimics. At the beginning of this project, a C-linked glycopeptidomimetic (section 1.5. compound **3**) was cited as one of the most active SLe^x mimetics towards the selectins. Similarly, we began transforming this lead by designing a convergent approach that could be easily modified to incorporate varying peptide or peptoid chain lengths with a synthetic

handle for easy functional group manipulation. The solution chemistry route could lead to a multitude of SLe^x mimetics and theoretically applied to solid phase chemistry to manufacture libraries of SLe^x mimetics.

The backbone of the target molecule consisted of varying protected amino acids and amine groups to find the appropriate spacing of the functional groups (hydroxyls and carboxylic acid) for optimum binding affinities. The backbone of all the linkers contained a peptoid functionality. Polypeptoids are oligomeric N-substituted glycines (Figure 2.1.1.).[2] These polyamides are not found in nature and differ from polypeptides since the nitrogen and not the α-carbon are substituted. Peptoids are new synthetic peptide isotere that may be biologically active and metabolically stable.

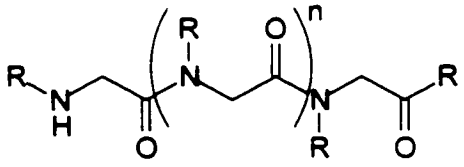

Figure 2.1.1. General structure of a polypeptoid (N-substituted oligoglycine).[2]

The carbohydrate portion of the convergent approach began with the essential L-fucose moiety that was modified to an α-C-linked carboxylic acid. This sugar acid was coupled to a proline ring that provided rigidity to the molecule in place of the GlcNAc which may decrease entropic costs for selectin binding. Also, the chirality of the proline ring provided another point of

diversification as either L- or D-proline could be used to try to achieve the proper conformation for selectin binding (Scheme 2.1.1.).

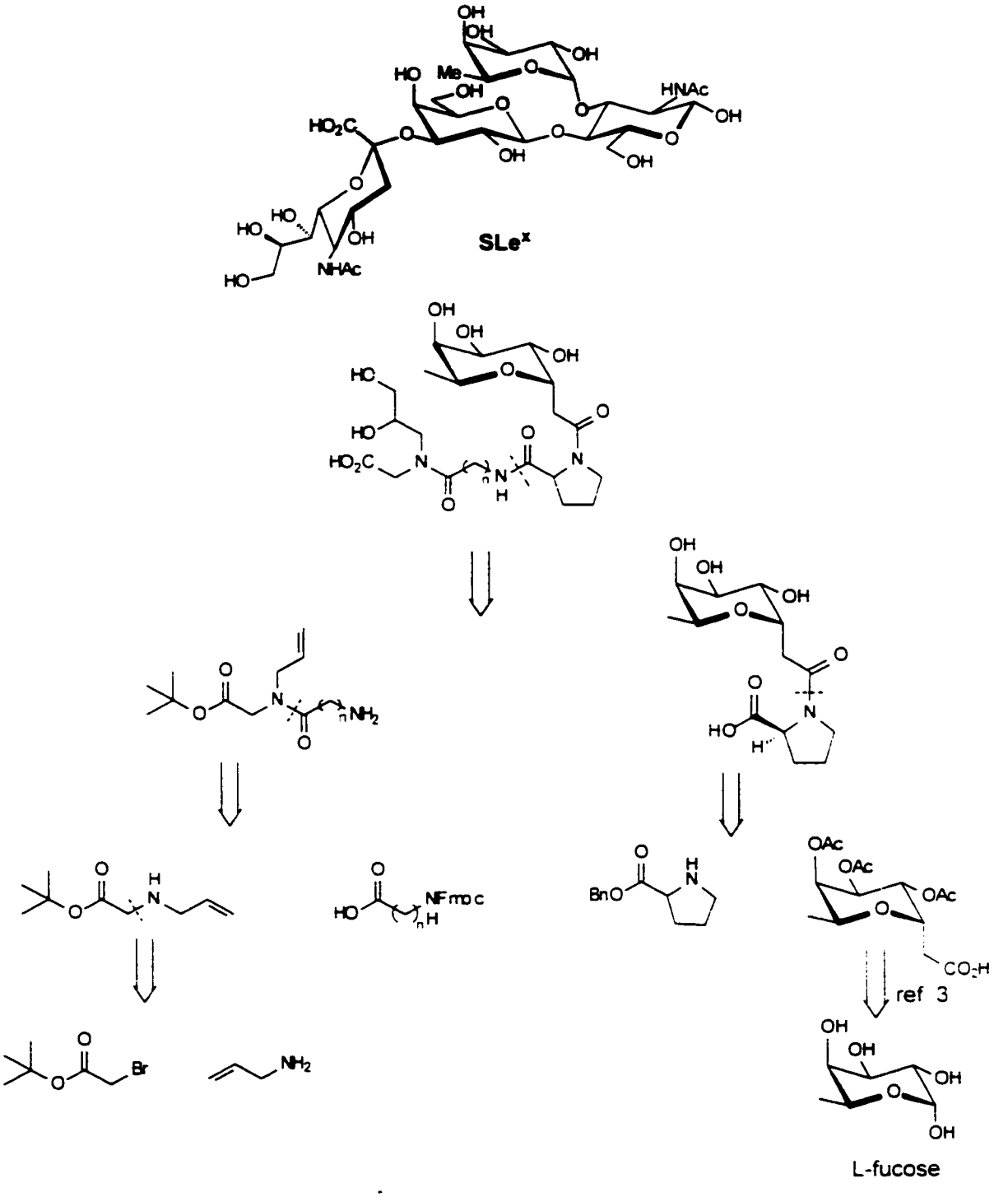

Scheme 2.1.1. Retrosynthetic scheme of SLe^x target glycomimetics.

2.2.2. Convergent Approach using L-Proline

The α-C-linked fucosyl carboxylic acid derivative **6** was synthesized from L-fucose using a literature procedure.[3] This consisted of peracetylation, displacement of the anomeric acetyl group by allyl moiety using BF_3OEt_2 and TMSOTf, Zemplén deacetylation, recrystallization, reacetylation, ozonolysis, and oxidation producing **6** in an overall yield of 59% (Scheme 2.1.2.).

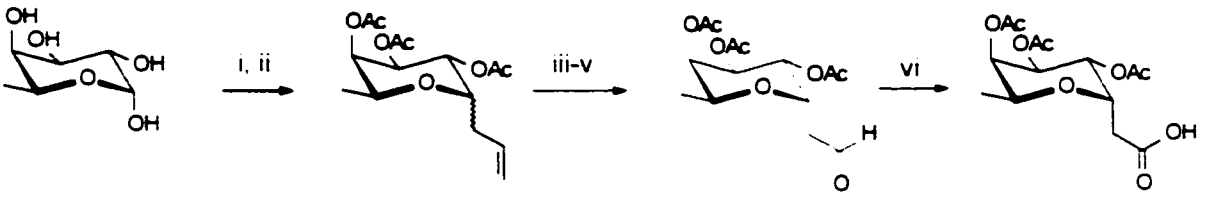

L-fucose **2** **5** **6**

Scheme 2.1.2. Overall synthesis of C-carboxylic acid 2, 3, 4-tri-O-acetyl-α-fucoside **6**. Reagents and conditions: (i) Ac_2O (9eq), C_5H_5N, 7hr, 0°C-rt, 99%; (ii) allyl-TMS (2eq), BF_3OEt_2 (2eq), TMSOTfl (1eq), CH_3CN, 4hr, 0°C-rt, 94%; (iii) 1N NaOMe, MeOH, rt, 3hr, recrystallization (EtOAc), 75%; (iv) (Ac_2O) (9eq), py, 4hr, 0°C-rt, 99%; (v) O_3, CH_2Cl_2,1hr, -78°C, 100%; (vi) NaH_2PO_4 (pH=6), 1M $KMnO_4$, t-BuOH, 1hr, rt, 85%.[4]

The allylation step (ii) produced a mixture of α and β-anomers (typically 14:1 α/β) that were inseparable using silica gel column chromatography. Only the α-anomer was desired since it had a similar orientation to that of the fucosyl residue in the SLe^x target molecule. Wong *et al.*[3] also faced this problem of an anomeric mixture and devised a route to obtain purely the α-anomer. In order to separate the anomers, the C-allyl fucosyl moiety was deacetylated using

Zemplén conditions and then recyrstallized from ethyl acetate yielding only the α-anomer **4**. The crystalline product was then reacetylated, ozonolyzed and oxidized with potassium permanganate to produce the desired α-C-linked fucosyl acid residue **6**. The ^{1}H and ^{13}C NMR of **6** was almost identical to the literature reference. The ^{1}H NMR of the product indicated that it consisted of essentially one isomer. The coupling constant for the H-1 proton and the H-2 proton (dd, $J_{1,2}$ = 5.6 Hz, $J_{2,3}$ = 9.8 Hz) indicate that this isomer was the α-anomer of **6** (Figure 2.1.2.).

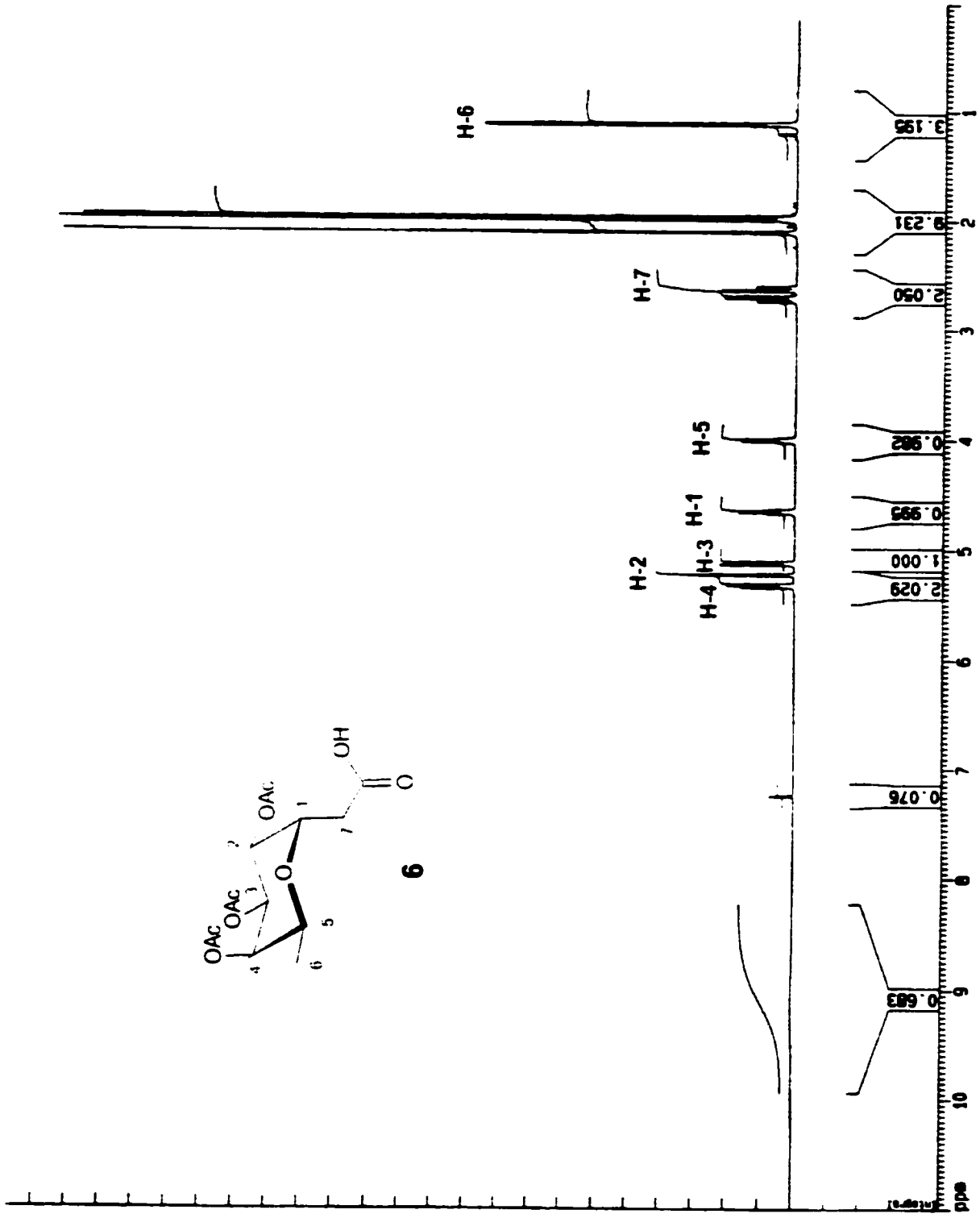

Figure 2.1.2. ^{1}H NMR (500 MHz, $CDCl_3$) of 2-(2, 3, 4-tri-O-acetyl-α-L-fucopyranosyl)ethanoic acid **6**.

In an effort to increase the yield of the carboxylic acid derivative **6**, other oxidation reactions were examined. These included sodium chlorite as the oxidizing agent[5] and refluxing in potassium permanganate.[6] The oxidation of the aldehyde derivative **5** using sodium chlorite to form the carboxylic acid derivative **6** had major impurities and was difficult to isolate. The oxidation of the allyl derivative **4** directly to the carboxylic acid derivative **6** used harsh potassium permanganate refluxing conditions. The refluxed reaction was attempted since it would reduce the number of synthetic steps. However, the yield of this reaction was low (14%) and not practical in a multi-step synthesis. Thus it was determined that the phosphate/permanganate oxidation of the aldehyde derivative **5** to form the carboxylic acid derivative **6** (Scheme 2.1.3.) was the most effective of the three oxidation reactions.

The carboxylic acid derivative **6** was coupled to L-proline benzyl ester, followed by hydrogenation to afford **8**. Deacetylation of **8** was done to examine the conformation of the unprotected mimic of the Fuc-α-1,3-GlcNAc portion of SLe^x (Scheme 2.1.3.).

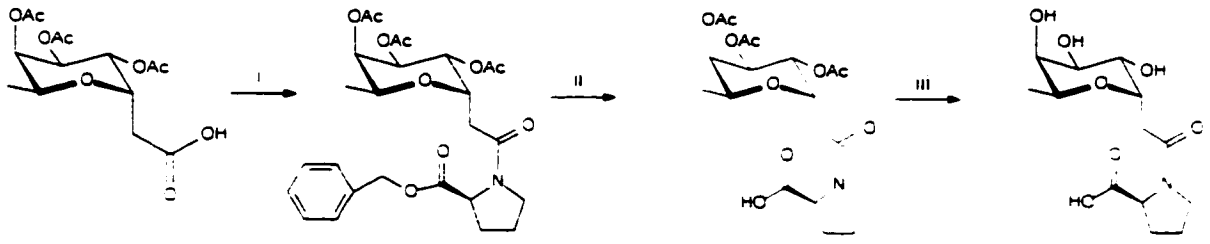

Scheme 2.1.3. Coupling of **6** with L-proline benzyl ester to form **7** followed by sequential deprotections. Reagents and conditions: (i) L-Pro-OBn (1.2eq), PyBOP (1.3eq), NMM (2eq), CH_2Cl_2, 4hr, rt, 99%; (ii) H_2,10% Pd/C, MeOH, 30min, 93%; (iii) 1N NaOMe, MeOH, rt, 3hr, 100%.

Compound **6** was coupled to L-proline benzyl ester using several different coupling reagents. The first one tried was TBTU (1.5eq) and DIPEA (1.8eq) which gave good yields (80%) but had long reaction times (>24hr) and required an initial work-up followed by silica gel chromatography to purify the product. The other coupling reagent tested was BOP (1.8eq) and NMM (2eq) which afforded the 2, 3, 4-tri-O-acetyl-α-L-fucosyl-L-proline benzyl ester derivative **7** in higher yields (87%). The solvents of the crude mixture were removed under reduced pressure and the residue was directly purified by silica gel column chromatography. This coupling reaction was somewhat faster (4hr), and had higher yields which could be attributed to fewer steps in the purification process. However, one main drawback of BOP was that it is highly carcinogenic. PyBOP is a derivative of BOP that is significantly less carcinogenic and still retains the same coupling capabilities as BOP. PyBOP (1.3eq) and NMM (2eq) were also used to couple **6** to L-proline benzyl ester which afforded the desired product **7** in very high yield (99%) with the same reaction time as BOP (4hr). The high yields, simplicity and reduced toxicity of PyBOP made it a preferred coupling reagent for most of the reactions in this study.

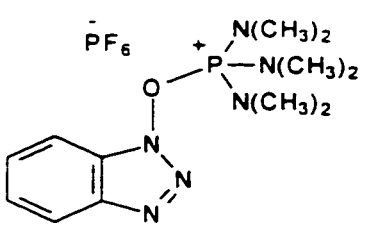

BOP

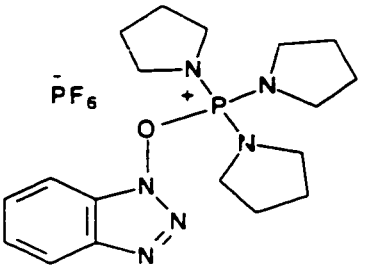

PyBOP

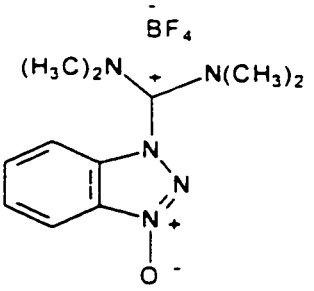

TBTU

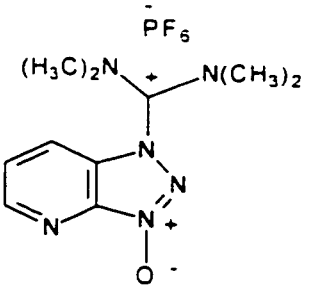

HATU

Figure 2.1.3. Coupling reagents of interest.

The ^{1}H and ^{13}C NMR of **7** was complicated by the presence of rotamers. Initially, it was thought that possibly some β-anomer (or other impurity) might be present. The ^{1}H NMR of compound **7** had three equal singlets for the acetyl groups which is consistent for a single compound. The rotamers were formed upon coupling the protected proline ring to the carboxylic acid of the fucosyl residue resulting in the formation of an amide bond. Amides have partial sp^2 character between the C and N that arises from the contribution of the resonance structure B (Figure 2.1.4.). This causes the geometric and magnetic non-

equivalence of the nitrogen substituents even if these groups are identical (e.g. N,N-dimethlyformamide). There also might be long-range coupling between the N-substituents and the R group directly attached to the carbonyl.[7] The partial planar amide has a large barrier to rotation (13 - 20 kcal/mol)[8] about the C-N bond. These factors lead to a complex NMR that is difficult to interpret and assign.

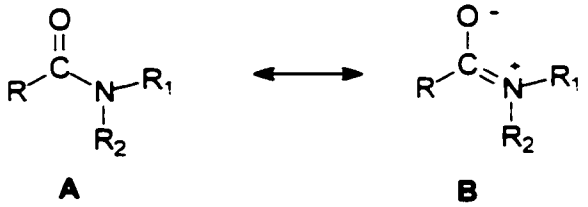

Figure 2.1.4. Resonance structures of amide bond.

To verify that this was indeed the case, a variable temperature ^{1}H NMR experiment was performed on compound **7**. At room temperature the exchange was slow and both rotamers were observed, whereas at high temperatures (<70°C) the exchange was fast and a single resonance was observed on the NMR time scale. The sample was dissolved in DMSO (bp = 189°C) to allow for very high temperatures (if necessary) for coalescence (where the two rotamer peaks become one). The ^{1}H NMR of compound **7** at room temperature can be seen in Figure 2.1.5. and the stacked plot of the variable temperature ^{1}H NMR for compound **7**can be seen in Figure 2.1.6.

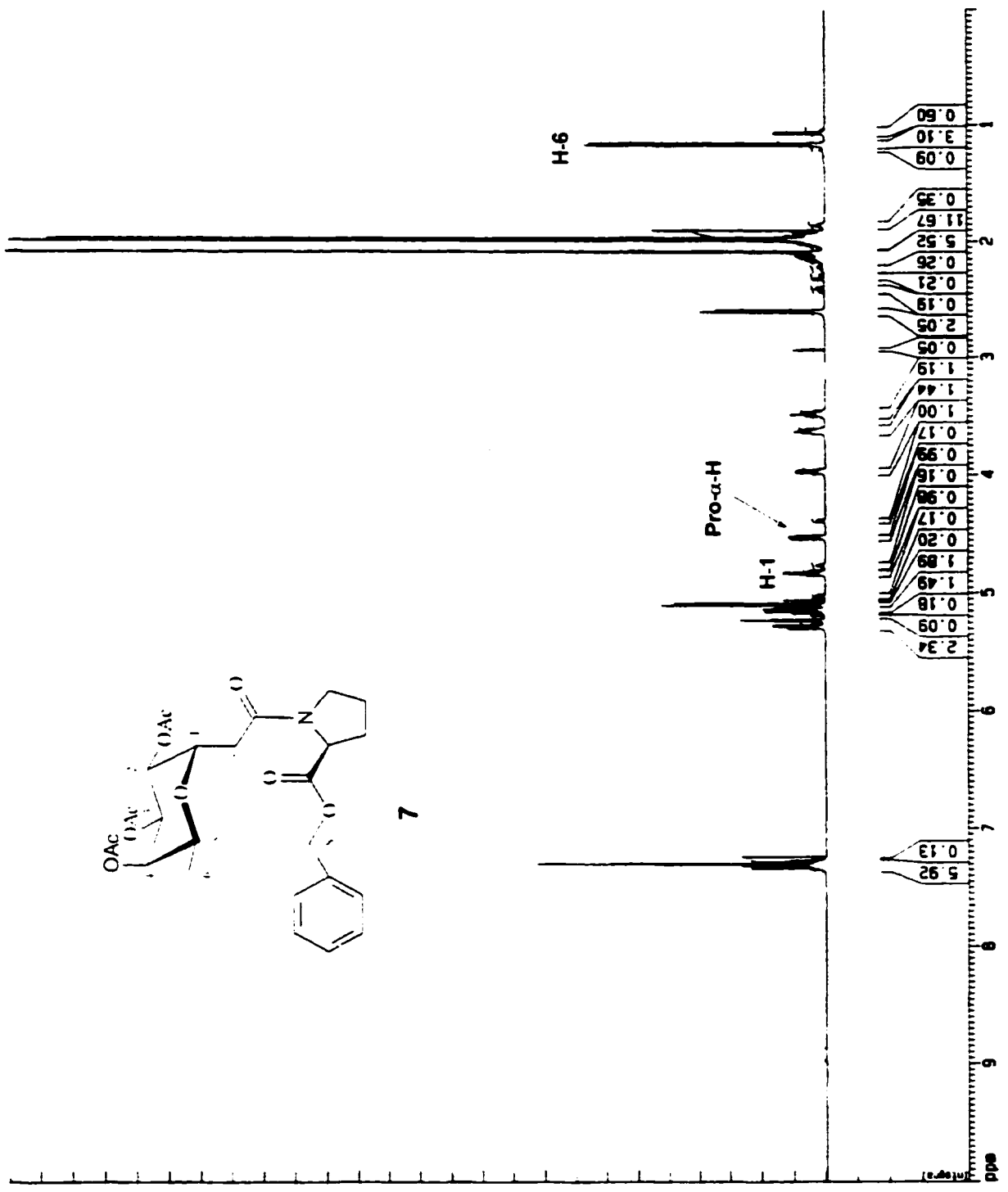

Figure 2.1.5. ^{1}H NMR (500 MHz, $CDCl_3$) of compound **7**.

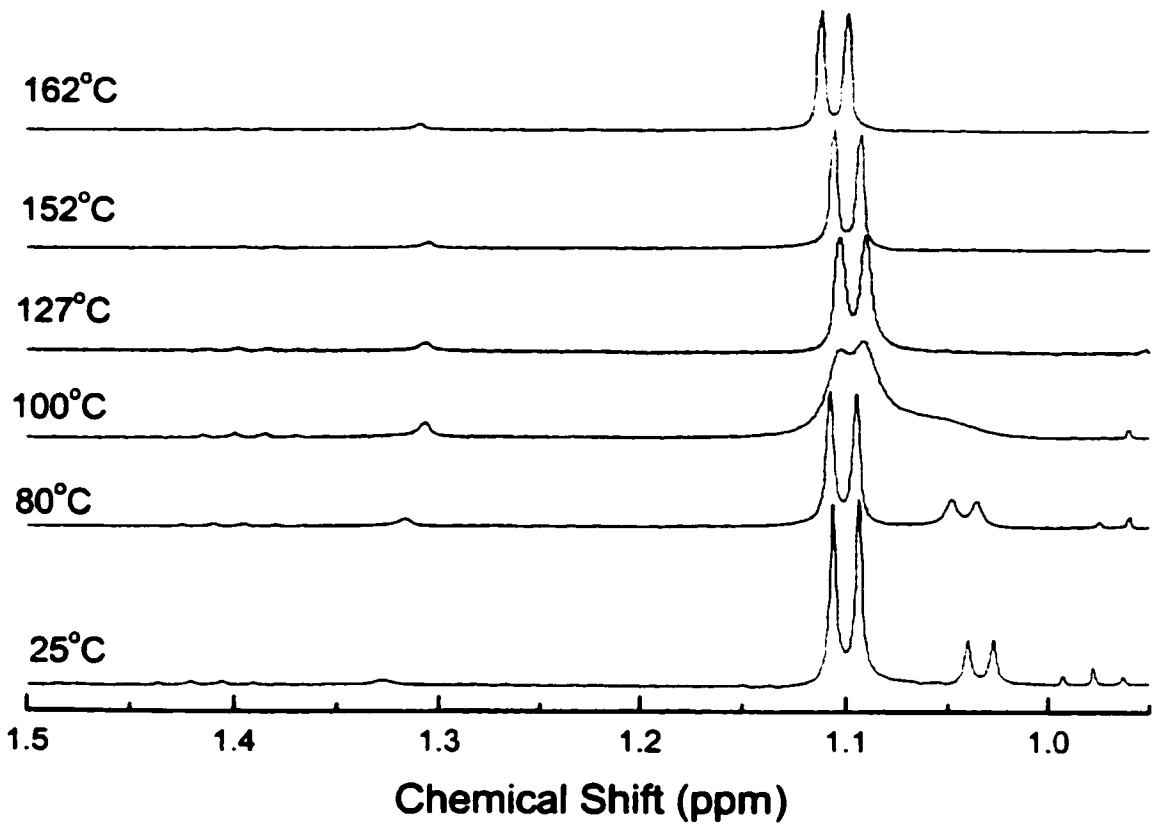

Figure 2.1.6. Typical coalescence of rotamer peaks in variable temperature ^{1}H NMR of compound **7** shown in stacked plot spectra.

At δ 1.1 ppm it is evident from the stacked temperature plot that the H-6 protons of the fucosyl residue coalesced at 127°C. At 152°C most of the peaks due to rotamers coalesced simplifying and broadening the signals present in the ^{1}H NMR spectrum proving the existence of a mixture of rotamers (4:1) in compound **7**. The $\Delta G°$ for the difference in energy of the rotamers was calculated to be +0.84 kcal/mol ($\Delta G° = -RT\ln k_{eq}$) at room temperature. This is in agreement with the literature value for the energy difference of *trans* to *cis* pyrrolidine (Figure 2.1.7) (ca. +2 kcal/mol).[8] The $\Delta G°$ value indicated the

relatively minor difference in energies of the two rotamers implying that effectively there are two possible analogues for the selectin built into one compound. If the rotamer mixture of the mimetic had a high affinity to a selectin, then NMR spectroscopic and/or X-ray crystallographic techniques could be employed to determine which rotamer configuration had the proper bioactive conformation. This information could then be used to design other analogues that would replace the amide bond with other functional groups (e.g. alkenes) that would lock the compound in the bioactive structure.

Debenzylation of **7** to yield the carboxylic acid derivative **8** was achieved by hydrogenation. A slight impurity was present in the crude reaction product and thus purification by silica gel column chromatography was required. In our interest to determine the probable solution conformation of mimetic we decided to deacetylate the α-L-fucosyl-L-proline carboxylic acid derivative **8** to form the deprotected compound **9**. We wanted to investigate the possibility of through-space interactions between the sugar moiety and the proline substituents that would indicate whether the molecule was behaving as a *cis*-proline or *trans*-proline (Figure 2.1.7.).

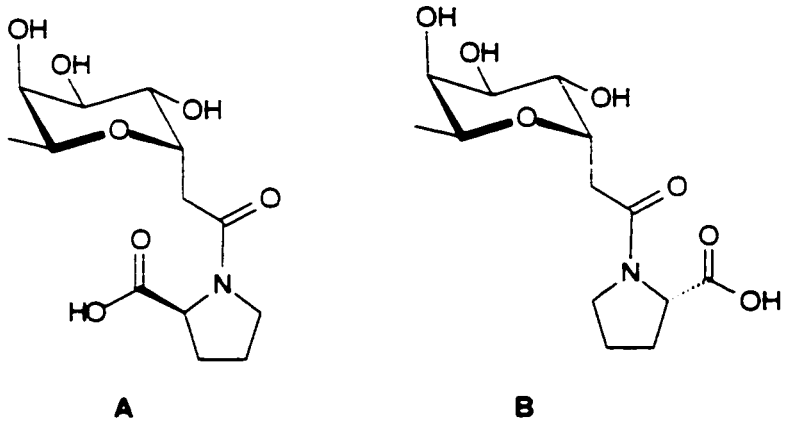

Figure 2.1.7. (a) *Cis*-α-L-fucose-L-proline: (b) *Trans*-α-L-fucose-L-proline.

Two NMR experiments performed on **9** (NOESY and nOe) showed no definitive interactions through-space that would imply a *cis*-proline. It, however, was difficult to separate the protons of interest due to overlapping proton frequencies. A single doublet for the fucosyl methyl group (H-6) was clearly visible and did not show the effect of a corresponding rotamer as it had in compounds **7** and **8**. This may imply that the methyl group of the fucosyl residue is far from the amide rotamers in compound **9**.

The preparation of the acetylated α-L-fucosyl-L-proline carboxylic acid derivative completed one half of the convergent approach. The other half involved synthesizing a peptide isotere (ψ - peptide) backbone that would incorporate the necessary hydroxyl groups of the galactose moiety and an anionic group that would take the place of the sialic acid moiety in approximately the same atom spacing as SLe^x. There are 9 atoms (starting with the anomeric O of the fucosyl residue) in the backbone of SLe^x to the carboxylic acid of the

sialic acid residue (Scheme 2.1.1.). Four of these atoms are represented by the fucosyl-proline residue leaving 5 atoms for the ψ - peptide backbone. The ψ-peptide backbone was synthesized by reacting t-butyl bromoacetate with allylamine to give **10** that was coupled to Fmoc-glycine or Fmoc-β-alanine to afford **11** and **12** respectively. Each peptoid branch was then deprotected to afford **13** and **14** (Scheme 2.1.4.).

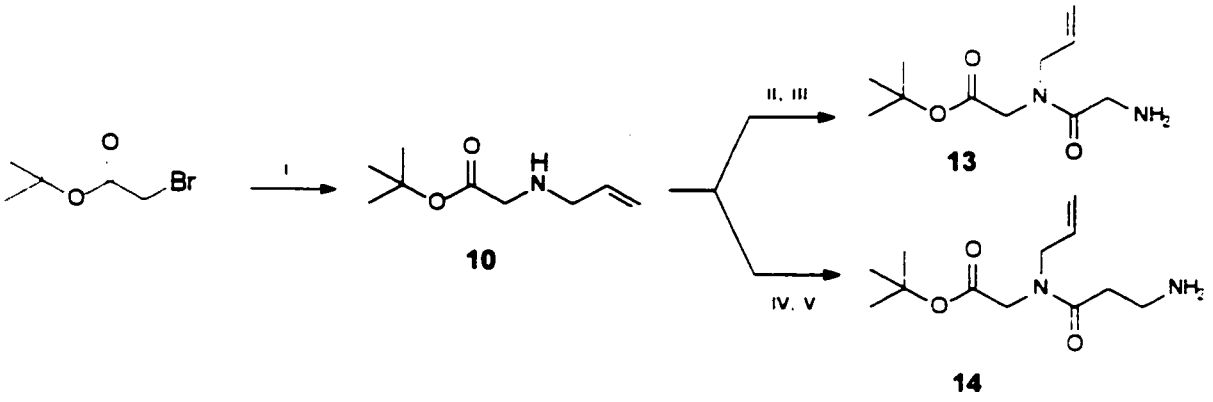

Scheme 2.1.4. Synthesis of SLe^x ψ-peptide backbones. Reagents and conditions: (i) allylamine (1.2eq), DIPEA (1.5eq), CH_3CN, 10min, 0°C, 86%; (ii) Fmoc-glycine (1.2eq), BOP (1.3eq), NMM (2eq), CH_2Cl_2, 6hr, rt, 88%; (iii) 20% piperidine/CH_3CN, 20min, rt, 100%; (iv) Fmoc-β-alanine (1.2eq), PyBOP (1.3eq), NMM (2eq), CH_2Cl_2, 4hr, rt, 99%; (v) 20% piperidine/CH_3CN, 30min, rt, 94%.

Monoalkylation of allylamine using the above procedure (i) could result in poor yields if not properly monitored. The primary amine can easily and quickly become dialkylated losing its capacity for further coupling reactions to extend the backbone chain. In order to reduce the risk of dialkylation, the allylamine was diluted in dioxane and t-butyl bromoacetate diluted in dioxane was slowly added via a dropping funnel. The dropping rate was extremely slow (1 drop every 15s) and thus the reaction took at least 24 hours for completion. As well, it was

difficult to monitor the reaction via TLC as t-butyl bromoacetate was not visible by molybdate, 1% $KmnO_4$ / 2% Na_2CO_3 dip or UV. Therefore, ^1H NMR analysis of the ongoing reaction was required to determine the completion of the reaction. This procedure gave the mono-alkylated product in higher yields. The reaction time, however, was too long and it was too time consuming determining the completion of the reaction via NMR analysis, thus this procedure was abandoned.

The coupling of Fmoc-glycine (ii) and Fmoc-β-alanine (iv) were accomplished using BOP and PyBOP with NMM respectively. As discussed earlier, PyBOP again gave better yields than BOP and had a shorter reaction time. The Fmoc groups of the peptoid branches were easily removed using 20% piperidine in acetonitrile (iii) and (iv). The deprotection of the Fmoc-glycine chain stained as one purple spot with ninhydrin as expected on TLC. However, the deprotection of the Fmoc-β-alanine chain showed two purple spots close together, one being approximately twice as intense as the other. Initially, the minor spot was thought to be an impurity, although 200 MHz NMR analysis of the combined spots gave the correct integration for **14**. One possible explanation for the two spots was that the two peptoid rotamers had a significant enough barrier to rotation to be visible on the time scale of the TLC. This seemed unusual, however, the 500 MHz NMR ^1H and ^{13}C showed evidence of two rotamers (Figure 2.1.8.).

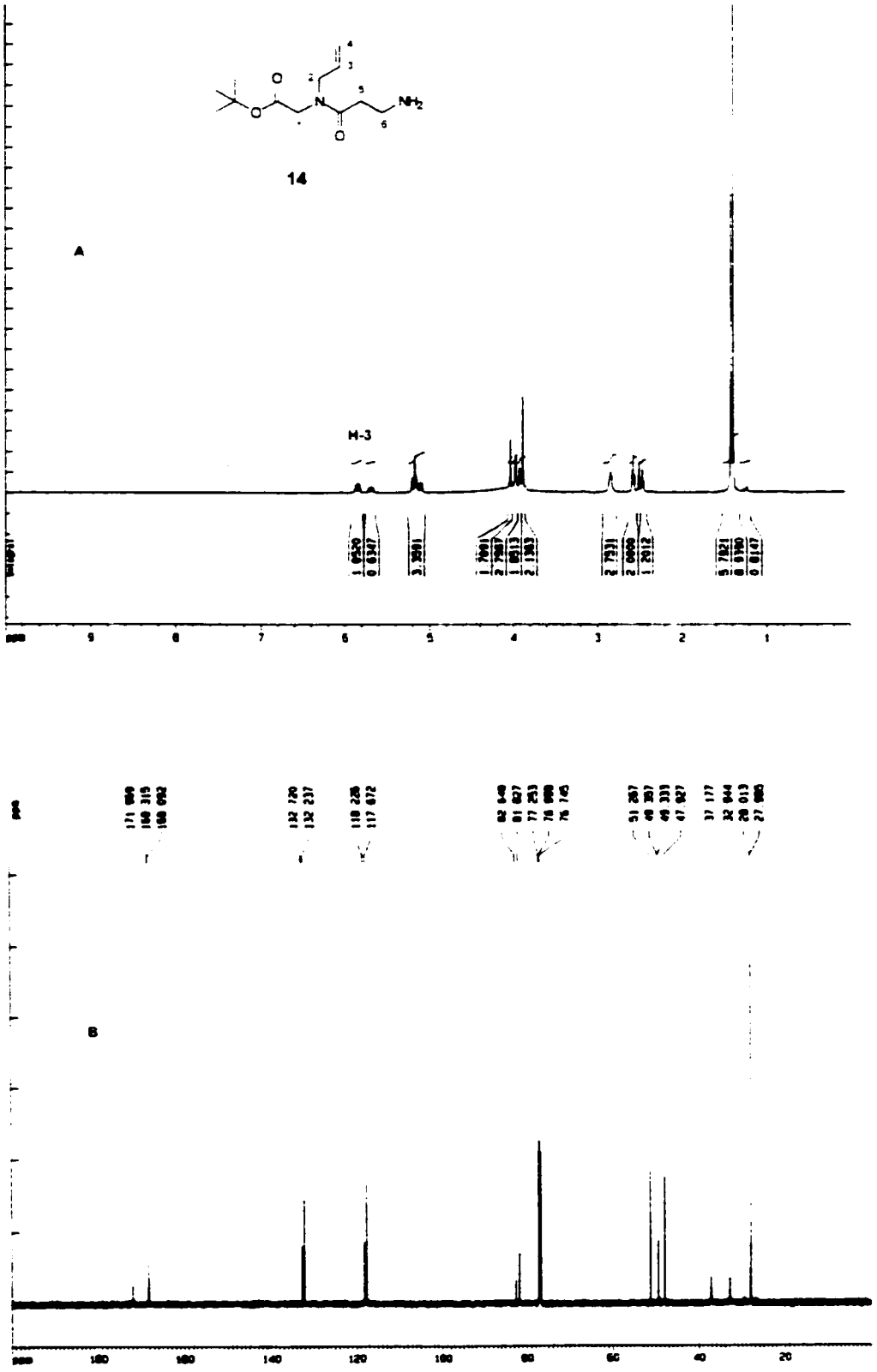

Figure 2.1.8. (a) ^{1}H NMR (500 MHz, $CDCl_3$) of compound **14**; (b) ^{13}C NMR (125.7 MHz, $CDCl_3$) of compound **14**.

A variable temperature ^{1}H NMR experiment was executed to decide if the extra peaks in the proton and carbon spectra were attributable to a rotamer mixture. At δ 5.75 ppm in Figure 2.1.9., it is clear that the H-3 of the alkene in compound **14** coalesces from two peaks at 300 K into one broad peak at 360 K. This result combined with the carbon spectrum showed almost twice the number of peaks expected for this compound. This is consistent with the existence of two rotamers which do not interconvert on the NMR time scale.

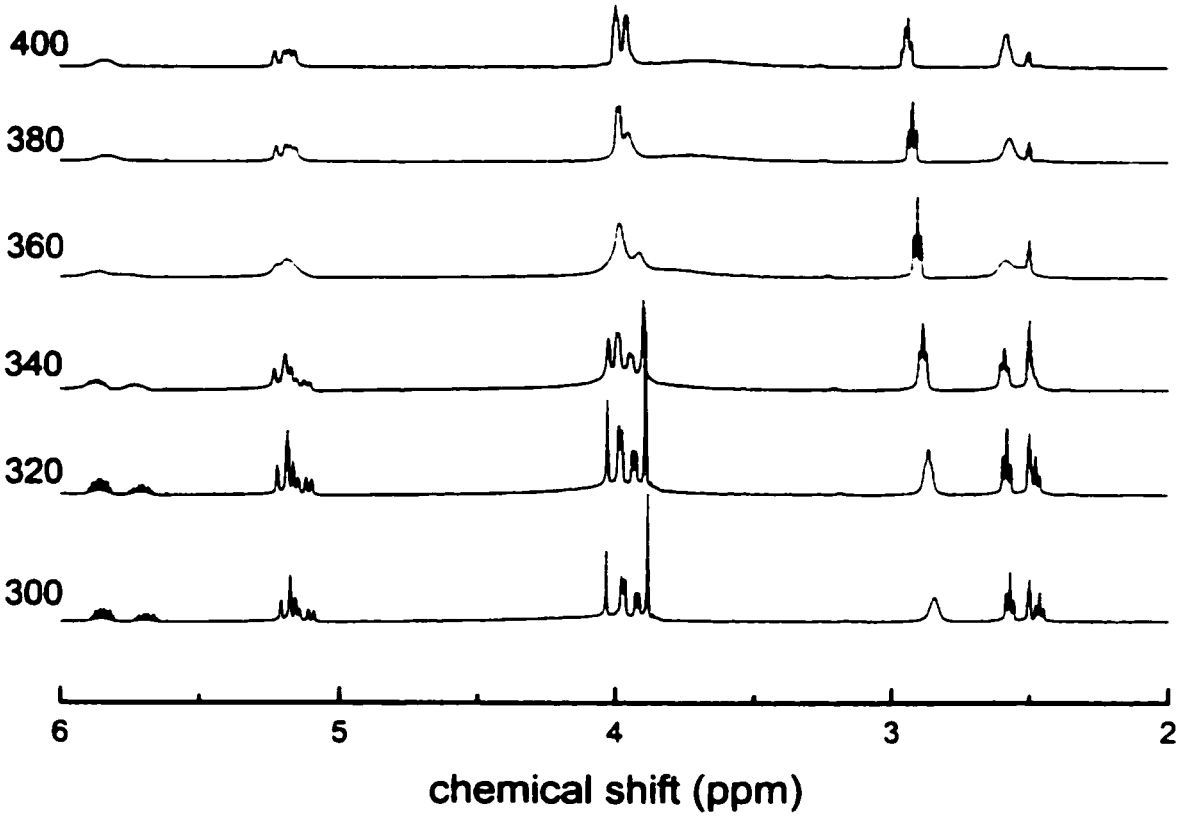

Figure 2.1.9. Variable temperature ^{1}H NMR stacked plot of compound **14**.

Analysis of **13** by 500 MHz NMR spectrometry also showed the presence of two rotamers. It is interesting to note that the ΔG° value for the energy difference of

the *trans* and *cis* conformation of compound **14** was calculated to be +0.47 kcal/mol which is almost half of the ΔG° value for compound **7** (+0.84 kcal/mol). This seems intuitively correct as the rotamer ratio for **14** was approximately 2:1 indicating that the difference between the two conformation minimas is very small and thus closer to equal populations than the rotamers of compound **7** which had a rotamer mixture of 4:1.

Now that the two halves of the mimetic were formed, a coupling reaction was required to connect the two pieces in this convergent approach. The coupling reagent used initially was BOP with NMM as it had performed well with past reactions and was easy to use and purify the crude amide product. Our first attempt was to couple **8** and **13** to form a possible glycomimetic. However, as seen in Scheme 2.1.5., the peptoid branch **13** was ideally suited to couple to itself and form an intramolecular ring **15**.

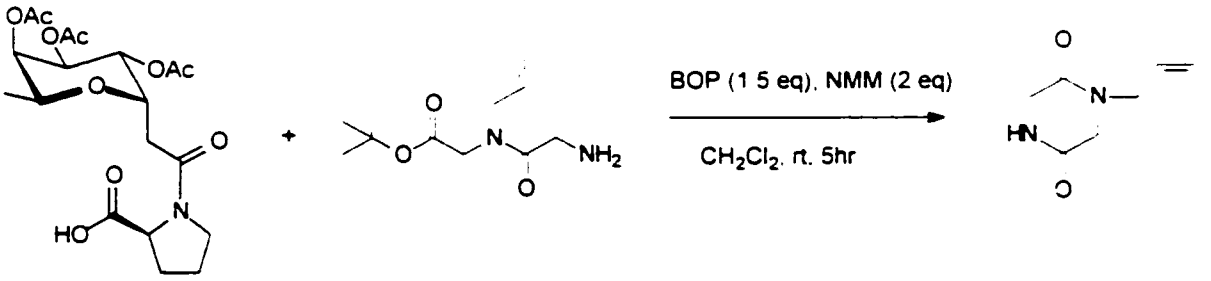

8 13 15

Scheme 2.1.5. Intramolecular ring formation of peptoid branch.

Actually, **13** was able to form an intramolecular ring upon standing for 3-4 hours. Therefore, it was necessary that the coupling reagent react quickly with the substrates in order for the reaction to occur. The similar reactivity of PyBOP to BOP ruled out its candidacy to couple these two segments so a different approach was required (Scheme 2.1.6.).

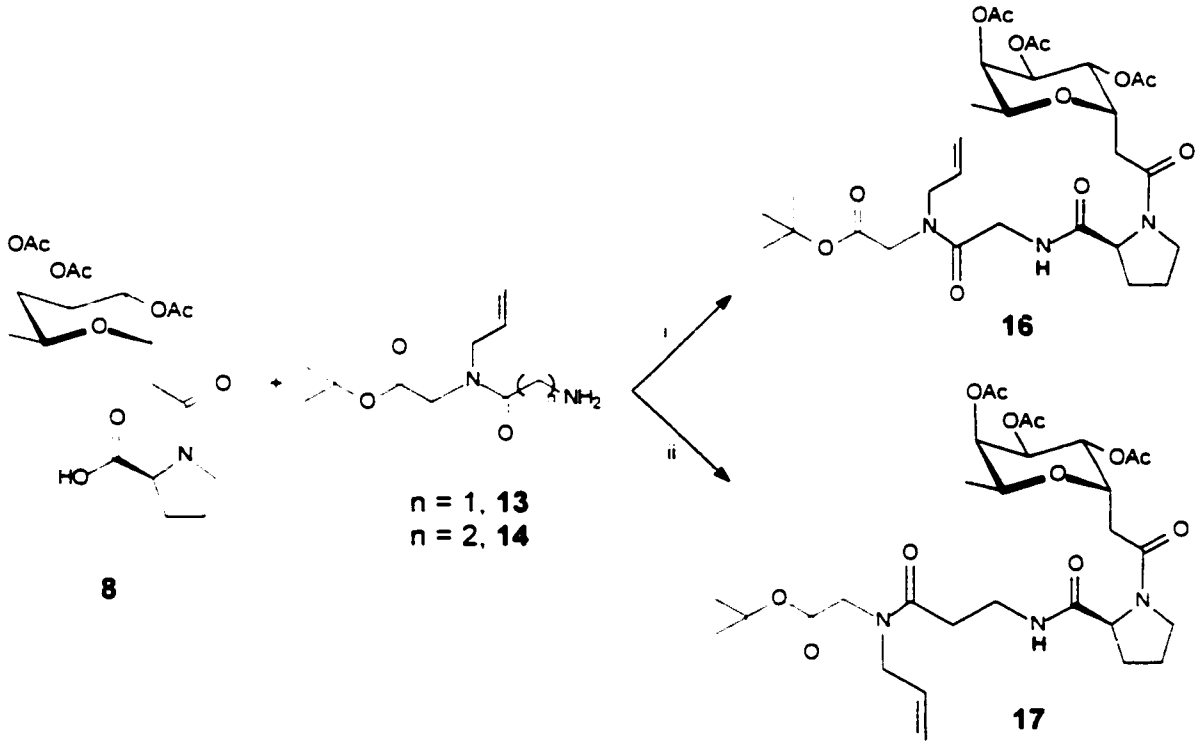

Scheme 2.1.6. Coupling of α-fucosyl-L-proline with ψ-peptide chains **13** and **14**. Reagents and conditions: (i) DCC (1.1eq), N-hydroxysuccinimide (1.05eq), **13** (1.6eq), DIPEA (cat), CH_2Cl_2, 26hr, rt, 82%; (ii) **14** (1.3eq), HATU (1.06eq), DIPEA (3eq), DMF, 2hr, rt, 97%.

The next attempt was to make an activated ester of the carboxylic acid derivative using the coupling reagent DCC and N-hydroxysuccinimide. Once this reaction

was complete, **13** and a catalytic amount of DIPEA were added to the same flask. The activated ester successfully coupled with the free amine of **13** in this one-pot synthesis to give **16** in good yield. The formation of **16** was verified using NMR experiments. The ^{1}H and the ^{13}C spectra both indicated the presence of rotamers which again complicated the NMR analysis (Figure 2.1.10.).

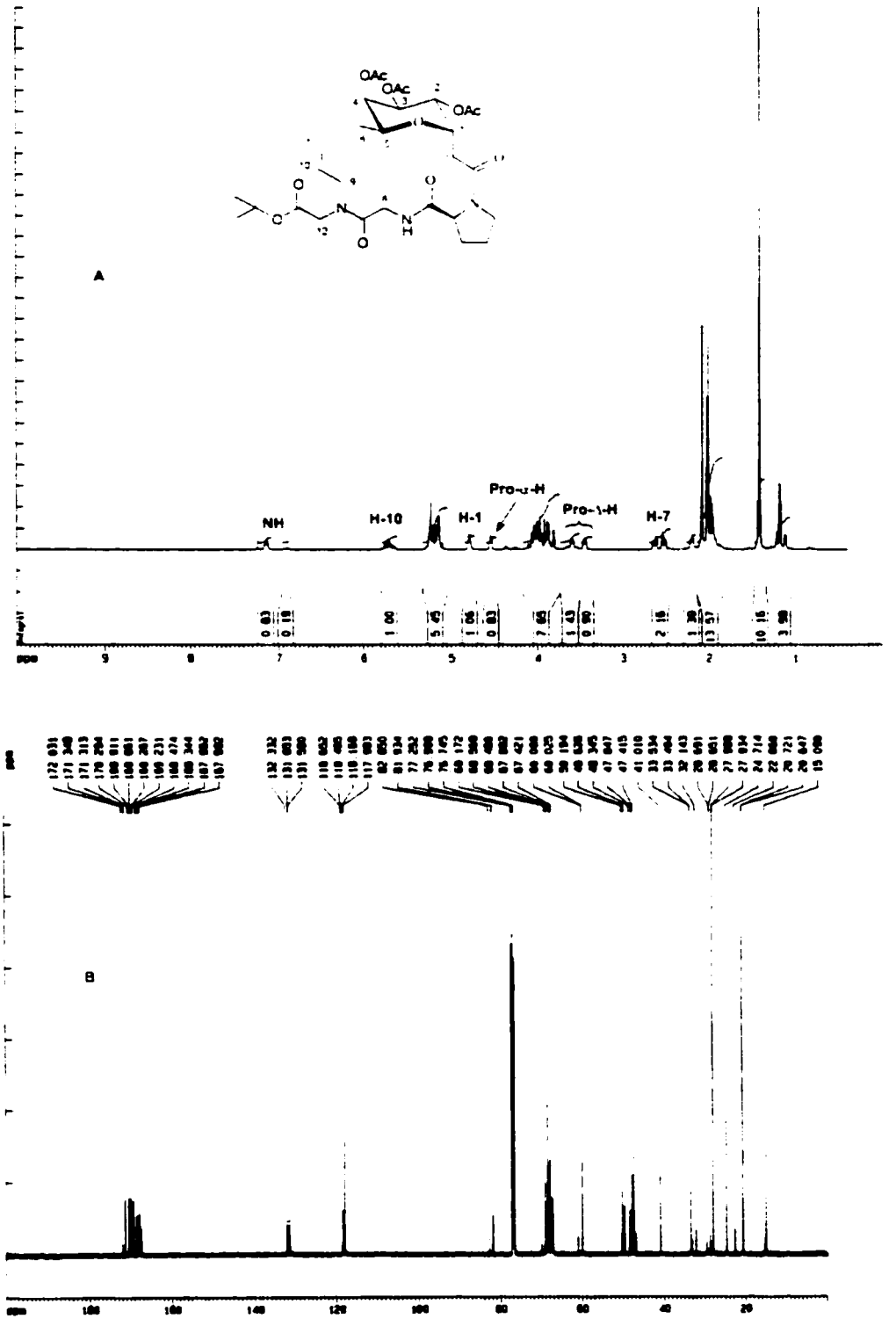

Figure 2.1.10. (a) ^{1}H NMR (500 MHz, $CDCl_3$) of compound **16**; (b) ^{13}C NMR (125.7 MHz, $CDCl_3$) of compound **16**.

Variable temperature NMR experiments were performed which confirmed the presence of rotamers. The key features of compound **16** were evident such as the amide peak at δ 7.13 ppm, the allylic H-10 at δ 5.70 ppm, the proline protons, the anomeric H-1 at δ 4.78 ppm, the acetates and the t-butyl group all having the proper integration confirm the successful synthesis of **16.** This reaction established a convergent synthetic route to other mimetics, however, the reaction time was very long. To solve this problem, we tried the coupling reagent HATU that was proven to have fast reaction times and capable of coupling sterically hindered compounds.[9] Coupling of **8** and **14** appeared to be done almost immediately as seen by TLC. The solution was stirred for an additional 2 hours to ensure that the reaction was complete. NMR analysis confirmed that **17** had been formed and the presence of more than one rotamer made the spectrum quite complicated. Increased yield, simplified procedure and a shorter reaction time was attained using this coupling reagent providing increased practicality to the proposed convergent approach to synthesizing SLe^x mimetics.

2.2.3. Convergent Approach using D-Proline

The chiral centre of the rigid proline ring was employed as an additional point of diversification to give another series of SLe^x mimetics. L-Proline was replaced by D-proline and coupled to the α-L-fucosyl carboxylic acid reside **6** to give **18**. The benzyl ester was removed to give **19** and removal of the acetates afforded the completely deprotected glycomimetic precursor **20** (Scheme 2.1.7.).

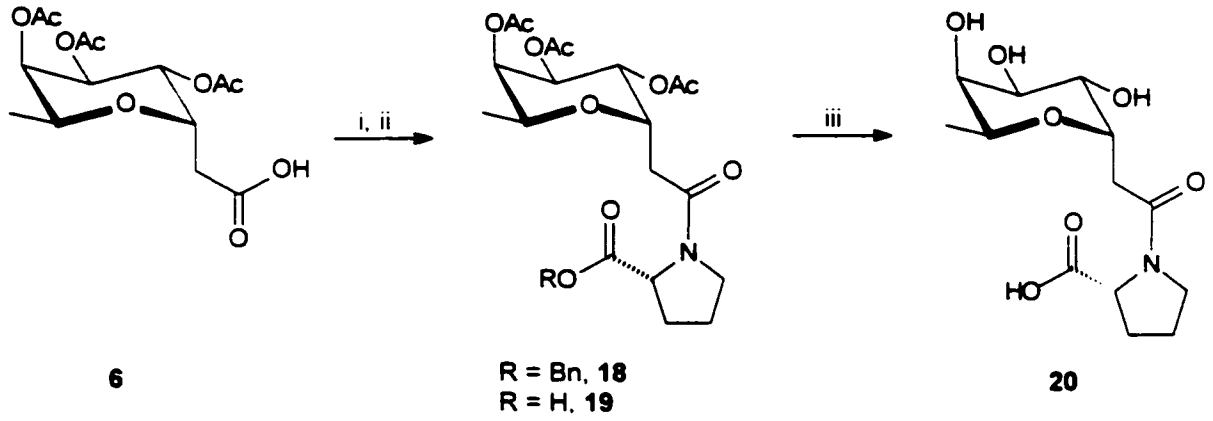

6 R = Bn, **18** R = H, **19** **20**

Scheme 2.1.7. Coupling of **6** with D-proline benzyl ester to form **18** followed by sequential deprotections. Reagents and conditions: (i) D-Pro-OBn (1.2eq), PyBOP (1.2eq), NMM (2eq), CH_2Cl_2, 4hr, rt, 96%; (ii) H_2,10% Pd/C, MeOH, 30min, 100%; (iii) 1N NaOMe, MeOH, rt, 2hr, 100%.

The above procedures were similar to the L-proline series except that the debenzylation of **18** afforded product **19** without need for additional purification. The fully deprotected glycopeptide **20** was also analyzed for solution conformation using NMR techniques and found not to have any unexpected through-space bond interactions. The doublet of the H-6 fucosyl protons (Figure 2.1.11.) was clearly visible and did not show corresponding peaks attributed to the presence of rotamers as it had in compounds **18** and **19**. This may imply that the fucosyl methyl group was not near the amide bond.

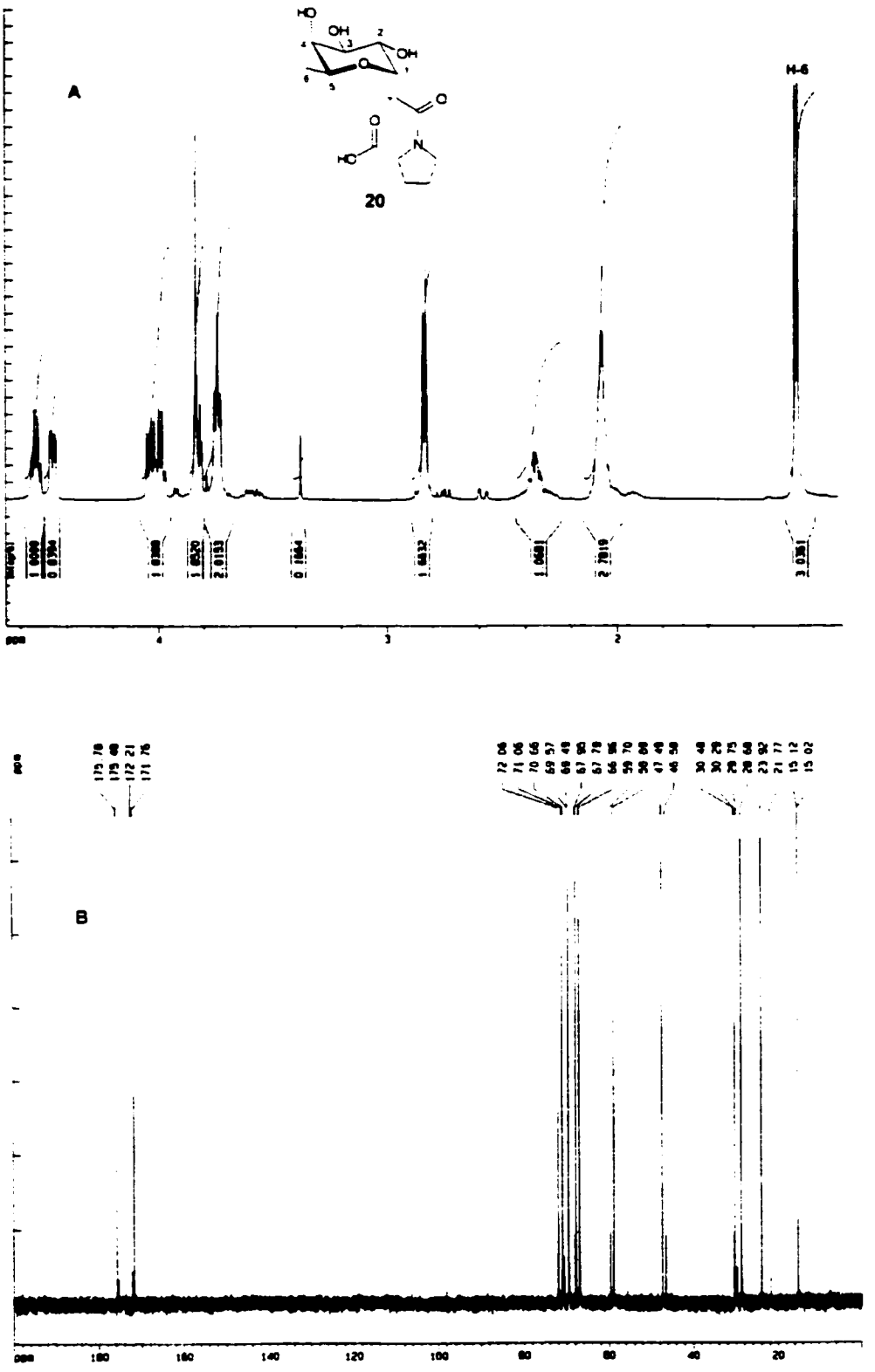

Figure 2.1.11. (a) ^{1}H NMR (500 MHz, $CDCl_3$) of compound **20**; (b) ^{13}C NMR (125.7 MHz, $CDCl_3$) of compound **20**.

Compound **19** was coupled to the peptoid backbones **13** and **14** to afford **21** and **22** respectively (Scheme 2.1.8.).

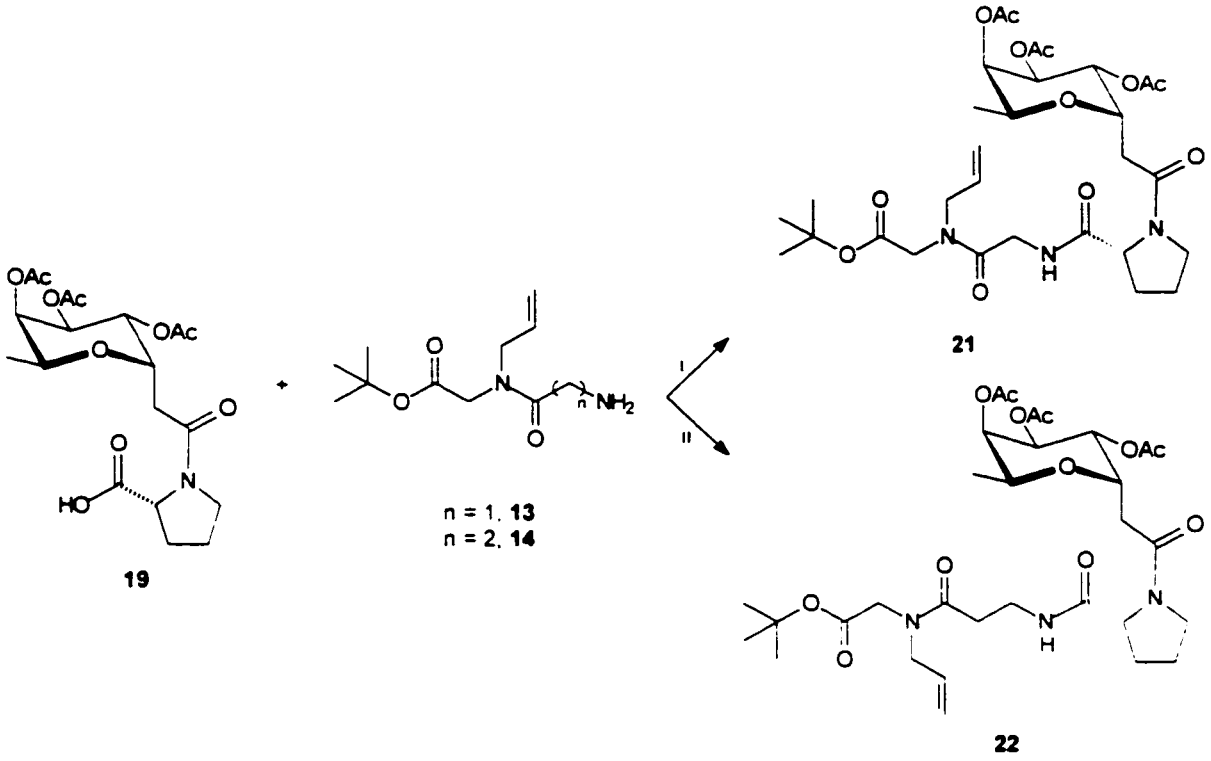

Scheme 2.1.8. Coupling of α-fucosyl-D-proline with ψ-peptide chains **13** and **14**. Reagents and conditions: (i) **13** (1.2eq), HATU (1.05eq), DIPEA (3eq), DMF, 18hr, rt, 65%; (ii) **14** (1.3eq), HATU (1.06 eq), DIPEA (3eq), DMF, 2hr, rt, 97%.

Compound **21** was obtained with a lower yield than the other HATU reactions as this was the initial trial of the HATU reagent. Subsequent HATU coupling reactions were optimized by adding additional equivalents of the free amine and the coupling reagent. The ^{1}H NMR showed a mixture of rotamers that had the chemical shifts of all the important groups which confirmed the formation of products **21** and **22** (Figure 2.1.12.).

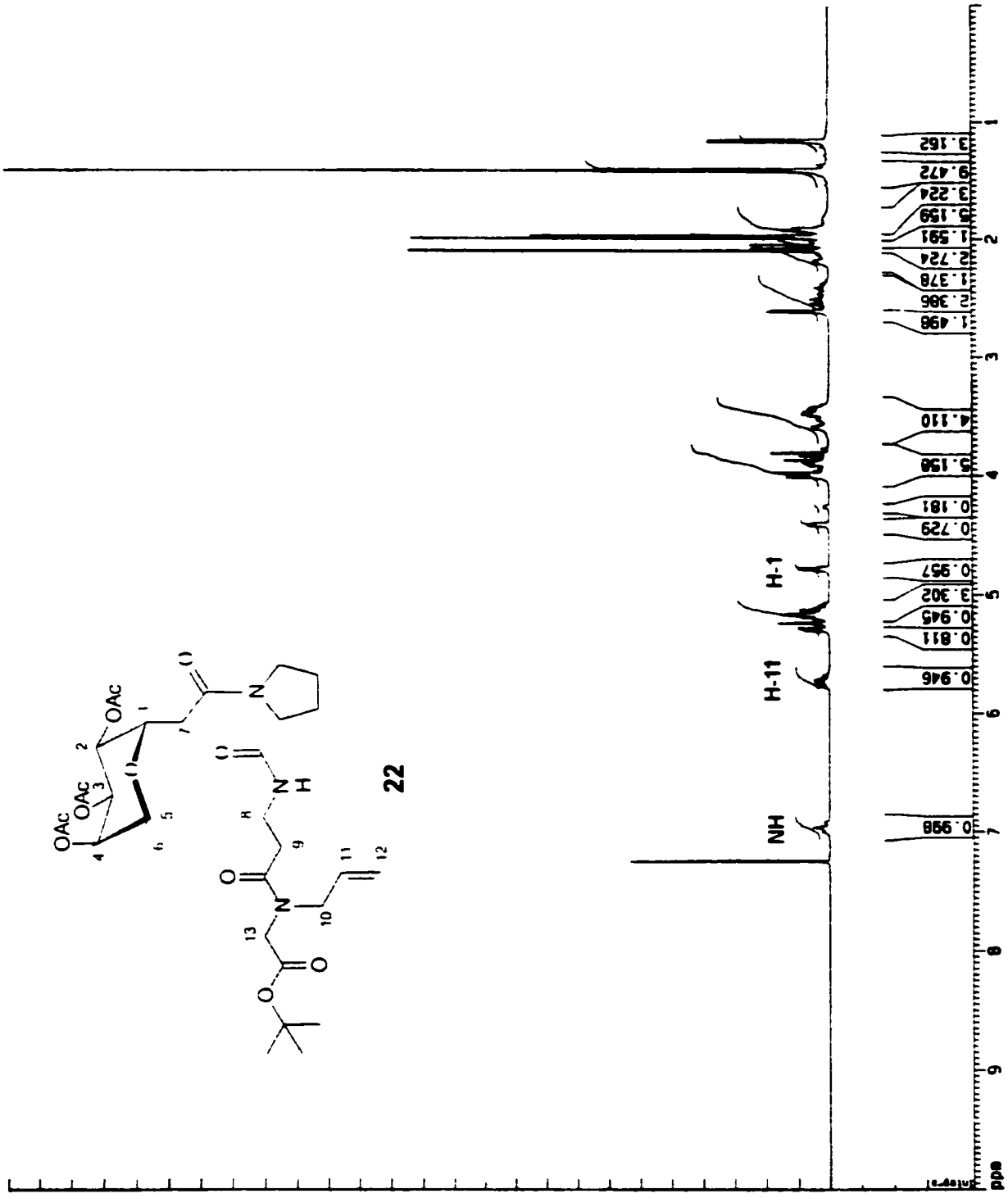

Figure 2.1.12. ^{1}H NMR (500 MHz, $CDCl_3$) of compound **22**.

Unfortunately, there was only sufficient time to transform one of the four convergent mimetic precursors into its mimetic and the α-L-fucosyl-D-proline-β-alaninyl derivative **22** appeared to be the most promising from preliminary molecular modelling analysis. The α-L-fucosyl-D-proline-β-alaninyl derivative mimicked the necessary Fuc-α-1,3-GlcNAc moiety and provided the proper atom spacing for placing the essential hydroxyl groups of the Gal moiety on the functionalizable alkene. Hydroxylation of the alkene was successfully achieved using a catalytic amount of osmium tetroxide and NMO to form **23** (Scheme 2.1.9.).

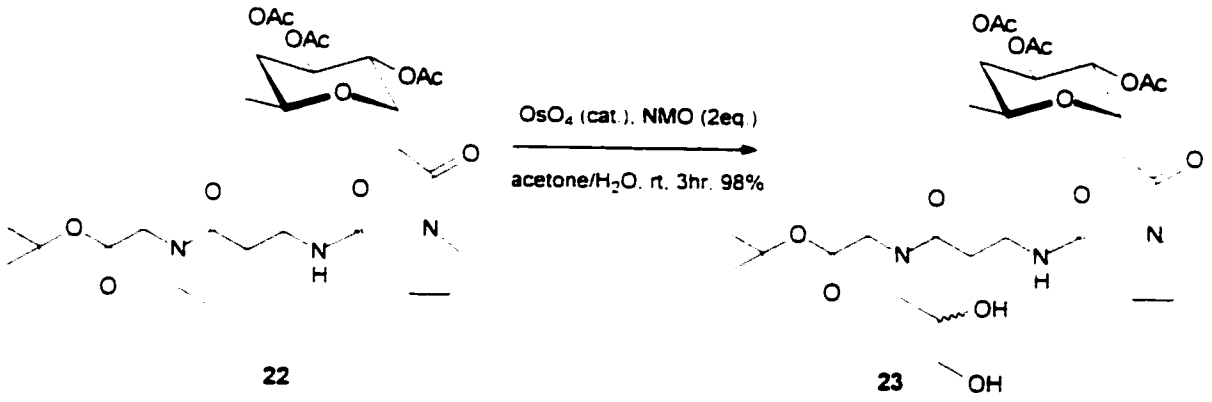

Scheme 2.1.9. Catalytic hydroxylation of **22** to form SLe^x mimetic precursor **23**.

The Sharpless AD-mix-α was initially used to stereoselectively hydroxylate the alkene functionality. However, TLC analysis revealed many spots present in the mixture and thus the product was discarded. A simplified and reliable

approach using a catalytic amount of osmium tetroxide was tested and gave good yields of the desired compound **23**. Unfortunately, the presence of multiple rotamers masked the diastereomeric ratio of this reaction. The disappearance of the allylic proton H-11 at δ 5.73 ppm and the decreased integration and simplification of the peaks around δ 5.2 ppm indicated the absence of the double bond (Figure 2.1.13.). The detection of the molecular ion by ESI-MS gave further evidence of the formation of the hydroxylated compound **23**.

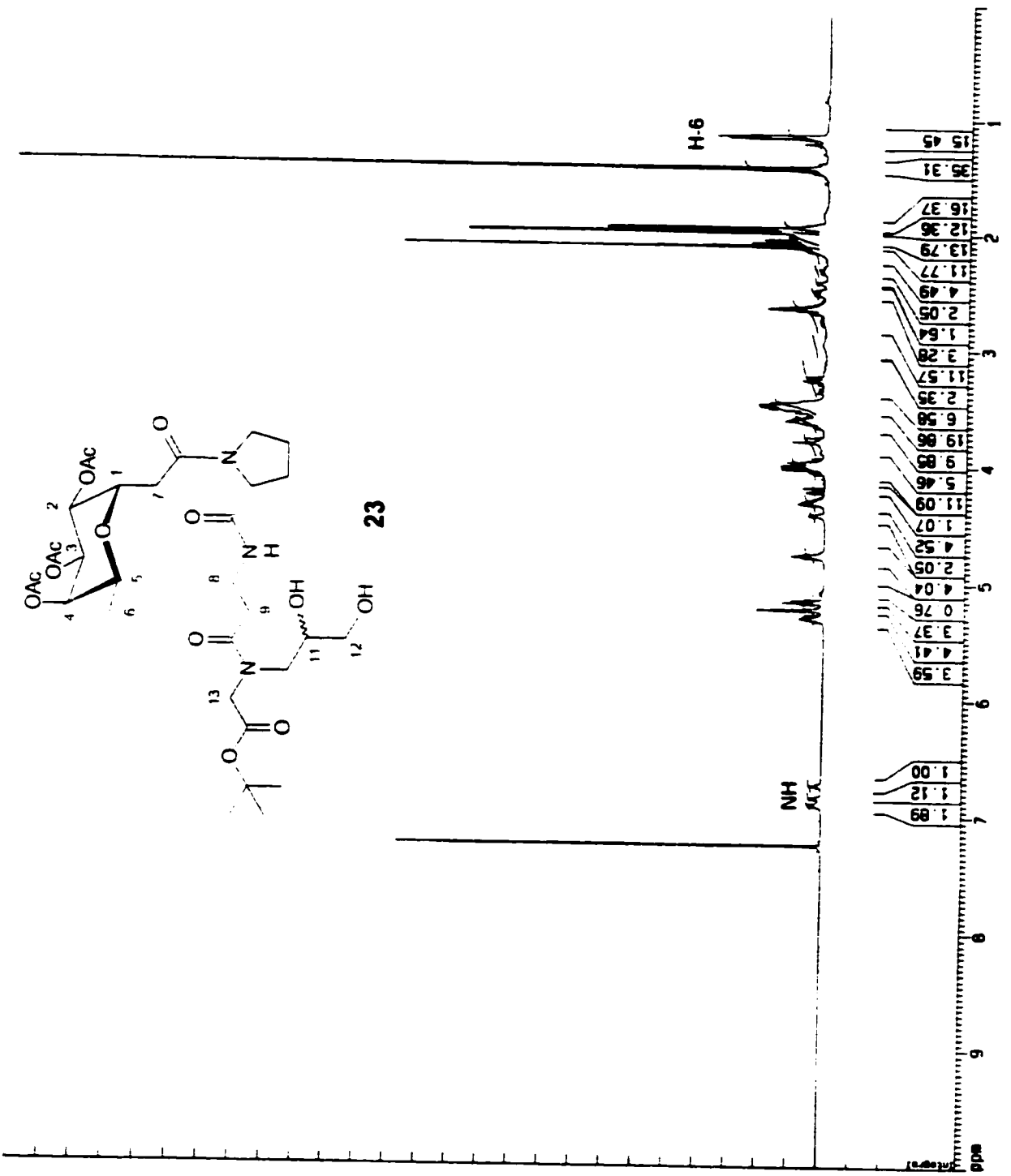

Figure 2.1.13. ^{1}H NMR (500 MHz, $CDCl_3$) of compound **23**.

The removal of the t-butyl ester protecting group was accomplished with 10% TFA in dichloromethane at room temperature in 30 minutes to yield two products (Scheme 2.1.10.).

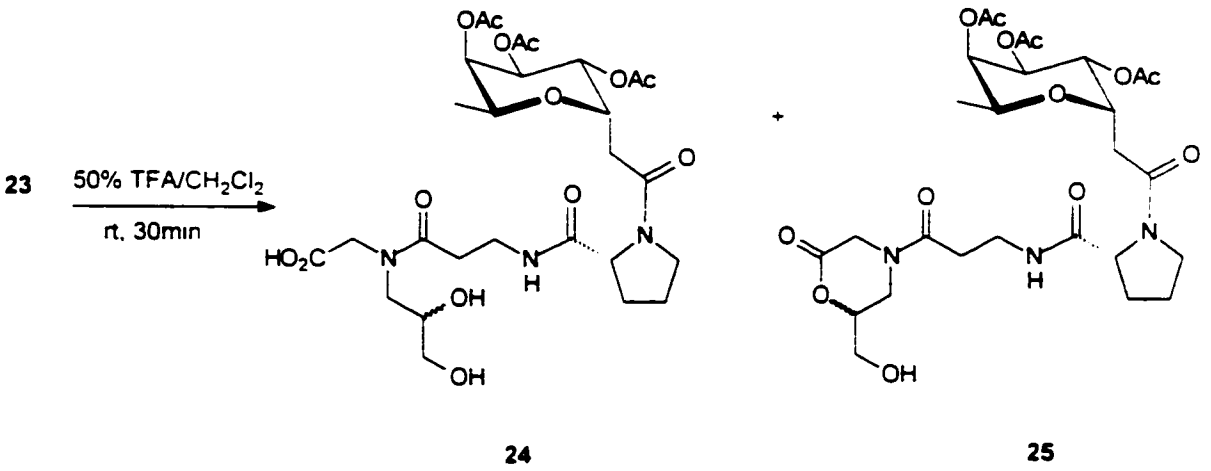

Scheme 2.1.10. Deprotection of ψ-peptide backbone to form compounds **24** and **25**

The lactonization of **23** in the presence of acid was expected and unavoidable. In order to achieve the proper atomic spacing for the carboxylic group and hydroxyl groups of the mimetic, the secondary hydroxyl was unfortunately positioned to form a thermodynamically stable six-membered ring. TLC analysis showed the presence of one major and one minor spot. Mass spectral analysis of the crude product showed the presence of both molecular ions. The major spot had a higher Rf value and was purified by silica gel column chromatography. The ESI-MS of this product only showed the molecular ion of the unwanted lactonized derivative **25**. Another deprotection of **23** under the

same conditions gave the expected mixture of products in approximately the same proportion, however, this time the products were not separated. The crude mixture residue was dissolved in methanol and a modified Zemplén reaction removed the acetyl protecting groups and opened up the lactone ring in a one-pot synthesis yielding a mixture of four rotamers. (Scheme 2.1.11.).

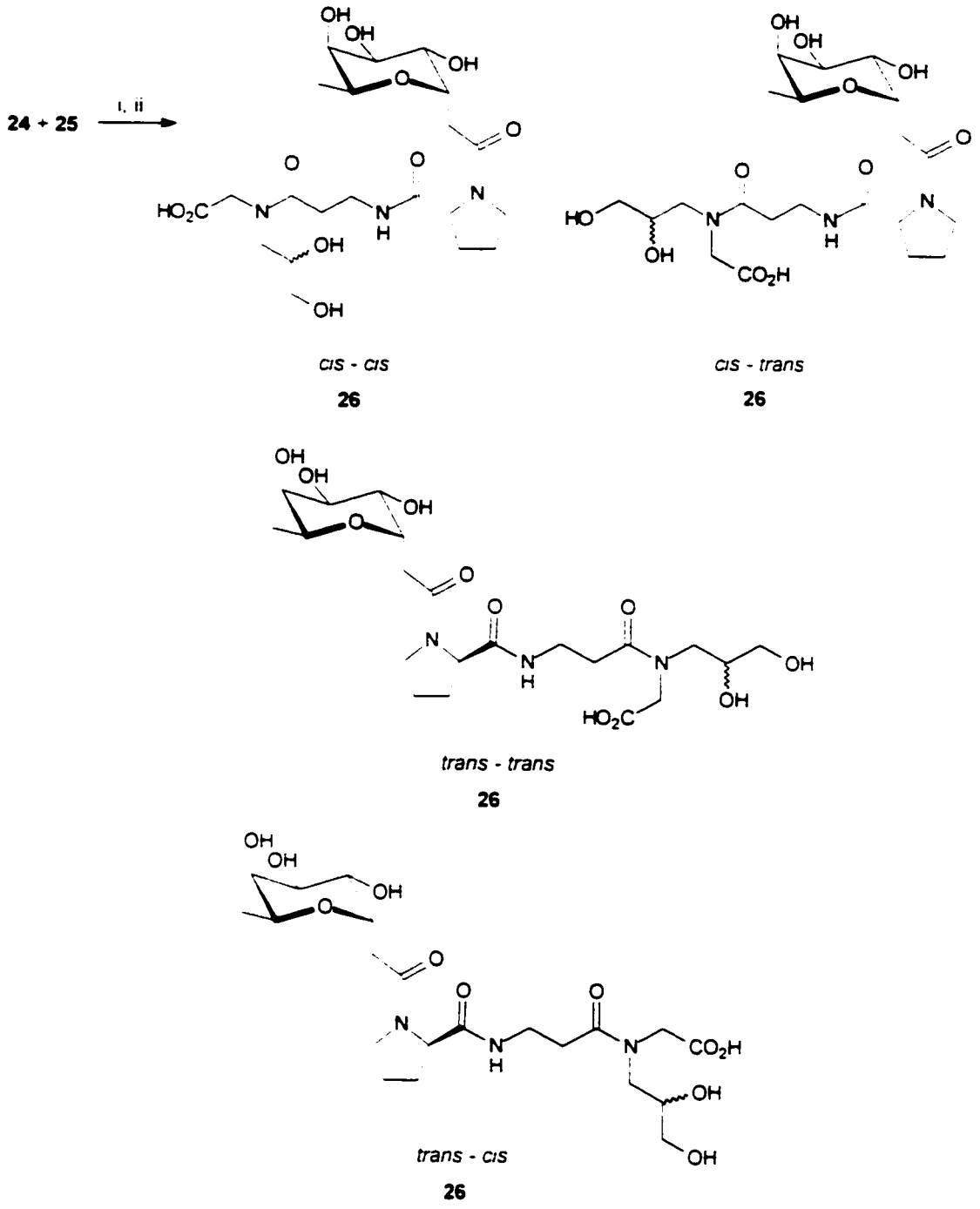

Scheme 2.1.11. Modified Zemplén to form the SLe^x mimetic **26**. Reagents and conditions: (i) 0.1M NaOMe, MeOH, rt, 1hr; (ii) 0.01M NaOH, MeOH, rt, 1hr, 100%.

The overall yield of SLe^x glycomimetic **26** was 52% which is quite high considering it is a 12-step synthesis. This equates to an average yield of 95% per reaction. Almost half of the reactions in this synthetic route were quantitative protection and deprotection steps.

Compound **26** incorporates all the necessary features of a simple and stable SLe^x mimetic that could potentially have stronger selectin binding affinities than the natural SLe^x ligand. It has a tri-hydroxylated fucosyl residue connected through an enzyme-resistant α-carbon that is linked to a rigidifying proline ring mimicking the Fuc and GlcNAc portion of SLe^x. The hydroxyl groups representing those of the Gal moiety are present on the ψ - peptide branch and the carboxylic acid replaces the sialic acid fragment of the natural ligand. This convergent synthetic pathway affords ample opportunities to diversify the rigidifying group and the length of the peptide backbone. It also provides a site for functional group manipulation at the double bond. This alkene can be converted into many different groups such as a mono-hydroxylated branch, an aldehyde, an epoxide, or a carboxylic acid, which could have potential to increase the SLe^x-selectin interactions.

The formation of glycomimetic **26** was confirmed by the absence of the t-butyl and acetate groups, the approximate integration of the ^1H spectrum (Figure 2.1.14.) and the presence of the molecular ion in a positive ESI-MS and negative ESI-MS.

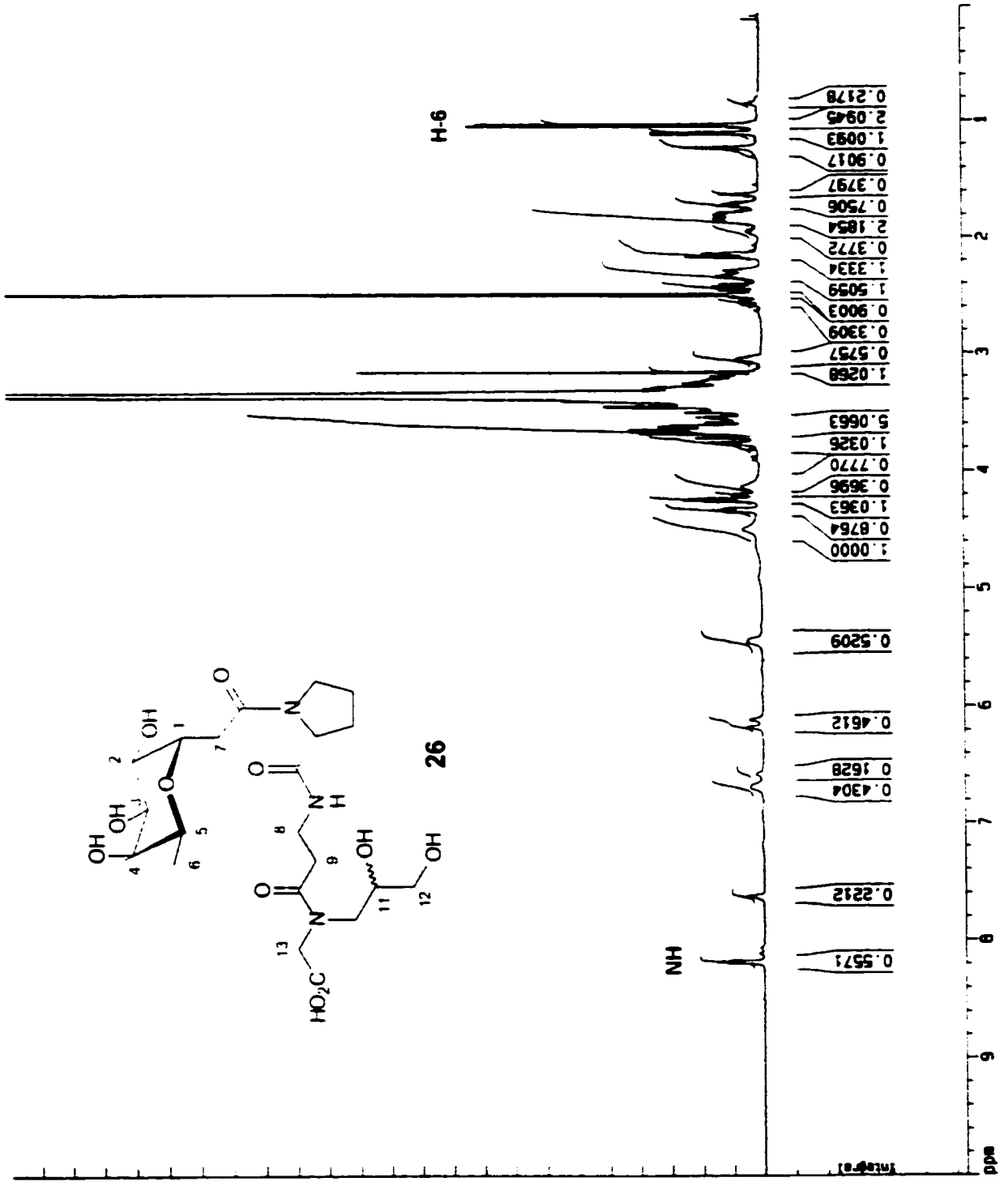

Figure 2.1.14. ^{1}H NMR (500 MHz, $CDCl_3$) of compound **26**.

The peaks for the hydroxyl groups were visible this time in the ^{1}H NMR spectrum and were confirmed by deuterium exchange in DMSO. The two signals of the fucosyl methyl group indicated that there were rotamers at room temperature in the ratio of 2:1 when DMSO is used as a solvent. This implies that the methyl group is relatively close to the amide bond and suggests that the unprotected molecule could be adopting a *cis*-proline, hair-pin configuration, as it does in the bioactive conformation of SLe^x. NOESY and nOe experiments were done on compound **26** but the results were uninterpretable due to the presence of water inherently present in DMSO. An additional variable temperature NMR experiment confirmed the presence of rotamers (Figure 2.1.15.).

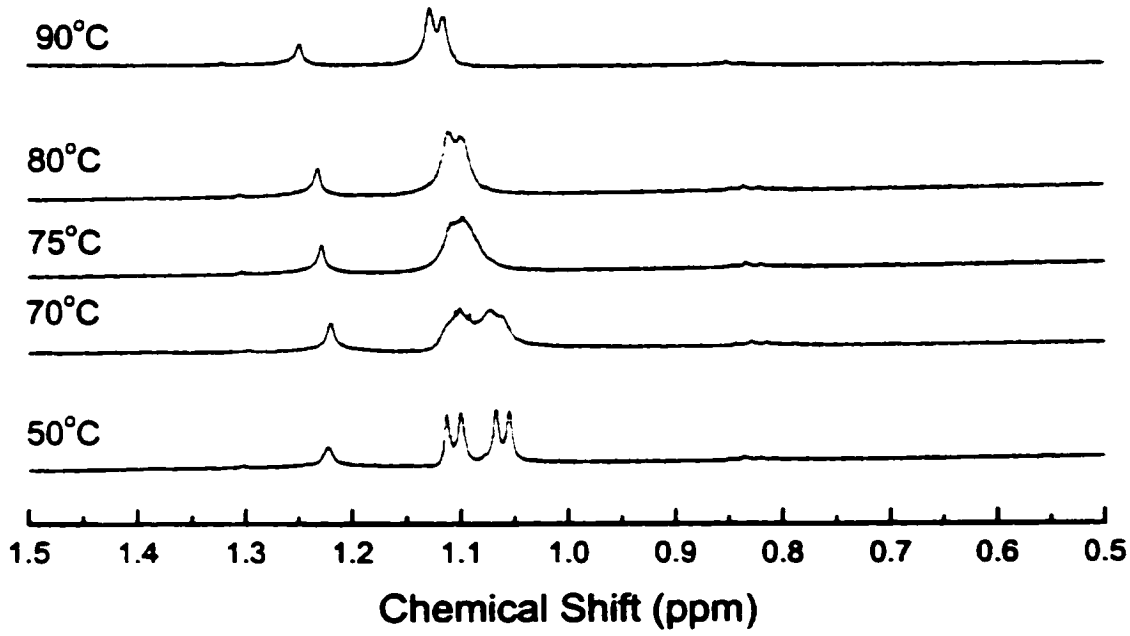

Figure 2.1.15. Variable temperature ^{1}H NMR stacked plot of compound **26**.

The population of the two major rotamers were approximately equal at 50°C using the methyl signals at δ 1.1 ppm as probes. These populations correlate with the relatively low $\Delta G°$ value (0.41 kcal/mol) at room temperature. The fucosyl methyl signals coalesced at 75°C (+/- 2°C). The energy of activation of the amide bond rotation in the glycomimetic **26** was determined using this coalescence value. It was calculated to be +17.5 kcal/mol using the equation $E_a = 2.3RT_c[10.32 + \log(T_c/\pi\Delta\nu/\sqrt{2})]$. This can be compared to the energy of activation for a typical amide bond (E_a = +21 kcal/mol for N,N-dimethylformamide).[8] The possible through-space interaction between the carbohydrate moiety and the ψ - peptide backbone of **26** prompted an interest in modelling this compound using computational software and comparing it to the proposed bioactive solution conformer of SLe^x.

2.2.4. Molecular Modelling

The conformation of oligosaccharides can be defined by the dihedral angles of the glycosidic linkage formed between the anomeric centre of one sugar and hydroxyl of another sugar. The conformational properties of glycosidic bonds are important determinants in the overall configuration of the oligosaccharide. The glycosidic dihedral angles are defined by two torsional angles ϕ and ψ. In a 1-4 linkage the ϕ dihedral angle is defined as H_1-C_1-O_1-C_4 and the ψ dihedral angle is defined as C_1-O_1-C_4-H_4. An example of one set of SLe^x dihedral angles is labelled in Figure 2.1.16.[10]

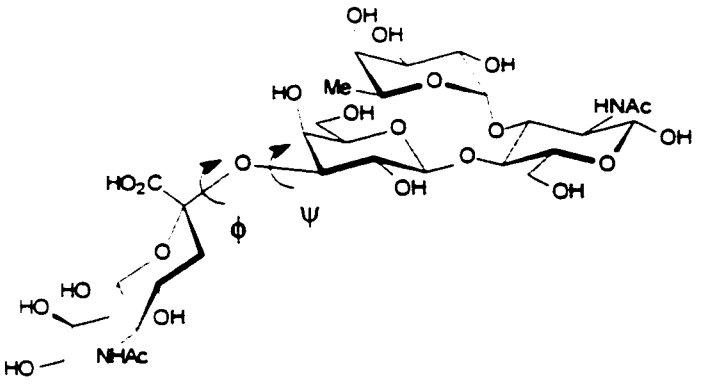

SLe^x

Figure 2.1.16. Dihedral angles ϕ and ψ of sialic acid-galactose glycosidic linkage.

Table 2.1.1. Glycosidic torsion angles of the bioactive conformation of SLe^x.[11]

NeuAc-Gal	Gal-GlcNAc	Fuc-GlcNAc
ϕ /ψ	ϕ /ψ	ϕ /ψ
-43° / -12°	+45°/ +19°	+29°/ +41°

Using the torsion angle values of Table 2.1.1., the 3-D model of the bioactive form of SLe^x bound to E-selectin was modelled using CAChe computational software and the P-selectin bound conformation was modelled using the calculations of the full relaxation matrix analysis of transferred-nOe spectra (Figure 2.1.17.).[12]

a)

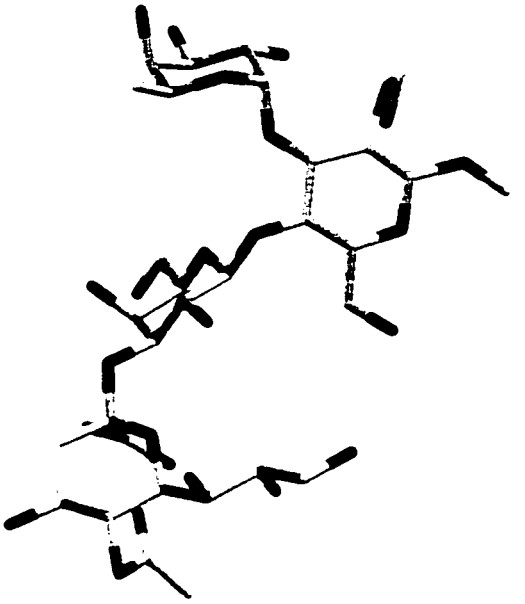

b)

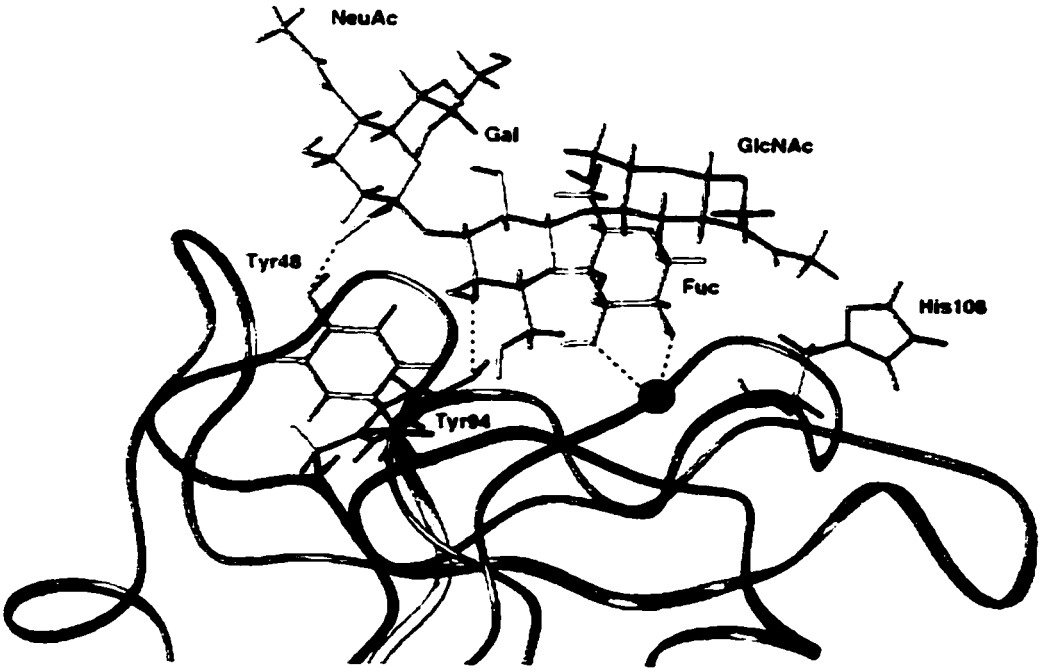

Figure 2.1.17. (a) Three-dimensional computer generated molecular model of bound SLe^x using CAChe (b) NMR solution conformation of possible alignment of SLe^x with P-selectin.

Preliminary modelling of mimetic **26** had some promising results. The distance from the α-L-fucosyl-anomeric oxygen to the carboxylate group is 9Å in the SLe^x bioactive form which corresponds precisely with the distance of a local minimum of the glycomimetic **26** from the α-fucosyl-anomeric-carbon to the carboxylic acid group. The global minimum is not necessarily the bioactive form of the oligosaccharide as there are many examples of compounds that have binding conformations significantly different from their lowest energy conformation.[13] The difference in the energy barrier for a local minimum, compared to the global minimum, is often low and easily overcome if it has the proper binding conformation for a protein. Therefore, further refinement of the molecular model of SLe^x mimetic **26** is required to definitively determine which of the local minima best mimic the bioactive conformation of SLe^x.

2.3. Conclusions

It is evident that the high overall yield and the numerous options for diversity allow this convergent synthesis to be a viable route to construct series of glycomimetics. The knowledge gained from the solution chemistry can be applied to solid-phase chemistry to manufacture libraries of glycopeptides in search of stable, high affinity, simplistic selectin antagonists. As well, the development of chemoenzymatic and enzymatic one-pot programmable syntheses has the potential to develop toward automated glycomimetic assembly.[14]

As the accessibility of carbohydrates and glycomimetics increases, the context of the research has expanded to include new ideas and designs for anti-inflammatory drugs. Future work has begun to target other key steps in the inflammation cascade. For example, the disruption of the sulfation[15] and biosynthethic[16] pathways of SLe^x, as well as, the inhibition of signal transduction leading to the expression of selectins and/or extravasation[17], and rolling.[18] The combination of these strategies and the continued crusade to understand the complex cell surface interactions is destined to direct the design of highly selective, extremely potent carbohydrate-based inhibitors. These inhibitors could eventually take the form of 'sugar-loaded', 'sugar-coated' pills for the treatment of asthma, arthritis, strokes, heart attack recovery and even cancer.[19]

2.4. Experimental Methods

2.4.1. General Methods

^1H NMR and ^{13}C NMR spectra were obtained on Brüker AMX500, Brüker Avance 300 or Varian Gemini 200 instruments at 500, 300 and 200 MHz for protons and 125.7, 75.4 and 50.3 MHz for carbons, respectively. Proton chemical shifts (δ) are relative to internal standard deuterated chloroform ($CDCl_3$) at δ 7.24 ppm, methanol (CD_3OD) at δ 4.87 ppm and δ 3.31 ppm or toluene (C_7D_8) at δ 7.09 ppm, δ 7.00 ppm, δ 6.98 ppm and δ 2.09 ppm. Carbon chemical shifts are given relative to internal standard $CDCl_3$ at δ 77.0 ppm. CD_3OD at δ 49.15 ppm and C_7D_8 δ 137.86 ppm, δ 129.24 ppm, δ 128.33 ppm, δ 125.49 ppm and δ 20.4 ppm. Abbreviations used to record NMR multiplicities were reported

using singlet (s), broad singlet (bs), doublet (d), doublet of doublets (dd), doublet of doublet of doublets (ddd), triplet (t), quartet (q) and multiplet (m). Special analyses were performed by first order approximations and were based on shift correlation spectroscopy (COSY), heteronuclear multiple quantum coherence (HMQC), and 1- and 2-dimensional distortionless enhancement by polarization transfer (DEPT) experiments. Spectra were reported via first analysis basis and coupling constants under 1Hz were disregarded. Peaks listed of the compounds with rotamer mixtures are of the major rotamer. Rotamers were confirmed by variable temperature ^{1}H NMR spectroscopy in DMSO and D_2O.

Mass spectra (FAB, EI, CI) were recorded on a Kratos Concept II instrument. Xenon and cesium were used as the neutral carrier atoms and in FAB-MS experiments. Electron Spray Ionization (ESI) was recorded on a Micromass Qualtro LC having a capillary voltage of 3.5-4.5 kv and water/acetonitrile 1/1 was the usual solvent.

Melting points were determined on a Gallenkamp apparatus and are uncorrected.

Optical rotation ($[\alpha]_D$) values were determined using a Perkin-Elmer model 241 set at the sodium D line (589 nm) and were run at room temperature.
Infrared spectra were obtained using a Bomem-Michelson MB-100 FT/IR spectrophotometer neat on potassium bromide plates.

Reactions were followed by thin-layer chromatography using Kieselgel 60 F_{254} precoated 0.25 mm thick aluminium or glass backed plates. The reagents used for compound detection include ammonium molybdate (2.5% w/v) in 10%

(v/v) aqueous sulfuric acid, iodine, ninhydrin (0.4% w/v) in aqueous pyridine (4% v/v) or potassium permanganate (1% w/v) with sodium carbonate (2% w/v) in water or short wave UV light.

Purifications were performed by gravity or flash chromatography on silica gel 60 (230 – 400 mesh, E. Merck No 9385). Solvents were reagent grade and evaporated under reduced pressure using a Büchi rotary evaporator connected to a water aspirator, air aspirator, or air vacuum.

All reactions, unless stated otherwise were carried out in oven dried flasks under an argon or nitrogen atmosphere. Dichloromethane was dried over CaH_2 and distilled and pyridine was dried over NaOH pellets prior to use. All chemical reagents were obtained from commercial suppliers and used as is except for Amberlite IR-120 (H) ion – exchange resin which was rinsed with deionized water and then methanol before use as a synthetic reagent.

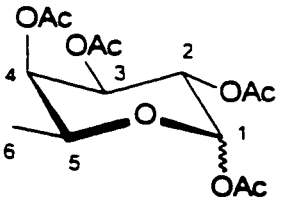

1, 2, 3, 4 Tetra-*O*-acetyl-α-L-fucopyranoside (1)[3]

Acetic anhydride (62.1 mL, 0.658 mol) was added to a solution of α-L-fucose (12.0 g, 73.1 mmol) dissolved in dry pyridine (45 mL) cooled to 0°C kept under N_2 gas. The reaction mixture was allowed to warm to room temperature and the progress of the reaction was followed by TLC (hexane/ethyl acetate 2/1) until complete disappearance of the starting material (7 hours). Methanol (80 mL) was added at 0°C to the reaction mixture and allowed to stir for an additional 2 hours. After concentration, workup consisted of transferring the reaction mixture to an Erlenmeyer flask and adding saturated $NaHCO_3$ (500 mL) until foaming ceased. Ether (300 mL) was added and the two layers were separated. The organic layer was washed successively with distilled water (400 mL x 1) and 2 mL of concentrated HCl, saturated $NaHCO_3$ solution (100 mL x 1) and10% HCl (100 mL x 2). The organic layer was dried over $NaSO_4$ and evaporation of the solvents in vacuo yielded a white solid having an α:β ratio of 7:1 (α:β ratios vary for each reaction from 1:1 to 15:1) (99% yield); mp = 69 – 70°C; ^{1}H NMR ($CDCl_3$, 500 MHz): α δ(ppm) 6.30 (d, 1H, H-1, $J_{1,2}$ = 3.0 Hz), 5.30 (m, 3H, H-2, H-3, H-4)

4.23 (q, 1H, H-5, $J_{5,6}$ = 6.5 Hz), 2.14, 2.11, 1.97, 1.96 (4s, 12H, $COC\underline{H}_3$), 1.12 (d, 3H, H-6, $J_{5,6}$ = 6.5 Hz); β δ(ppm) 5.64 (d, 1H, H-1, $J_{1,2}$ = 9.3 Hz), 5.30 (m, 1H, H-2), 5.03 (dd, 1H, H-3, $J_{2,3}$ = 10.4 Hz, $J_{3,4}$ = 3.5 Hz), 5.23 (dd, 1H, H-4, $J_{3,4}$ = 3.4 Hz, $J_{4,5}$ = 0.8 Hz) 3.92 (dq, 1H, H-5, $J_{4,5}$ = 1.0 Hz, $J_{5,6}$ = 6.5 Hz), 2.15, 2.07, 2.00, 1.95 (4s, 12H, $COC\underline{H}_3$), 1.19 (d, 1H, H-6, $J_{5,6}$ = 6.4 Hz); ^{13}C NMR ($CDCl_3$, 125.7 MHz): α δ(ppm) 170.5, 170.1, 169.9, 169.1 ($\underline{C}OCH_3$), 89.9 (C-1), 70.6, 67.8, 66.5 (C-2, C-3, C-4), 67.2 (C-5), 20.8, 20.6, 20.5, 20.5 ($CO\underline{C}H_3$), 15.9 (C-6); EI-MS, m/z = 355.1 (44%), $[M + Na]^+$ calcd for $C_{14}H_{20}O_9Na$. The ^1H and ^{13}C NMR spectral data are essentially identical to the reported literature values.[3]

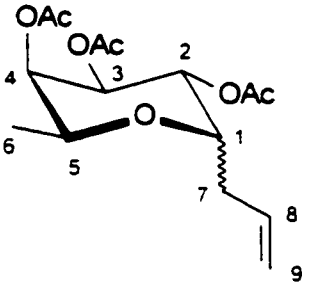

3-(2, 3, 4-Tri-*O*-acetyl-α,β-L-fucopyranosyl)propene (2)[3]

Allyltrimethylsilane (5.43 mL, 34.2 mmol), trimethylsilylmethyl - trifluoromethanesulfonate (0.34 mL, 1.71 mmol) and boron trifluoride diethyl etherate (4.33 mL, 34.2 mmol) were added dropwise via syringe to a solution of **1** (5.68 g, 17.1 mmol) in dry acetonitrile (60 mL), cooled to 0°C under N_2 atmosphere. The reaction mixture was removed from the cold bath after 30 minutes and stirred at room temperature. The course of the reaction was

monitored by TLC (hexane/ethyl acetate 2/1) until disappearance of the starting material (4 hours). The organic layer was washed successively with saturated $NaHCO_3$ solution (100 mL x 2) and brine solution (100 mL x 1). Aqueous layers were extracted with dichloromethane (150 mL x 3). Organic layers were combined and dried over $NaSO_4$ and the solvent was removed under reduced pressure. The concentrate was purified by column chromatography on silica gel with ethyl acetate/hexane 1/10 as eluent to yield a clear, colourless oil having an α:β ratio of 14:1 (94% yield). ^1H NMR, ^{13}C NMR, MS data are listed for the purified α-anomer, compound **4**. The α:β ratios of this reaction vary from 20:1 to 4:1

3-(2, 3, 4-Tri-*O*-acetyl-α,β-L-fucopyranosyl)propene (2)

Allyltrimethylsilane (34.1 mL, 0.215 mol), and boron trifluoride diethyl etherate (39.6 mL, 0.322 mol) were added dropwise via syringe to a solution of **1** (23.76 g, 71.5 mmol) in dry acetonitrile (60 mL), cooled to 0°C under N_2 atmosphere. The reaction mixture was allowed to warm to room temperature. The course of the reaction was monitored by TLC (hexane/ethyl acetate 2/1) until disappearance of the starting material (7 days). Purification procedures of **2** were the same as above (93% yield).

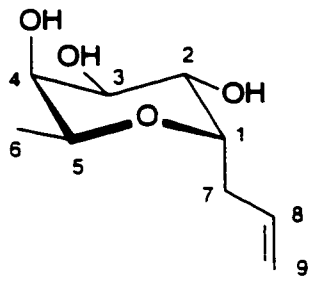

3-(2, 3, 4-Tri-*O*-hydroxyl-α-L-fucopyranosyl)propene (3)[3]

3-(2, 3, 4-tri-*O*-acetyl-α,β-L-fucopyranosyl)propene (0.793 g, 2.52 mmol) was dissolved in dry methanol (15 mL) and 1M sodium methoxide solution in methanol (0.6 mL) was added dropwise until solution was basic (pH = 10). The course of the reaction was monitored by TLC (hexane/ethyl acetate 2/1) until complete disappearance of the starting material (3 hours). Amberlite IR-120 (H) ion – exchange resin was rinsed with deionized water followed by methanol and then added to the solution until neutral (pH = 7). The reaction mixture was then suction filtered and concentrated. The crude product was purified by recrystallization using ethyl acetate to yield white, needle crystals (75% yield); mp = 152.5 - 153°C; $[\alpha]_D^{23}$ = -122.0° (c = 1.0, MeOH); ^{1}H NMR ($CDCl_3$, 500 MHz): δ (ppm) 5.82 (m, 1H, H-8), 5.09 (ddd, 1H, H-9, $H_{8,9\ trans}$ = 17.1 Hz, $^2J_9$ = 2.0 Hz, $^4J_{9,?}$ = 1.5 Hz), 5.02 (ddd, 1H, H-9, $H_{8,9\ cis}$ = 10.3 Hz, $^2J_9$ = 2.1 Hz, $^4J_{9,?}$ = 1.1 Hz), 4.82 (s, 3H, O<u>H</u>), 3.94 (m, 1H, H-1), 3.88 (dd, 1H, H-2, $J_{1,2}$ = 5.6 Hz, $J_{2,3}$ = 8.9 Hz) 3.83 (dq, 1H, H-5, $J_{4,5}$ = 2.0 Hz, $J_{5,6}$ = 6.5 Hz), 3.69 (dd, 1H, H-4, $J_{3,4}$ = 3.5 Hz, $J_{4,5}$ = 2.1 Hz), 3.66 (dd, 1H, H-3, $J_{2,3}$ = 8.9 Hz, $J_{3,4}$ = 3.5 Hz), 2.45, 2.35 (m, 2H, H-7), 1.19 (d, 3H, H-6, $J_{5,6}$ = 6.5 Hz); ^{13}C NMR ($CDCl_3$, 125.7 MHz): δ

(ppm) 137.0 (C-8), 116.7 (C-9), 75.9 (C-1), 72.6 (C-4), 72.2 (C-3), 69.8 (C-2), 68.8 (C-5), 30.8 (C-7), 16.4 (C-6); FAB-MS, m/z = 189.1 (38%), $[M + 1]^+$ calcd for $C_9H_{17}O_4$. The ^1H and ^{13}C NMR spectral data are essentially identical to the reported literature values.[3]

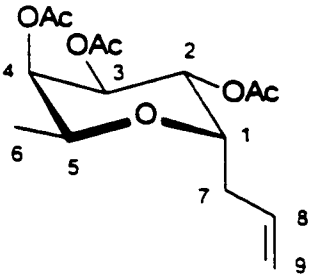

3-(2, 3, 4-Tri-*O*-acetyl-α-L-fucopyranosyl)propene (4)[3]

Acetic anhydride (18.1 mL, 0.191 mol) was added to a solution of **3** (4.00 g, 21.3 mmol) dissolved in dry pyridine (25 mL) cooled to 0°C kept under N_2 gas. The reaction mixture was allowed to warm to room temperature and the progress of the reaction was followed by TLC (hexane/ethyl acetate 2/1) until complete disappearance of the starting material (4 hours). Methanol (50 mL) was added at 0°C to the reaction mixture and allowed to stir for an additional 2 hours. After concentration, workup consisted of transferring the reaction mixture to an Erlenmeyer flask and adding saturated $NaHCO_3$ (500 mL) until foaming ceased. Ether (300 mL) was added and the two layers were separated. The organic layer was washed successively with distilled water (400 mL x 1) and 2 mL of concentrated HCl, saturated $NaHCO_3$ solution (100 mL x 1) and10% HCl (100 mL x 2). The organic layer was dried over $NaSO_4$ and evaporation of the

solvents in vacuo yielded a clear oil (99% yield); $[\alpha]_D^{23}$ = -102.1° (c = 1.0, $CHCl_3$) ^1H NMR ($CDCl_3$, 500 MHz): δ (ppm) 5.74 (m, 1H, H-8), 5.28 (dd, 1H, H-2, $J_{1,2}$ = 5.6 Hz, $J_{2,3}$ = 10.0 Hz), 5.24 (dd, 1H, H-4, $J_{3,4}$ = 3.3 Hz, $J_{4,5}$ = 1.8 Hz), 5.19 (dd, 1H, H-3, $J_{2,3}$ = 10.0 Hz, $J_{3,4}$ = 3.4 Hz), 5.08 (m, 2H, H-9), 4.25 (m, 1H, H-1), 3.94 (dq, 1H, H-5, $J_{4,5}$ = 1.5 Hz, $J_{5,6}$ = 6.4 Hz) 2.48, 2.25 (m, 2H, H-7), 2.12, 2.02, 1.98 (3s, 9H, $COCH_3$), 1.11 (d, 3H, H-6, $J_{5,6}$ = 6.4 Hz); ^{13}C NMR ($CDCl_3$, 125.7 MHz): δ (ppm) 170.6, 170.1, 169.9 ($COCH_3$), 133.8 (C-8), 117.3 (C-9), 71.9 (C-1), 70.7 (C-4), 68.5 (C-3), 68.2 (C-2), 65.6 (C-5), 30.6 (C-7), 20.77, 20.7, 20.6 ($COCH_3$), 15.9 (C-6); FAB-MS, m/z = 315.1 (21%), $[M + 1]^+$ calcd for $C_{15}H_{23}O_7$, HRMS calcd for $C_{15}H_{23}O_7$ 315.1444, found 315.1425. The ^1H and ^{13}C NMR spectral data are essentially identical to the reported literature values.[3]

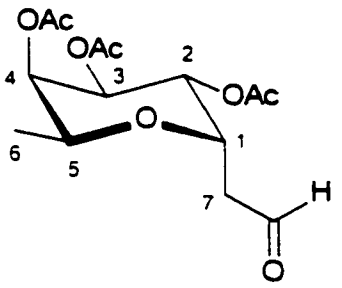

2-(2, 3, 4-Tri-*O*-acetyl-α-L-fucopyranosyl)ethanal (5)[3]

3-(2, 3, 4-Tri-O-acetyl-α-L-fucopyranosyl)propene (1.00 g, 3.18 mmol) was dissolved in dry dichloromethane (20 mL) and the solution was purged with oxygen for 10 min at –78°C. Ozone was then bubbled through the reaction solution until the colour of the solution turned blue. Completion of the reaction was confirmed by TLC (hexane/ethyl acetate 2/1). The solution was then purged

with oxygen for another 10 min at –78°C to remove excess ozone. Dimethylsulfide (40 mL) was added to the clear, colourless solution. The reaction mixture was allowed to reach room temperature and stirred for an additional 24 hours. The solution was concentrated and the residue was co-evaporated with toluene to remove dimethylsulfoxide produced during the reaction yielding a light yellow oil (100% yield). Further purification could be obtained by column chromatography on silica gel using hexane/ethyl acetate 1/1 as eluent yielding a clear, colourless oil (90% yield); $[\alpha]_D^{23}$ = -62.6° (c = 5.0, $CHCl_3$); ^{1}H NMR ($CDCl_3$, 500 MHz): δ (ppm) 9.71 (dd, 1H, C<u>H</u>O, $^4J_{ald,7}$ = 2.6 Hz, $^4J_{ald,7'}$ = 1.5 Hz), 5.32 (dd, 1H, H-2, $J_{1,2}$ = 5.6 Hz, $J_{2,3}$ = 9.7 Hz), 5.25 (dd, 1H, H-4, $J_{3,4}$ = 3.4 Hz, $J_{4,5}$ = 2.2 Hz), 5.13 (dd, 1H, H-3, $J_{2,3}$ = 9.7 Hz, $J_{3,4}$ = 3.4 Hz), 4.83 (m, 1H, H-1), 3.95 (dq, 1H, H-5, $J_{4,5}$ = 2.1 Hz, $J_{5,6}$ = 6.4 Hz), 2.76 (ddd, 1H, H-7, $^4J_{ald,7}$ = 2.7 Hz, $^2J_{7,7'}$ = 8.2 Hz, $J_{1,7}$ = 16.5 Hz), 2.71 (ddd, 1H, H-7', $^4J_{ald,7'}$ = 1.5 Hz, $^2J_{7,7'}$ = 8.9 Hz, $J_{1,7'}$ = 5.8 Hz), 2.12, 2.01, 1.99 (3s, 9H, COC<u>H</u>$_3$), 1.13 (d, 3H, H-6, $J_{5,6}$ = 6.4 Hz); ^{13}C NMR ($CDCl_3$, 125.7 MHz): δ (ppm) 198.6 (<u>C</u>HO), 170.4, 170.0, 169.7 (<u>C</u>OCH$_3$), 70.1 (C-4), 68.4 (C-3), 67.4 (C-1), 67.3 (C-2), 66.9 (C-5), 41.6 (C-7), 20.7, 20.7, 20.6 (CO<u>C</u>H$_3$), 15.8 (C-6);); IR (thin film): ν (cm^{-1}) 1746 (CHO); CI-MS, m/z = 317 (13%), $[M + 1]^+$ calcd for $C_{14}H_{21}O_8$, The ^{1}H and ^{13}C NMR spectral data are essentially identical to the reported literature values.[3]

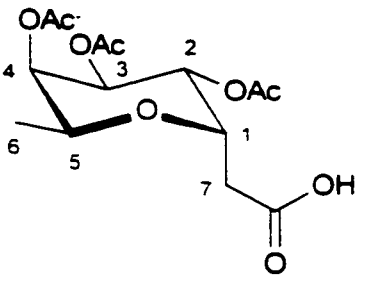

2-(2, 3, 4-Tri-*O*-acetyl-α-L-fucopyranosyl)ethanoic acid (6)[7]

To a solution of **5** (1.01 g, 3.20 mmol) dissolved in t-butyl alcohol (5.6 mL) was added a buffer solution (pH = 6) of sodium phosphate monobasic (5.6 mL) and 1M potassium permanganate (7.0 mL). The course of the reaction was followed by TLC (hexane/ethyl acetate 1/1) until complete disappearance of the aldehyde (1 hour). The reaction was quenched with cold saturated sodium sulphite until the mixture turned from purple to brown (5 mL) followed by addition of dilute acid until the solution became clear (20 mL). Workup consisted of extracting with ethyl acetate (200 mL x 3) and washing with dilute acid (200 mL x 1), water (200 mL x 1) and then brine (200 mL x 1). The organic layers were combined and dried over sodium sulphate, filtered and concentrated. The crude product was further purified by dissolving it in ether at 0°C and dilute sodium bicarbonate until the pH of the aqueous layer was 8. The contents of the flask were transferred to a separatory funnel and the bottom aqueous layer was removed and then re-acidified using dilute HCl. The aqueous layer was then extracted with ether (150 mL x 3) and the organic layers were combined and dried over sodium sulphate, filtered and concentrated to yield a white powder (85% yield); mp = 122.4 - 1123.1°C; $[\alpha]_D^{23}$ = -83.3° (c = 1.0, $CHCl_3$) ^1H NMR

($CDCl_3$, 500 MHz): δ (ppm) 9.15 (bs, 1H, CO_2H), 5.33 (dd, 1H, H-2, $J_{1,2}$ = 5.6 Hz, $J_{2,3}$ = 9.8 Hz), 5.22 (m, 1H, H-4), 5.12 (dd, 1H, H-3, $J_{2,3}$ = 9.8 Hz, $J_{3,4}$ = 3.3 Hz), 4.65 (m, 1H, H-1), 4.00 (dq, 1H, H-5, $J_{4,5}$ = 1.5 Hz, $J_{5,6}$ = 6.4 Hz), 2.72 (dd, 1H, H-7, $J_{1,7}$ = 8.9 Hz, $^2J_{7,7'}$ = 15.4 Hz), 2.62 (dd, 1H, H-7', $J_{1,7'}$ = 5.6 Hz, $^2J_{7,7'}$ = 15.4 Hz), 2.11, 1.99, 1.97 (3s, 9H, $COC\underline{H}_3$), 1.11 (d, 3H, H-6, $J_{5,6}$ = 6.4 Hz); ^{13}C NMR ($CDCl_3$, 125.7 MHz): δ (ppm) 175.8 ($\underline{C}O_2H$), 170.5, 170.1, 169.6 ($\underline{C}OCH_3$), 70.2 (C-4), 69.4 (C-1), 68.4 (C-3), 67.3 (C-2), 66.9 (C-5), 32.8 (C-7), 20.6 ($CO\underline{C}H_3$ x2), 20.6 ($CO\underline{C}H_3$), 15.7 (C-6); FAB-MS, m/z = 333.1 (100%), $[M + 1]^+$ calcd for $C_{14}H_{21}O_9$, HRMS calcd for $C_{14}H_{21}O_9$ 333.1186, found 333.1117. The ^1H and ^{13}C NMR spectral data are essentially identical to the reported literature values.[7]

2-(2, 3, 4-Tri-*O*-acetyl-α-L-fucopyranosyl)ethanoic acid (6)

Sulfamic acid (43.2 mg, 0.478 mmol) dissolved in 0.5 mL of distilled water and sodium chlorite (30.9 mg, 0.319 mmol) dissolved in 0.5 mL of distilled water was added to a solution of **5** (100 mg, 31.9 mmol) dissolved in THF/H_2O (5/1). The reaction was monitored via TLC (hexane/ethyl acetate 1/1) until disappearance of majority of starting material (4 hours). The organic solvent was removed in vacuo. Workup consisted of extracting the crude product with ethyl acetate (50 mL x 3), washing with water (50 mL x 1) followed by brine (50 mL x 1) and then water (50 mL x 1). The organic layers were combined and dried over $NaSO_4$ and evaporation of the solvents in vacuo yielded a cloudy yellow oil (80% crude yield).

2-(2, 3, 4-Tri-*O*-acetyl-α-L-fucopyranosyl)ethanoic acid (6)

C-allyl 2, 3, 4-tri-*O*-acetyl-α-fucoside (399 mg, 1.27 mmol), dissolved in t-butanol (5.5 mL) and potassium permanganate (802 mg, 5.08 mmol) dissolved in water (25 mL) were mixed with acetone and cooled to 0°C. The reaction was left to warm to room temperature (2 hours) and then refluxed for 90 minutes. The reaction was complete by TLC (chloroform/methanol 9/1) analysis. The mixture was then filtered and acetone was removed under reduced pressure. The aqueous residue was then acidified with 10% HCl and extracted with ether (150 mL x 3). The organic phase was then washed with cold 10% HCl (150 mL x 1), distilled water (150 mL x 1) and brine (150 mL x 1). The organic layer was dried over $MgSO_4$. filtered and concentrated yielding a white solid (14% yield).

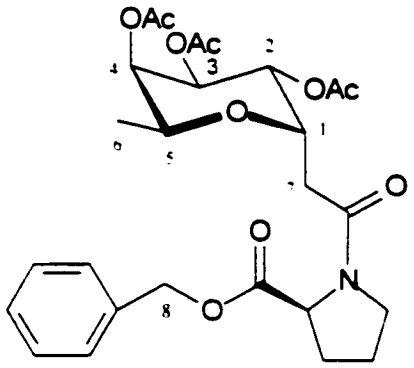

2, 3, 4-Tri-*O*-acetyl-α-L-fucose-L-proline benzyl ester derivative (7)

L-Proline benzyl ester (618 mg, 2.56 mmol) was added to a solution of **6** (707 mg, 2.13 mmol) dissolved in dry dichloromethane (50 mL). The coupling reagent PyBOP (1.44 g, 2.76 mmol) was then added followed by NMM (0.83 mL,

7.64 mmol) to reach pH = 8 and stirred under N_2 atmosphere. The reaction was judged complete by TLC (hexane/ethyl acetate 1/1) after four hours. The solvents were removed in vacuo and the crude mixture was transferred directly to a silica gel column. The purified product was eluted using hexane/ethyl acetate 1/1 as a running solvent. The compound obtained was a white solid in 5:1 rotamer mixture (99% yield). Other coupling reagents examined were TBTU (1.5eq.) with DIPEA (1.8eq.) and BOP (1.8eq.) and NMM (2eq.) which afforded **8** in 80% and 87% respectively. m.p. = 58.2 - 59.2°C; $[\alpha]_D^{23}$ = -96.8° (c = 1.0, $CHCl_3$); ^{1}H NMR ($CDCl_3$, 500 MHz): δ (ppm) 7.30 (m, 5H, Ph-H), 5.28 (dd, 1H, H-2, $J_{1,2}$ = 5.0 Hz, $J_{2,3}$ = 8.8 Hz), 5.23 (m, 1H, H-4), 5.14 (dd, 1H, H-3, $J_{2,3}$ = 9.0 Hz, $J_{3,4}$ = 3.4 Hz), 5.10 (d, 2H, H-8, ^2J = 8.7 Hz), 4.83 (dd, 1H, H-1, $J_{1,7}$ = 6.1 Hz), 4.77 (dd, 1H, Pro-α-H, $J_{\alpha,\beta cis}$ = 6.4 Hz, $J_{\alpha,\beta trans}$ = 11.9 Hz), 3.97 (dq, 1H, H-5, $J_{4,5}$ = 2.8 Hz, $J_{5,6}$ = 6.5 Hz), 3.63 (m, 1H, Pro-Δ-H), 3.49 (m, 1H, Pro-Δ-H'), 2.60 (d, 2H, H-7, $J_{1,7}$ = 6.1 Hz), 2.16 (m, 1H, Pro-β-H), 2.09, 1.99, 1.97 (3s, 9H, $COCH_3$), 1.98 (m, 3H, Pro-β-H, Pro-γ-H), 1.16 (d, 3H, H-6, $J_{5,6}$ = 6.5 Hz); ^{13}C NMR ($CDCl_3$, 125.7 MHz): δ (ppm) 171.9, 170.4, 170.0, 169.8 (O-C=O), 168.3 (N-C=O), 135.6 (C-ipso-Ph), 128.5, 128.2, 128.0 (Ph-C), 69.6 (C-4), 68.6 (C-3), 68.0 (C-2), 67.8 (C-1) 67.6 (C-5), 66.7 (C-8), 58.7 (Pro-α-C), 47.0 (Pro-Δ-C), 33.3 (C-7), 29.0 (Pro-β-C), 24.6 (Pro-γ-C), 20.7 ($CO\underline{C}H_3$ x2), 20.6 ($CO\underline{C}H_3$), 15.4 (C-6); ESI-MS, m/z = 520.2 (29%), $[M + 1]^+$ calcd for $C_{26}H_{34}NO_{10}$, m/z = 542.1 (18%), $[M + Na]^+$ calcd for $C_{26}H_{33}NO_{10}Na$.

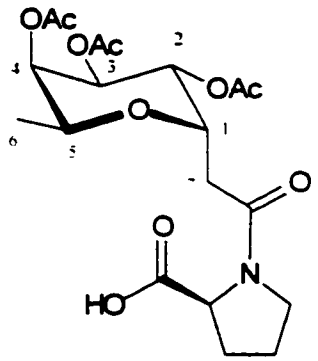

2, 3, 4-Tri-*O*-acetyl-α-L-fucose-L-proline carboxylic acid derivative (8)

Compound **7** (500 mg, 0.963 mmol) was dissolved in reagent grade methanol (20 mL). A slurry of reagent grade methanol and 10% palladium weight on activated carbon (5 mL, 333 mg respectively) was added to the reaction mixture. Hydrogen gas was bubbled through the reaction mixture. TLC analysis (ethyl acetate) confirmed that the reaction was completed in 30 minutes. A minor impurity was detected during debenzylation and thus silica gel column chromatography was necessary for purification. The product eluted with the running solvent of methanol/chloroform 1/9 with 0.1% acetic acid. Removal of the solvents in vacuo yielded a white solid in a 6:1 rotamer mixture (93% yield); mp = 78.2 - 79.0°C; $[\alpha]_D^{23}$ = -117.2° (c = 0.78, MeOH); ^{1}H NMR ($CDCl_3$, 500 MHz): δ (ppm) 7.25 (vbs, H, CO_2H), 5.29 (dd, 1H, H-2, $J_{1,2}$ = 5.0 Hz, $J_{2,3}$ = 8.8 Hz), 5.23 (m, 1H, H-4), 5.16 (dd, 1H, H-3, $J_{2,3}$ = 9.8 Hz, $J_{3,4}$ = 3.4 Hz), 4.80 (dd, 1H, H-1, $J_{1,7}$ = 5.9 Hz), 4.30 (dd, 1H, Pro-α-H, $J_{\alpha,\beta cis}$ = 2.9 Hz, $J_{\alpha,\beta trans}$ = 7.5 Hz), 3.99 (dq, 1H, H-5, $J_{4,5}$ = 2.8 Hz, $J_{5,6}$ = 6.5 Hz), 3.61 (m, 1H, Pro-Δ-H), 3.48 (m, 1H, Pro-Δ-H'), 2.64 (d, 2H, H-7, $J_{1,7}$ = 5.9 Hz), 2.24 (m, 1H, Pro-β-H), 2.10, 2.05, 2.00 (3s, 9H, $COCH_3$), 2.04 (m, 1H, Pro-β-H), 1.98 (m, 2H, Pro-γ-H), 1.16 (d, 3H,

H-6, $J_{5,6}$ = 6.5 Hz); ^{13}C NMR ($CDCl_3$, 125.7 MHz): δ (ppm) 176.4 (CO_2H), 174.1, 170.5, 170.2 ($\underline{C}OCH_3$), 169.9 (N-C=O), 69.6 (C-4), 68.7 (C-3), 67.1 (C-2), 66.8 (C-1) 67.2 (C-5), 59.4 (Pro-α-C), 47.5 (Pro-Δ-C), 33.3 (C-7), 28.2 (Pro-β-C), 24.7 (Pro-γ-C), 20.7, 20.6, 20.6 ($CO\underline{C}H_3$), 15.4 (C-6); IR (thin film): ν (cm^{-1}) 3500 - 2800 (CO_2H), 1746 (C=O), 1641 (N-C=O); CI-MS, m/z = 430 (11%), $[M + 1]^+$ calcd for $C_{19}H_{28}NO_{10}$.

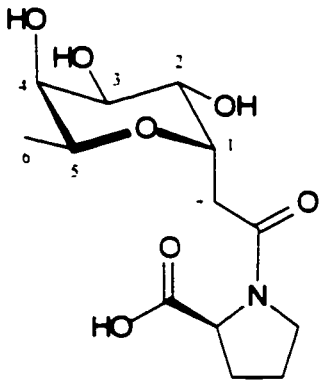

2, 3, 4-Tri-hydroxy-α-L-fucose-L-proline carboxylic acid derivative (9)

To a solution of **8** (57.0 mg, 0.133 mmol) dissolved in reagent grade methanol (5 mL) was added 0.1M sodium methoxide solution in methanol (2.0 mL) dropwise until solution was basic (pH = 10). The course of the reaction was monitored by TLC (methanol/chloroform 3/7) until complete disappearance of the starting material (3 hours). Amberlite IR-120 (H) ion – exchange resin was rinsed with methanol and then added to the solution until neutral (pH = 7). The reaction mixture was then suction filtered and concentrated yielding a white solid (100% yield); mp = 41.5 - 42.4°C; $[\alpha]_D^{23}$ = -94.6° (c = 0.71, MeOH); ^1H NMR (D_2O, 500

MHz): δ (ppm) 4.85 (m, 1H, H-1), 4.51 (dd, 1H, Pro-α-H, $J_{\alpha,\beta cis}$ = 4.2 Hz, $J_{\alpha,\beta trans}$ = 9.1 Hz), 4.06 (dd, 1H, H-2, $J_{1,2}$ = 6.1 Hz, $J_{2,3}$ = 9.8 Hz), 4.01(q, 1H, H-5, $J_{5,6}$ = 6.4 Hz), 3.86 (m, 1H, H-3), 3.83 (m, 1H, H-4), 3.81 (m, 1H, Pro-Δ-H), 3.72 (m, 1H, Pro-Δ-H'), 2.93 (dd, 1H, H-7, $J_{1,7}$ = 10.2 Hz, $J_{7,7'}$ = 15.8 Hz), 2.80 (dd, 1H, H-7' $J_{1,7'}$ = 3.6 Hz, $J_{7,7'}$ = 15.8 Hz), 2.38 (m, 1H, Pro-β-H), 2.10 (m, 3H, Pro-β-H, Pro-γ-H), 1.23 (d, 3H, H-6, $J_{5,6}$ = 6.5 Hz); ^{13}C NMR (D_2O, 125.7 MHz): δ (ppm) 175.6 (CO_2H), 171.9 (N-C=O), 72.0 (C-1), 70.8 (C-3), 69.4 (C-4), 67.8 (C-5) 66.9 (C-2). 58.9 (Pro-α-C), 47.4 (Pro-Δ-C), 23.0 (C-7), 28.6 (Pro-β-C), 23.9 (Pro-γ-C), 15.0 (C-6); ESI-MS, m/z = 304.0 (5.2%), $[M + 1]^+$ calcd for $C_{13}H_{22}NO_7$.

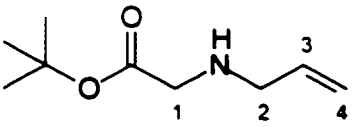

N-Allylglycine t-butyl ester (10)

Distilled allyl amine (0.92 mL, 12.0 mmol) was added to a solution of DIPEA (2.70 mL, 15.5 mmol) in dry acetonitrile (1 mL). The reaction mixture was cooled to 0°C and t-butyl bromoacetate (1.40 mL, 9.48 mmol) was added via syringe under N_2. After 5 minutes a white solid began to precipitate out of solution. TLC analysis (hexane/ethyl acetate 1/1) revealed one major and one minor spot had formed after 10 minutes indicating that the primary amine was starting to become dialkylated. The reaction was stopped immediately and the contents of the flask were transferred to a silica gel column with eluent hexane/ethyl acetate 1/6 for purification. The product obtained was a colourless,

clear oil (86% yield); ^{1}H NMR ($CDCl_3$, 500 MHz): δ (ppm) 5.78 (ddd, 1H, H-2, $J_{2,3}$ = 6.0 Hz, $J_{3,4cis}$ = 8.3 Hz, $J_{3,4'trans}$ = 16.2 Hz), 5.10 (d, 1H, H-4, $J_{3,4}$ = 8.3 Hz), 3.21 (s, 2H, H-1), 3.17 (d, 2H, H-2, $J_{2,3}$ = 6.0 Hz), 1.72 (bs, 1H, NH), 1.41 (s, 9H, C-$(CH_3)_3$); ^{13}C NMR ($CDCl_3$, 125.7 MHz): δ (ppm) 171.5 (C=O), 136.2 (C-2), 116.2 (C-4), 80.9 (C-$(CH_3)_3$), 51.7 (C-2), 50.7 (C-1) 28.0 (C-$(CH_3)_3$); EI-MS, m/z = 172 (0.4%), $[M+1]^+$ calcd for $C_9H_{18}NO_2$, m/z = 114 (5.8%), $[M-C_4H_9]^+$ calcd for $C_5H_9NO_2$, m/z = 70 (47.3%), $[M-C_5H_9O_2]^+$ calcd for C_4H_9N.

N-Allylglycine t-butyl ester (10)

Allylamine (0.46 mL, 6.15 mmol) and DIPEA (1.34 mL, 7.69 mmol) were dissolved in 1,4-dioxane (50 mL). t-butyl-bromoacetate dissolved in 1,4-dioxane (50 mL) was added very slowly (1 drop every 15s) via a dropping funnel. Small (approx. 5 mg) ^{1}H NMR samples were analyzed periodically to determine that the reaction was complete in 24 hours. The solvent was removed under reduced pressure and the concentrate was purified by silica gel column chromatography with hexane/ethyl acetate 8/1 as eluent. A clear, colourless oil was obtained (90% yield).

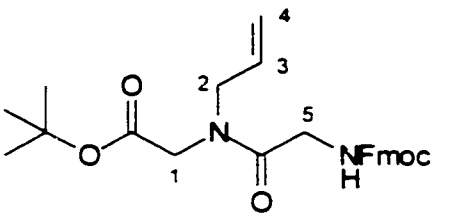

N-Fmoc-glycyl-N-allylglycine t-butyl ester (11)

Fmoc-glycine (1.99 g, 7.05 mmol) was added to a solution of N-allylglycine t-butyl ester (1.00 g, 5.87 mmol) dissolved in dry dichloromethane (60 mL). Coupling reagent BOP (3.37 g, 7.64 mmol) was then added, followed NMM (1.30 mL, 11.8 mmol) to obtain pH = 8 as measured by pH paper. The reaction mixture stirred for 6 hours, after which time, the reaction was judged complete by TLC (hexane/ethyl acetate 1/1). The solvents were removed under reduced pressure and the concentrate was purified using silica gel chromatography with hexane/ethyl acetate 6/1 as an eluent. The product obtained was a thick, cloudy oil (88% yield); ^{1}H NMR ($CDCl_3$, 500 MHz): δ (ppm) Fmoc 8H: 7.74 (d, 2H, J = 7.6 Hz), 7.59 (d, 2H, J = 7.4), 7.37 (m, 2H), 7.79 (m, 2H), 5.79 (m, 2H, H-3, NH), 5.20 (m, 2H, H-4), 4.35 (d, 2H, H-6, J = 6.7), 4.21 (m, 1H, H-7), 4.11 (m, 1H, H-2), 4.07 (d, 1H, H-5), 4.00 (s, 1H, H-1), 3.97 (d, 1H, H-2'), 3.92 (d, 1H, H-5'), 3.84 (s, 1H, H-1'), 1.45 (s, 9H, C-$(CH_3)_3$); ^{13}C NMR ($CDCl_3$, 125.7 MHz): δ (ppm) 168.7 (C=O), 167.9 (N-C=O), 156.1 (N-CO_2), 143.9, 141.3 (quaternary-Fmoc-C), 131.6 (C-3), 127.6, 127.0, 125.2, 119.9 (Fmoc-C), 118.1 (C-4), 82.1 (C-$(CH_3)_3$), 67.1 (C-6), 50.3 (C-5) 48.1 (C-1), 47.1 (C-7), 42.5 (C-2), 28.0 (C-$(CH_3)_3$); FAB-MS, m/z = 451.2 (33%), $[M+1]^+$ calcd for $C_{26}H_{31}N_2O_5$, HRMS calcd for $C_{26}H_{31}N_2O_5$ 451.2233, found 451.2190.

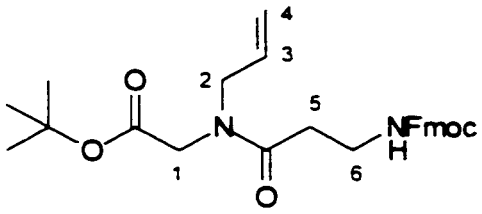

N-Fmoc-β-alaninyl-N-allylglycine t-butyl ester (12)

Fmoc-β-alanine (2.76 g, 8.87 mmol) was added to a solution of N-allylglycine t-butyl ester (1.23 g, 7.39 mmol) dissolved in dry dichloromethane (75 mL). PyBOP (5.00 g, 9.61 mmol) and NMM (1.6 mL, 14.8 mmol) were added and the pH was 8 as measured by pH paper. The reaction mixture stirred for 4 hours, after which time, the reaction was judged complete by TLC (hexane/ethyl acetate 1/1). The solvents were removed under reduced pressure and the concentrate was purified using silica gel chromatography with ether/hexanes 6/4 as an eluent. The product obtained was a clear, colourless oil (98% yield). Another coupling reagent examined was EDC (1.1eq) with HOBt (1.1eq) and DIPEA (2.0eq) afforded **12** in 80% yield. ^{1}H NMR ($CDCl_3$, 500 MHz): δ (ppm) Fmoc 8H: 7.73 (d, 2H, J = 6.6 Hz), 7.57 (d, 2H, J = 6.4), 7.30 (m, 4H), 5.74 (m, 1H, H-3), 5.65 (bs, 1H, NH), 5.17 (m, 2H, H-4), 3.96 (bm, 7H, H-1, H-2, H-7, H-8), 3.52 (m, 2H, H-6), 2.58 (m, 2H, H-5), 1.45 (s, 9H, C-$(CH_3)_3$); ^{13}C NMR ($CDCl_3$, 125.7 MHz): δ (ppm) 172.2 (C=O), 168.3 (N-C=O), 156.4 (N-CO_2), 144.0, 141.2 (quaternary-Fmoc-C), 132.2 (C-3), 127.6, 127.0, 125.1, 120.0 (Fmoc-C), 117.5 (C-4), 81.8 (C-$(CH_3)_3$), 66.7 (C-7), 51.2, 48.0 (C-1, C-2) 47.2 (C-8), 36.8 (C-6),

32.9 (C-5), 28.0 (C-($\underline{C}H_3)_3$); FAB-MS, m/z = 465.2 (4%), $[M+1]^+$ calcd for $C_{27}H_{33}N_2O_5$.

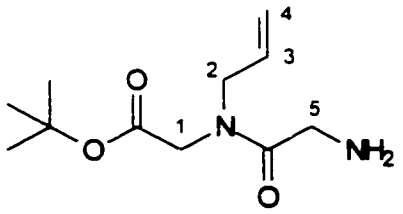

Glycyl-N-allylglycine-t-butyl ester (13)

The removal of the Fmoc protecting group from N-Fmoc glycyl-N-allylglycine t-butyl ester was accomplished by dissolving **11** (208 mg, 0.48 mmol) in 10 mL of freshly prepared 20% piperidine in acetonitrile solution. The white solid precipitate of dibenzylfulvene formed after five minutes. TLC (methanol/chloroform 3/7) confirmed that the reaction was complete. The presence of a purple stain with ninhydrin indicated that a primary amine had been formed. The solvents were removed under vacuo and the residue was purified using silica gel column chromatography. A gradient elution consisting of pure chloroform, methanol/chloroform (2/100) followed by methanol/chloroform (5/100) yielded a clear oil with a rotamer mixture of 5:1(100% yield); ^1H NMR ($CDCl_3$, 500 MHz): δ (ppm) 5.71 (m, 1H, H-3), 5.15 (m, 2H, H-4), 3.90 (m, 4H, H-1, H-2), 3.50 (bs, 2H, H-5), 1.65 (bs, 2H, NH_2), 1.41(s, 9H, C-$(CH_3)_3$); ^{13}C NMR ($CDCl_3$, 125.7 MHz): δ (ppm) 168.4 (C=O), 165.8 (N-C=O), 132.2 (C-3), 117.5 (C-4), 81.8 ($\underline{C}$-$(CH_3)_3$), 50.0 (C-2), 48.1 (C-1) 42.9 (b, C-5), 28.0 (C-($\underline{C}H_3)_3$); ESI-MS, m/z = 229.1 (100%), $[M+1]^+$ calcd for $C_{11}H_{21}N_2O_3$, m/z = 457.2 (68%),

$[2M+1]^+$ calcd for $C_{22}H_{41}N_4O_6$, m/z = 685.3 (9.85%), $[3M+1]^+$ calcd for $C_{33}H_{61}N_6O_9$.

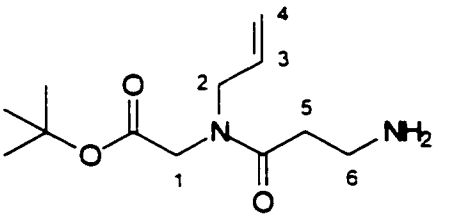

β-Alaninyl-N-allylglycine-t-butyl ester (14)

The removal of the Fmoc protecting group from N-Fmoc-β-alaninyl-N-allylglycine t-butyl ester was accomplished by dissolving **12** (670 mg, 1.49 mmol) in 14 mL of freshly prepared 20% piperidine in acetonitrile solution. The white solid precipitate of dibenzylfulvene formed after five minutes. TLC (methanol/chloroform 3/7) confirmed that the reaction was complete since the two spots stained purple with ninhydrin indicating the presence of a primary amine. The two spots were attributed to the two rotamers present in the compound and was confirmed by variable temperature NMR analysis. The contents of the flask were concentrated under vacuo and purified using silica gel column chromatography. A gradient elution consisting of pure chloroform, methanol/chloroform (2/100) followed by methanol/chloroform (5/100) yielded a clear oil with a rotamer mixture of 11:5 (99% yield); ^{1}H NMR ($CDCl_3$, 500 MHz): δ (ppm) 5.76 (m, 1H, H-3), 5.15 (m, 2H, H-4), 4.71 (bs, 2H, NH_2), 3.93 (m, 4H, H-1, H-2), 3.15 (bs, 2H, H-6), 2.67 (m, 2H, H-5), 1.41(s, 9H, C-$(CH_3)_3$); ^{13}C NMR ($CDCl_3$, 125.7 MHz): δ (ppm) 172.0 (C=O), 168.3 (N-C=O), 132.2 (C-3), 117.7

(C-4), 81.8 (C-(CH_3)$_3$), 51.3, 47.9 (C-1, C-2) 37.2 (C-6), 32.9 (C-5), 28.0 (C-(CH_3)$_3$); ESI-MS, m/z = 243.1 (60%), $[M+1]^+$ calcd for $C_{12}H_{22}N_2O_3$, m/z = 485.3 (10%), $[2M+1]^+$ calcd for $C_{24}H_{45}N_4O_6$.

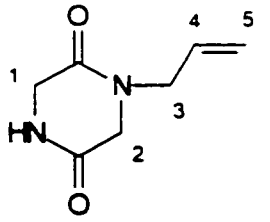

Intramolecular ring formation of glycyl-N-allylglycine-t-butyl ester (15)

Reaction of **8** (100 mg, 0.233 mmol) with **13** (100 mg, 0.466 mmol) using BOP (155 mg, 0.350 mmol) and NMM (0.06 mL, 0.466 mmol) at pH = 8, as the coupling reagent was dissolved in dry dichloromethane (35 mL). TLC analysis (methanol/chloroform 5/100) showed the formation of a product after 30min but there was still unreacted starting material. The reaction stirred for another 4½ hours and then was concentrated under reduced pressure. The residue was purified by silica gel column chromatography with 10% methanol/chloroform as eluent yielding white, needle crystals. NMR and MS analysis confirmed that the free amine formed the intramolecular ring **15**. mp = 134.3 - 134.8°C; ^{1}H NMR ($CDCl_3$, 200 MHz): δ (ppm) 6.88 (bs, 1H, NH), 5.70 (m, 1H, H-4), 5.27 (m, 2H, H-5), 4.02 (m, 6H, H-1, H-2, H-3); ^{13}C NMR ($CDCl_3$, 50.3 MHz): δ (ppm) 166.1, 163.2 (N-C=O), 130.8 (C-4), 119.5 (C-5) 48.7, 48.5, 45.0 (C-1, C-2, C-3); EI-MS, m/z = 154 (24%), $[M]^+$ calcd for $C_7H_{10}N_2O_2$.

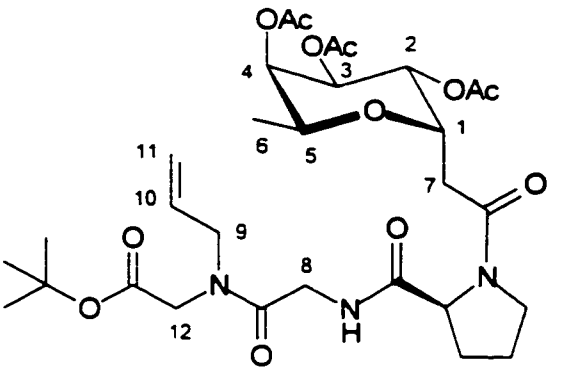

2, 3, 4-Tri-O-acetyl-α-L-fucosyl-L-proline-N-allyl-glycyl-glycine-t-butyl ester derivative (16)

2, 3, 4-Tri-O-acetyl-α-L-fucose-L-proline carboxylic acid derivative **8** (82.6 mg, 0.193 mmol), N-hydroxysuccinimide (24.0 mg, 0.208 mmol) and DCC (24.0 mg, 0.208 mmol) were dissolved in dry dichloromethane (20 mL) and stirred for 18 hours. Glycyl-N-allylglycine-t-butyl ester **13** (64 mg, 0.300 mmol) and two drops of DIPEA were added to the reaction flask under Ar atmosphere and allowed to stir overnight. After 8 hours, the reaction was judged complete by TLC (methanol/chloroform 5/100) and the solvents were removed under vacuo. The residue was purified by silica gel column chromatography using 3% methanol/chloroform as eluent to yield the pure compound as a white solid in 9:2 rotamer mixture (82% yield); mp = 77.9 – 78.2°C; $[\alpha]_D^{23}$ = -68.5° (c = 0.5, MeOH); ^{1}H NMR ($CDCl_3$, 500 MHz): δ (ppm) 7.13 (m, 1H, NH), 5.70 (m, 1H, H-10), 5.23 (m, 2H, H-2, H-4), 5.18 (m, 1H, H-3), 5.14 (m, 2H, H-11), 4.78 (m, 1H, H-1), 4.55 (m, 1H, Pro-α-H), 3.97 (bm, 7H, H-5, H-8, H-9, H-12), 3.60 (m, 1H, Pro-Δ-H), 3.44 (m, 1H, Pro-Δ-H'), 2.64 (m, 1H, H-7), 2.53 (m, 1H, H-7'), 2.20 (m, 1H, Pro-β-H), 2.07, 2.02, 2.00 (3s, 9H, $COCH_3$), 1.96 (m, 3H, Pro-β-H, Pro-γ-H),

1.41 (s, 9H, C-$(CH_3)_3$), 1.18 (d, 3H, H-6, $J_{5,6}$ = 6.5 Hz); ^{13}C NMR ($CDCl_3$, 125.7 MHz): δ (ppm) 171.3, 170.3, 169.9, 169.9, 169.2, 168.5, 167.9 (C=O), 131.7 (C-10), 118.0 (C-11), 81.9 (C-(CH_3)), 66.2, 68.6, (C-2, C-4), 68.5 (C-3), 67.9 (C-5), 67.4 (C-1), 60.0 (Pro-α-C), 50.2 (C-9), 48.6 (C-8), 47.9 (Pro-Δ-C), 41.1 (C-12), 33.5 (C-7), 28.0 (C-$(CH_3)_3$), 22.7, 20.7, 20.7 ($COCH_3$), 15.1 (C-6); FAB-MS, m/z = 640.4 (37%), $[M+1]^+$ calcd for $C_{30}H_{46}N_3O_{12}$; HRMS calcd for $C_{30}H_{46}N_3O_{12}$ 640.3082 found 640.3113.

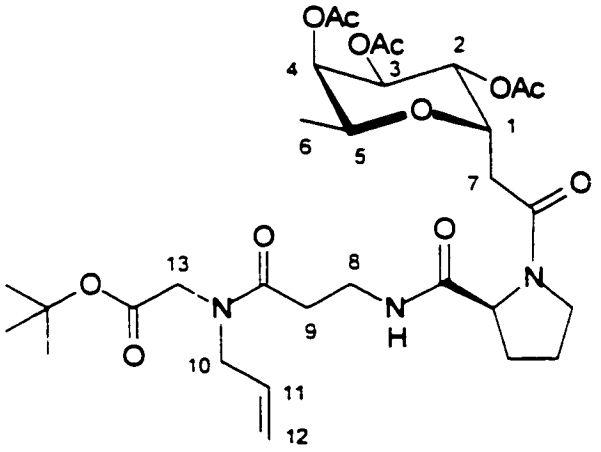

2, 3, 4-Tri-O-acetyl-α-L-fucose-L-proline-N-allyl-β-alaninyl-glycine-t-butyl ester derivative (17)

2, 3, 4-Tri-*O*-acetyl-α-L-fucose-L-proline carboxylic acid derivative **8** (132 mg, 0.307 mmol) and N-allyl-β-alaninyl-glycine-t-butyl ester **14** (100 mg, 0.413 mmol) were dissolved in DMF (2 mL) under a N_2 atmosphere. The coupling reagent used was HATU (138 mg, 0.322 mmol) with DIPEA (119 mg, 0.920 mmol) and the solution turned from deep yellow to pale yellow. The reaction stirred for 2 hours after which the reaction was judged complete by TLC

(methanol/chloroform 5/100). The solvent was removed under vacuo and the residue was purified by silica gel column chromatography using 1% methanol/chloroform as eluent to obtain a white solid having a rotamer mixture of 5:1 (97% yield); mp = 58.2 – 58.9°C; $[\alpha]_D^{23}$ = -84.7° (c = 3.19, MeOH); ^{1}H NMR ($CDCl_3$, 500 MHz): δ (ppm) 6.95 (m, 1H, NH), 5.73 (m, 1H, H-11), 5.23 (m, 2H, H-2, H-4), 5.14 (m, 3H, H-3, H-12), 4.77 (m, 1H, H-1), 4.41 (m, 1H, Pro-α-H), 3.90 (m, 5H, H-5, H-10, H-13), 3.55 (m, 1H, Pro-Δ-H), 3.47 (m, 2H, H-8) 3.41 (m, 1H, Pro-Δ-H'), 2.53 (bm, 4H, H-7, H-9), 2.15 (m, 1H, Pro-β-H), 2.08, 2.03, 2.00 (3s, 9H, $COCH_3$), 2.02 (m, 2H, Pro-γ-H), 1.91 (m, 1H, Pro-β-H), 1.41 (s, 9H, C-$(CH_3)_3$), 1.17 (d, 3H, H-6, $J_{5,6}$ = 6.6 Hz); ^{13}C NMR ($CDCl_3$, 125.7 MHz): δ (ppm) 171.9, 171.4, 170.3, 169.9, 169.1, 169.1, 168.4 (C=O), 131.4 (C-11), 117.4 (C-12), 81.7 (C-(CH_3)), 69.8, 68.6, (C-2, C-4), 68.4 (C-3), 67.8 (C-5), 67.5 (C-1), 60.2 (Pro-α-C), 51.2, 47.8 (C-10, C-13), 47.3 (Pro-Δ-C), 35.4 (C-8), 33.5 (C-7), 32.4 (C-9), 28.7 (Pro-β-C), 28.0 (C-(CH_3)$_3$), 24.7 (Pro-γ-C), 20.8, 20.7, 20.6 ($COCH_3$), 15.2 (C-6); ESI-MS, m/z = 654.2 (35%), $[M+1]^+$ calcd for $C_{31}H_{48}N_3O_{12}$.

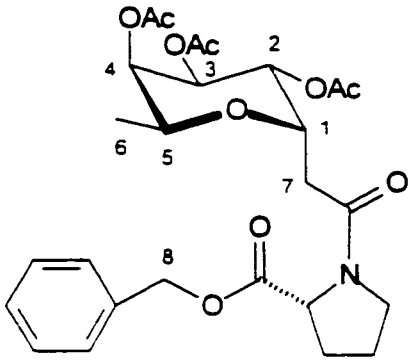

2, 3, 4-Tri-*O*-acetyl-α-L-fucose-D-proline benzyl ester derivative (18)

D-Proline benzyl ester (399 mg, 1.65 mmol) was added to a solution of compound **6** (457 mg, 1.38 mmol) dissolved in dry dichloromethane (30 mL). The coupling reagent PyBOP (931 mg, 1.79 mmol) was then added followed by NMM (0.50 mL, 4.82 mmol) to reach pH = 8 and stirred under N_2 atmosphere. The reaction was judged complete by TLC (hexane/ethyl acetate 1/1) after four hours. The solvents were removed in vacuo and the crude mixture was transferred directly to a silica gel column. The purified product was eluted using hexane/ethyl acetate 1/1 as a running solvent. The compound obtained was a white solid in 4:1 rotamer mixture (96% yield). mp = 59.6 - 59.9°C; $[\alpha]_D^{23}$ = -7.58° (c = 1.0, $CHCl_3$); ^1H NMR ($CDCl_3$, 500 MHz): δ (ppm) 7.31 (m, 5H, Ph-H), 5.32 (dd, 1H, H-2, $J_{1,2}$ = 5.1 Hz, $J_{2,3}$ = 8.9 Hz), 5.24 (m, 1H, H-4), 5.18 (m, 1H, H-3), 5.12 (d, 2H, H-8, ^2J = 12.5 Hz), 4.80 (dd, 1H, H-1, $J_{1,2}$ = 5.1 Hz, $J_{1,7}$ = 6.6 Hz), 4.50 (dd, 1H, Pro-α-H, $J_{\alpha,\beta cis}$ = 3.5 Hz, $J_{\alpha,\beta trans}$ = 8.8 Hz), 4.00 (dq, 1H, H-5, $J_{4,5}$ = 2.6 Hz, $J_{5,6}$ = 6.5 Hz), 3.63 (m, 1H, Pro-Δ-H), 3.50 (m, 1H, Pro-Δ-H'), 2.63 (d, 2H, H-7, $J_{1,7}$ = 6.6 Hz), 2.13 (m, 1H, Pro-β-H), 2.10, 1.99, 1.98 (3s, 9H, $COCH_3$), 2.02 (m, 1H, Pro-γ-H), 1.95 (m, 2H, Pro-β-H', Pro-γ-H'), 1.16 (d, 3H, H-6, $J_{5,6}$ = 6.5

Hz); ^{13}C NMR ($CDCl_3$, 125.7 MHz): δ (ppm) 171.8, 170.4, 169.5, 169.9 (O-C=O), 168.2 (N-C=O), 135.7 (C-ipso-Ph), 128.7, 128.3, 128.0 (Ph-C), 69.8 (C-4), 68.5 (C-3), 68.3 (C-1), 67.1 (C-2) 67.6 (C-5), 66.8 (C-8), 58.8 (Pro-α-C), 47.1 (Pro-Δ-C), 33.2 (C-7), 29.1 (Pro-β-C), 24.6 (Pro-γ-C), 20.7, 20.7, 20.7 ($CO\underline{C}H_3$), 15.5 (C-6); FAB-MS, m/z = 520.2 (100%), $[M + 1]^+$ calcd for $C_{26}H_{34}NO_{10}$.

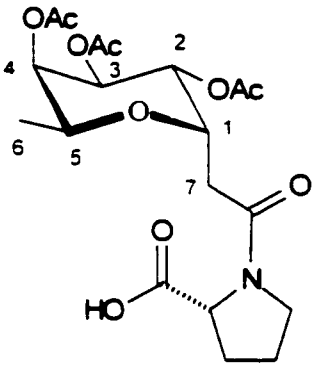

2, 3, 4-Tri-*O*-acetyl-α-L-fucose-D-proline carboxylic acid derivative (19)

Compound **18** (100 mg, 0.193 mmol) was dissolved in reagent grade methanol (11 mL). A slurry of reagent grade methanol and 10% palladium weight on activated carbon (5 mL, 67 mg respectively) was added to the reaction mixture. Hydrogen gas was bubbled through the reaction mixture. TLC analysis (ethyl acetate) confirmed that the reaction was completed in 15 minutes. Filtration followed by removal of the solvent in vacuo yielded a white solid in a 4:1 rotamer mixture (100% yield); mp = 101.0 - 101.8°C; $[\alpha]_D^{23}$ = -17.3° (c = 0.43, MeOH); ^1H NMR ($CDCl_3$, 500 MHz): δ (ppm) 5.20 (m, 3H, H-2, H-3, H-4), 4.76 (m, 1H, H-1), 4.43 (d, 1H, Pro-α-H, $J_{\alpha,\beta}$ = 6.9 Hz), 4.17 (d, 1H, H-5, $J_{5,6}$ = 5.8 Hz), 3.72 (m, 2H, Pro-Δ-H), 2.95 (dd, 1H, H-7, $J_{1,7}$ = 6.6 Hz, $^2J_{7,7'}$ = 15.7 Hz), 2.75 (dd,

1H, H-7', $J_{1,7'}$ = 5.3 Hz, $^2J_{7,7'}$ = 15.7 Hz), 2.17 (bm, 1H, Pro-β-H), 2.10, 1.94, 1.93 (3s, 9H, $COCH_3$), 2.04 (bm, 3H, Pro-β-H, Pro-γ-H), 1.09 (d, 3H, H-6, $J_{5,6}$ = 5.8 Hz); ^{13}C NMR ($CDCl_3$, 125.7 MHz): δ (ppm) 177.5 (CO_2H), 175.2, 174.5, 174.4 ($\underline{C}OCH_3$), 174.3 (N-C=O), 75.7 (C-4), 74.3 (C-3), 73.6 (C-1), 72.7 (C-2) 71.9 (C-5), 64.0 (Pro-α-C), 52.2 (Pro-Δ-C), 37.8 (C-7), 33.8 (Pro-β-C), 29.7 (Pro-γ-C), 25.1, 25.0, 24.9 ($CO\underline{C}H_3$), 20.6 (C-6); IR (thin film): ν (cm^{-1}) 3500 - 2800 (CO_2H), 1747 (C=O), 1644 (N-C=O); FAB-MS, m/z = 430.2 (100%), $[M + 1]^+$ calcd for $C_{19}H_{28}NO_{10}$.

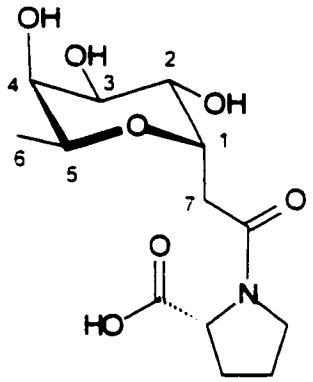

2, 3, 4-Tri-hydroxy-α-L-fucose-D-proline carboxylic acid derivative (20)

To a solution of **19** (60.0 mg, 0.140 mmol) dissolved in reagent grade methanol (5 mL) was added 0.1M sodium methoxide solution in methanol (2.0 mL) dropwise until solution was basic (pH = 10). The course of the reaction was monitored by TLC (methanol/chloroform 3/7) until complete disappearance of the starting material (2 hours). Amberlite IR-120 (H) ion – exchange resin was rinsed with methanol and then added to the solution until neutral (pH = 7). The reaction

mixture was then suction filtered and concentrated yielding a white solid (100% yield); mp = 103.4 - 104.4°C; $[\alpha]_D^{23}$ = -17.7° (c = 0.6, MeOH); ^{1}H NMR (D_2O, 500 MHz): δ (ppm) 4.53 (dd, 1H, H-1, $J_{1,2}$ = 6.5 Hz, $J_{1,7}$ = 13.2 Hz), 4.46 (dd, 1H, Pro-α-H, $J_{\alpha,\beta cis}$ = 3.7 Hz, $J_{\alpha,\beta trans}$ = 8.3 Hz), 4.03 (dd, 1H, H-2, $J_{1,2}$ = 6.5 Hz, $J_{2,3}$ = 9.0 Hz), 3.99(q, 1H, H-5, $J_{5,6}$ = 6.5 Hz), 3.83 (m, 2H, H-3, H-4), 3.74 (m, 2H, Pro-Δ-H), 2.83 (d, 2H, H-7, $J_{1,7}$ = 13.0 Hz), 2.35 (m, 1H, Pro-β-H), 2.06 (m, 3H, Pro-β-H, Pro-γ-H), 1.21 (d, 3H, H-6, $J_{5,6}$ = 6.3 Hz); ^{13}C NMR (D_2O, 125.7 MHz): δ (ppm) 175.8 (CO_2H), 171.8 (N-C=O), 72.1 (C-1), 71.1 (C-3), 69.5 (C-4), 67.80 (C-5) 67.0 (C-2), 58.9 (Pro-α-C), 47.5 (Pro-Δ-C), 30.3 (C-7), 28.7 (Pro-β-C), 23.9 (Pro-γ-C), 15.1 (C-6); ESI-MS, m/z = 304.1 (37%), $[M + 1]^+$ calcd for $C_{13}H_{22}NO_7$.

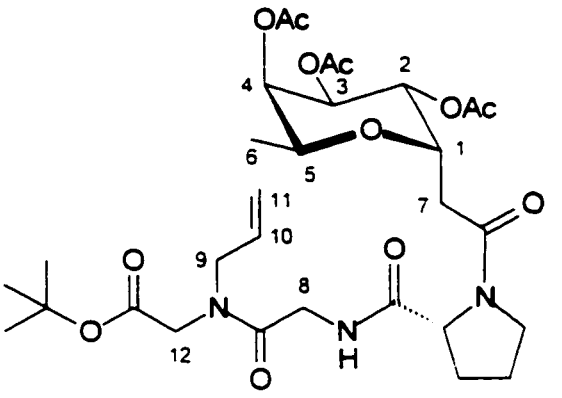

2, 3, 4-Tri-O-acetyl-α-L-fucose-D-proline-N-allyl-glycyl-glycine-t-butyl ester derivative (21)

Compound **19** (100 mg, 0.234 mmol) and glycyl-N-allylglycine-t-butyl ester **13** (70.0 mg, 0.281 mmol) were dissolved in DMF (3 mL). HATU (93.4 mg, 0.246 mmol) and DIPEA (0.12 mL; 0.702 mmol) were added and the reaction mixture turned from deep yellow to pale yellow. After 18 hours, the reaction was judged

complete by TLC (methanol/chloroform 5/100) and the solvent was removed under vacuo. The residue was purified by silica gel column chromatography using 1% methanol/chloroform as eluent to yield the pure compound as a white solid in 3:2 rotamer mixture (65% yield); mp = 70.9 – 71.9°C; $[\alpha]_D^{23}$ = -7.76° (c = 4.0, MeOH); ^{1}H NMR (acetone-d_6, 500 MHz): δ (ppm) 7.30 (m, 1H, NH), 5.92 (m, 1H, H-10), 5.20 (m, 5H, H-2, H-3, H-4, H-11), 4.78 (m, 1H, H-1), 4.51 (m, 1H, Pro-α-H), 4.18 (q, 1H, H-5, $J_{5,6}$ = 6.3 Hz), 4.02 (m, 6H, H-8, H-9, H-12), 3.76 (m, 1H, Pro-Δ-H), 3.65 (m, 1H, Pro-Δ-H'), 2.96 (dd, 1H, H-7, $J_{1,7}$ = 7.2 Hz, $^2J_{7,7'}$ = 16.0 Hz), 2.78 (dd, 1H, H-7', $J_{1,7'}$ = 3.4 Hz, $^2J_{7,7'}$ = 16.0 Hz), 2.23 (m, 1H, Pro-β-H), 2.10, 1.94, 1.95 (3s, 9H, $COCH_3$), 1.94 (m, 3H, Pro-β-H, Pro-γ-H), 1.42 (s, 9H, C-$(CH_3)_3$), 1.09 (d, 3H, H-6, $J_{5,6}$ = 6.4 Hz); ^{13}C NMR (acetone-d_6, 125.7 MHz): δ (ppm) 172.7, 172.2, 170.9, 170.3, 170.1, 169.6, 169.0 (C=O), 134.2 (C-10), 117.5 (C-11), 81.6 ($\underline{C}$-(CH_3)), 71.4, 69.2, 68.4 (C-2, C-3, C-4), 70.0 (C-1), 67.7 (C-5), 60.8 (Pro-α-C), 51.0, 50.0, 49.3 (C-8, C-9, C-12), 48.0 (Pro-Δ-C), 41.4 (C-7), 33.6 (Pro-β-C), 28.2 (C-($\underline{C}H_3)_3$), 23.3 (Pro-γ-C), 20.8 20.6, 20.5 ($CO\underline{C}H_3$), 16.4 (C-6); CI-MS, m/z = 640 (7.4%), $[M+1]^+$ calcd for $C_{30}H_{46}N_3O_{12}$.

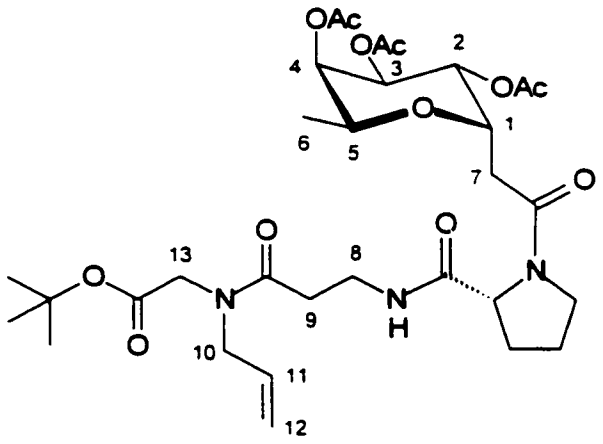

2, 3, 4-Tri-O-acetyl-α-L-fucose-D-proline-N-allyl-β-alaninyl-glycine-t-butyl ester derivative (22)

Compound **19** (207 mg, 0.484 mmol) and β-alaninyl-N-allylglycine-t-butyl ester **14** (144 mg, 0.595 mmol) were dissolved in DMF (1 mL) under N_2 atmosphere. HATU (219 mg, 0.559 mmol) and DIPEA (0.25 mL, 0.742 mmol) were added and the reaction mixture turned from deep yellow to pale yellow. After 2 hours, the reaction was judged complete by TLC (methanol/chloroform 5/100) and the solvent was removed under vacuo. The residue was purified by silica gel column chromatography using 2% methanol/chloroform as eluent to yield the pure compound as a white solid in 4:1 rotamer mixture (97% yield); mp = 57.3 – 58.4°C; $[\alpha]_D^{23}$ = -15.3° (c = 0.69, MeOH); ^{1}H NMR ($CDCl_3$, 500 MHz): δ (ppm) 6.96 (m, 1H, NH), 5.73 (m, 1H, H-11), 5.29 (dd, 1H, H-2, $J_{1,2}$ = 5.0 Hz, $J_{2,3}$ = 8.9 Hz), 5.23 (m, 1H, H-4), 5.16 (m, 3H, H-3, H-12), 4.78 (dd, 1H, H-1, $J_{1,7}$ = 6.5 Hz), 4.41 (m, 1H, Pro-α-H), 3.98 (m, 5H, H-5, H-10, H-13), 3.60 (m, 1H, Pro-Δ-H), 3.48 (m, 3H, Pro-Δ-H', H-8), 2.61 (d, 2H, H-7, $J_{1,7}$ = 6.5 Hz), 2.46 (bm, 2H, H-9), 2.19 (m, 1H, Pro-β-H), 2.10, 1.99, 1.97 (3s, 9H, $COCH_3$), 1.92 (m, 3H, Pro-

β-H, Pro-γ-H), 1.42 (s, 9H, C-$(CH_3)_3$), 1.17 (d, 3H, H-6, $J_{5,6}$ = 6.5 Hz); ^{13}C NMR ($CDCl_3$, 125.7 MHz): δ (ppm) 172.0, 171.3, 170.4, 170.1, 169.5, 169.1, 168.4 (C=O), 132.4 (C-11), 117.4 (C-12), 81.6 (C-(CH_3)), 69.7, 68.56, (C-4), 68.5, 68.4 (C-1, C-3), 68.0 (C-2), 67.7 (C-5), 60.2 (Pro-α-C), 51.2, 49.3 (C-10, C-13), 47.4 (Pro-Δ-C), 35.3 (C-8), 33.3 (C-7), 33.4 (C-9), 28.5 (Pro-β-C), 28.0 (C-$(CH_3)_3$), 24.7 (Pro-γ-C), 20.7 ($COCH_3$ x2), 20.6 ($COCH_3$), 15.6 (C-6); ESI-MS, m/z = 654.2 (21%), $[M+1]^+$ calcd for $C_{31}H_{48}N_3O_{12}$.

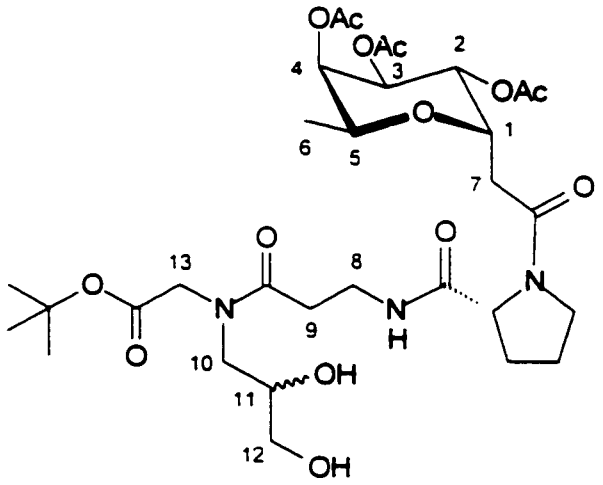

Compound 23

Compound **22** (100 mg, 0.153 mmol) and NMO (35.9 mg, 0.306 mmol) were dissolved in acetone (4.5 mL) and water (0.5 mL). A catalytic amount of osmium tetroxide (small crystal) was added and turned the reaction mixture from clear to yellow. The course of the reaction was monitored by TLC (methanol/chloroform 1/10) until complete disappearance of the starting material (3 hours). A solution of 10% sodium bisulfite was added (4.5 mL) and the crude

reaction mixture was washed with water (100 mL x 1) and extracted with CH_2Cl_2 (100 mL x 4). The organic layers were combined and dried over $NaSO_4$, filtered and the solvent was removed under reduced pressure. The concentrate was purified by silica gel column chromatography with 5% methanol/chloroform as eluent. The compound obtained was a white solid (98% yield); mp = 66.8 – 67.9°C; $[\alpha]_D^{23}$ = -13.7° (c = 0.5, MeOH); ^{1}H NMR ($CDCl_3$, 500 MHz): δ (ppm) 6.98 (m, 1H, NH), 5.30 (m, 1H, H-2), 5.23 (m, 1H, H-4), 5.17 (m, 1H, H-3), 4.77 (m, 1H, H-1), 4.32 (m, 1H, Pro-α-H), 4.00 (m, 3H, H-5, H-13), 3.61 (m, 2H, Pro-Δ-H, H-11), 3.48 (m, 7H, Pro-Δ-H', H-8, H-10, H-12), 2.65 (m, 2H, H-7), 2.40 (bm, 2H, H-9), 2.13 (m, 1H, Pro-β-H'), 2.11, 1.99, (2s, 6H, $COCH_3$), 2.05 (m, 3H, Pro-β-H, Pro-γ-H) 1.95 (2s, 3H, $COCH_3$), 1.44, 1.43, 1.43 (3s, 9H, C-$(CH_3)_3$), 1.16 (m, 3H, H-6); ^{13}C NMR ($CDCl_3$, 125.7 MHz). δ (ppm) 173.8 – 168.73 (cluster of C=O rotamer peaks), 82.3 (C-(CH_3)), 70.0 (C-4), 69.7(C-11), 68.7 (C-1), 68.3 (C-3), 67.7 (C-2), 67.6 (C-5), 63.9(C-12), 63.5 (C-10), 60.6 (Pro-α-C), 52.5 (C-13), 47.6 (Pro-Δ-C), 35.4 (C-8), 33.2 (C-7), 32.5 (C-9), 29.0 (Pro-β-C), 28.0 (C-$(CH_3)_3$), 24.7 (Pro-γ-C), 20.7, 20.7, 20.6 ($COCH_3$), 15.8 (C-6); ESI-MS, m/z = 688.1 (2%), $[M+1]^+$ calcd for $C_{31}H_{50}N_3O_{14}$.

Compound 23

Compound **22** (100 mg, 0.153 mmol) was dissolved in tert-butanol/water 1/1 (4 mL) and cooled to 0°C. The Sharpless reagent AD mix – α (0.159 mg) was added and the reaction was monitored by TLC (methanol/chloroform 1/10).

After stirring overnight, the reaction was still incomplete and many spots had formed. The reaction was discarded.

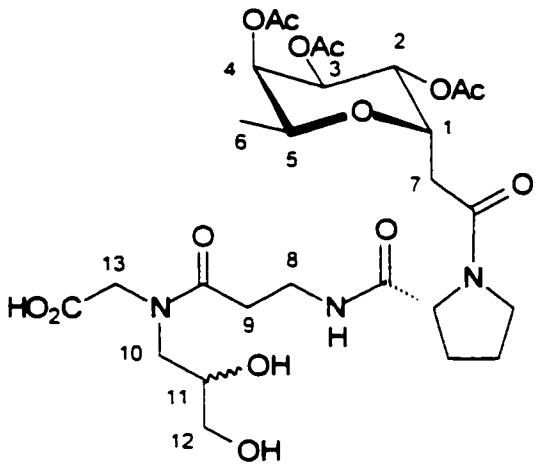

24

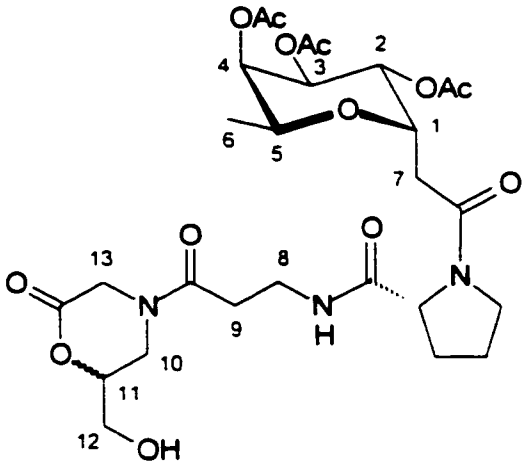

25

Compounds 24 and 25

Compound **23** was dissolved in trifluoroacetic acid/dry dichloromethane 1/1 (4.6 mL) under a N_2 atmosphere. The reaction was monitored by TLC (methanol/chloroform 1/5) until complete disappearance of the starting material (30 min). The solvents were removed under reduced pressure yielding both products **24** and **25** as a clear, colourless oil. Due to line broadening and mixture of products, not all peaks could be assigned with certainty. ^{1}H NMR ($CDCl_3$, 500 MHz): δ (ppm) 6.93 (bm, 1H, NH), 5.28 (m, 1H, H-2), 5.23 (m, 1H, H-4), 5.16 (m, 1H, H-3), 4.76 (m, 1H, H-1), 4.22 (m, 4H, Pro-α-H, H-11, H-13), 3.98 (m, 1H, H-5), 3.73 (m, 6H, Pro-Δ-H, H-8, H-12), 2.8-2.3 (bm, 2H, H-9), 2.67 (m, 2H, H-7), 2.12, 1.99, 1.97 (3s, 9H, $COCH_3$), 2.06 (m, 4H, Pro-β-H, Pro-γ-H) 1.15 (m, 3H, H-

6); ^{13}C NMR ($CDCl_3$, 125.7 MHz): δ (ppm) 171.0 – 169.0 (cluster of C=O rotamer peaks), 71.1 (C-4), 68.8 (C-1), 68.3 (C-3), 67.7 (C-2), 67.5 (C-5), 63.8 (C-12), 62.0 (C-10), 61.3 (C-13), 60.7 (C-11), 60.5 (Pro-α-C), 47.8 (Pro-Δ-C), 35.5 (C-8), 33.7, 33.4 (C-7, C-9), 29.1 (Pro-β-C), 24.7 (Pro-γ-C), 20.8, 20.7, 20.6 ($CO\underline{C}H_3$), 15.8 (C-6); ESI-MS, m/z = 632.1 (10%), $[M+1]^+$ calcd for $C_{27}H_{42}N_3O_{14}$ (compound **24**), ESI-MS, m/z = 613.1 (3%), $[M+1]^+$ calcd for $C_{27}H_{40}N_3O_{13}$ (compound **25**)

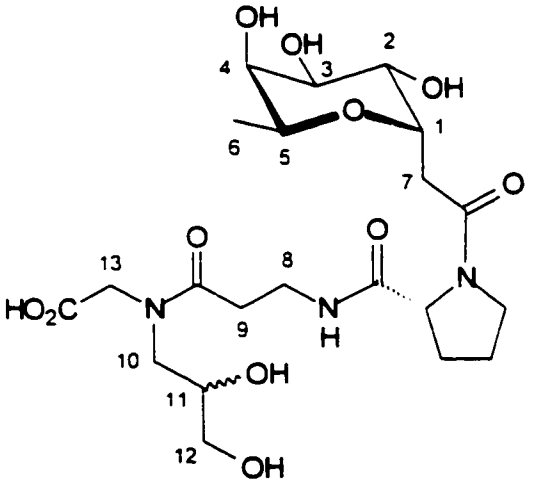

Compound 26

To a solution of **24** and **25** (20 mg) dissolved in reagent grade methanol (3 mL) was added 0.1M sodium methoxide solution in methanol (0.62 mL) dropwise until the solution was basic (pH = 10) under N_2 atmosphere. The course of the reaction was monitored by TLC (methanol/chloroform 1/5) until the two spots of products **24** and **25** decreased in Rf values (1 hour). The deacetylated products **24** and **25** were treated with 0.01M NaOH and the TLC system was changed (methanol/chloroform 3/5) and the reaction was judged complete after 1 hour.

Amberlite IR-120 (H) ion - exchange resin was rinsed with methanol and then added to the solution until slightly acidic (pH ≈ 6.5). The reaction mixture was filtered and the solvents were removed under reduced pressure yielding a beige solid. (100% yield); mp = 133.0 – 135.1°C; $[\alpha]_D^{23}$ = -26.5° (c = 0.37, MeOH); ^{1}H NMR (DMSO, 500 MHz): δ (ppm) 8.18 (t, 1H, NH, J = 5.8 Hz), 7.61, 6.88, 6.58, 6.06, 5.43 (rotamer peaks of OH), 4.34 (m, 1H, H-1), 4.25 (dd, 1H, Pro-α-H, $J_{\alpha,\beta cis}$ = 3.3 Hz, $J_{\alpha,\beta trans}$ = 8.3 Hz), 3.68 (m, 5H, H-2, H-3, H-4, H-5, Pro-Δ-H), 3.38 (m, 9H, H-8, H-10, H-11, H-12, H-13), 3.04 (m, 1H, Pro-Δ-H'), 2.43 (dd, 1H, H-7, $J_{1\,7}$ = 10.0 Hz, $J_{7\,7'}$ = 16.5 Hz), 2.31 (m, 2H, Pro-β-H), 2.17 (m, 1H, H-7'), 1.81 (m, 2H, Pro-γ-H), 1.69 (m, 2H, H-9), 1.04 (d, 3H, H-6, $J_{5,6}$ = 6.4 Hz); ^{13}C NMR (DMSO, 125.7 MHz): δ (ppm) 173.5, 172.6, 171.9, 170.0 (C=O), 71.7 (C-1), 70.1, 68.9, 68.8, 68.0, 67.4 (C-2, C-3, C-4, C-5, C-11), 63.7, 63.41 (C-10, C-12), 59.8 (Pro-α-C), 54.4 (C-13), 46.6 (Pro-Δ-C), 35.3, 34.9, 32.3, 31.5 (C-7, C-8, C-9, Pro-β-C), 22.6 (Pro-γ-C), 16.6 (C-6); (+)ESI-MS, m/z = 528.1 (4%), $[M+Na]^+$ calcd for $C_{21}H_{36}N_3O_{11}$, (-)ESI-MS, m/z = 504.0 (3%); $[M-1]^+$ calcd for $C_{21}H_{34}N_3O_{11}$.

References

(1) Simanek, E. E.; McGarvey, G. J.; Jablonowski, J. A.; Wong, C. H. *Chem. Rev.* **1998**, 98, 833.

(2) Zuckerman, R. N.; Kerr, J. M.; Kent, S. H.; Moos, W. H. *J. Am. Chem. Soc.* **1992**, 114, 10646.

(3) Uchiyama, T.; Woltering, T.J.; Wong, W.; Lin, C. C.; Kajimoto, T.; Takebayashi, M.; Weiz-Schmidt, G.; Asakura, T.; Noda, M.; Wong, C. H. *Bioorg. Med. Chem.* **1996**, 4, 1149.

(4) Abika, A.; Roberts, J. C.; Takemasa, T; Masamura, M. *Tetrahedron Lett.* **1986**, 27, 4537.

(5) Shishido, K.; Shitara, E.; Komatsu, H.; Hiroya, K.; Fukumoto, K.; Kametani, T. *J. Org. Chem.* **1986**, 51, 3007.

(6) Kokke, W.; Varkvisser, F. *J. Org. Chem.* **1974**, 39, 1535.

(7) Stewart, W. E.; Siddall, T. H. *Chem. Rev.* **1970**, 70, 517.

(8) Breznik, M.; Grdadolnik, S. G.; Giester, G.; Leban, I.; Kikelj, D.; *J.Org. Chem.* **2001**, 66, 7044.

(9) Carpino, L. A.; El-Faham, A.; Minor, C. A.; Albericio, F.; *J. Am. Soc. Chem. Commun.* **1994**, 201.

(10) Boons, G. J. In *Carbohydrate Chemistry*; Boons, G. J. Ed.; Blackie Academic & Professional: London, 1998; p 1.

(11) Harris, R.; Graham, R. K.; Field, R. A.; Milton, M. J.; Ernst, B.; Magnani, J. L.; Homans, S. W. *J. Am. Chem. Soc.* **1999**, 121, 2546.

(12) Poppe, L.; Brown, G. S.; Philo, J. S.; Pandurang, V. N.; Shah, B. H. *J. Am. Chem. Soc.* **1997**, 119, 1727.

(13) Deisenhofer, J. *Biochemistry*, **20**, 2361-2370.

(14) Koeller, K. M.; Wong, C. H.; *Chem. Rev.* **2000**, 100, 4465.

(15) Alon, R.; Hammer, D. A.; Springer, T. A. *Nature* **1996**, 379, 266.

(16) Chandrasekaran, E. V.; Jain, R. K.; Larsen, R. D.; Wlasichuk, K.; Matta, K. L. *Biochemistry* **1995**, 34, 2925.

(17) Kanwar, S.; Johnston, M. B.; Kubes, P. *Circ. Res.* **1995**, 77, 879.

(18) Alon, R.; Fuhlbrigge, R. C.; Findger, E. B.; Springer, T. A. *J. Cell. Biol.* **1996**, 135, 849.

(19) Sharon, N.; Lis, H. *Sci. Amer.* **1993**, 82.

Chapter 3. Olefin Metathesis: A Second Approach Towards the Synthesis of SLe^x Mimetics.

3.1. Introduction

Reactions involving carbon-carbon bond formation and cleavage are the most powerful tools available in modern synthetic design. Olefin metathesis reactions catalyzed by certain transition metals are capable of executing both of these processes. Redistribution of C-C double bonds is presently a very reliable, effective and relatively simple procedure in organic synthesis. The developments of novel metal carbene catalysts during the last decade, has played a significant role in making olefin metathesis an attractive alternative to previous olefin chemistry.

Previously, metal catalyzed olefin synthesis had been difficult to initiate and control as the use of poorly defined heterogeneous/homogeneous catalysts under harsh conditions had rendered them incompatible with many functional groups.[1] In order to improve catalytic design and activity, a greater understanding of the mechanism was necessary. The first proposed mechanism that was confirmed by experimental data and consistent with results was developed by Chauvin in 1971. The foundation of the mechanistic pathway proved to be dependent upon the formation of a metallacyclobutane intermediate via a [2+2] cycloaddition followed by a [2+2] cycloreversion as seen in Figure 3.1.1.[2]

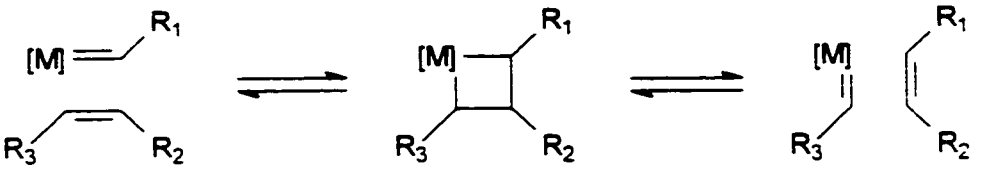

Figure 3.1.1. Initial mechanism proposed by Chauvin.[2]

Single component metal catalysts demonstrated the greatest potential for this mechanism. The first well-defined catalyst of this generation to be recorded were the molybdenum alkylidenes **1** of Schrock *et al.*[3] (Figure 3.1.2.). These catalysts which are highly active react with a variety of substrates and functional groups and are recently commercially available. Schrock's catalyst (**1**) is one of the few reagents that can perform olefin metathesis on tri- and tetra-substituted alkenes and is not affected by the electronic nature of the reactant. However, this early transition metal catalyst is limited in its design. The molybdenum centre is oxophilic and is sensitive to moisture and air in the solvent and in the substrates. These complications lead to a short shelf-life and make it difficult to prepare, and work with, as solvents need to be degassed and products purified and dried before each reaction.[4]

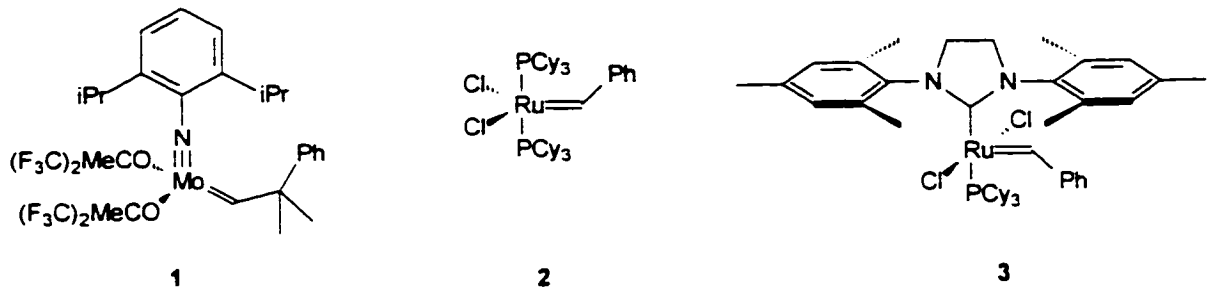

1 2 3

Figure 3.1.2. Transition metal catalysts of interest.

The problematic nature of Schrock's catalyst was, in part, overcome by the ruthenium transition metal catalysts of Grubbs *et al.*[5] These consisted of moisture and air tolerant and water soluble catalysts. The most effective of the early Grubbs' catalysts is the benzylidene ruthenium compound **2**.[6] This catalyst improved initiation rates and is tolerant to many functional groups thus increasing the scope of synthetic possibilities. The ruthenium carbene has long been commercially available since it is easy to prepare and is less prone to decomposition. The practicality and diversity of this catalyst has triggered an avalanche of ideas and research into this area of synthesis and in all areas of organic chemistry. Although, **2** is convenient to use and has a variety of applications, it also has synthetic limitations. For example, the benzylidene ruthenium is much less active than Schrock's catalyst and cannot react with electron poor or sterically hindered alkenes.

A new generation of catalysts has emerged to overcome the restrictions of these former transition metal catalysts. Grubbs and co-workers have created a "designer" catalyst (**3**) that is capable of the breadth and scope of the

benzylidene ruthenium catalyst while being as reactive as the early metal catalysts.[7] This saturated N-heterocyclic carbene (modified Grubbs') has all of the same excellent qualities as **2**, as well as, the capability of reacting with electron poor and sterically hindered substrates.[8]

The progression of metal carbene catalysts has optimized the utility of the metathesis mechanism in a variety of applications such as ring closing metathesis, ring opening metathesis and cross metathesis. These enticing applications have had profound implications on the rational of modern synthetic and retrosynthetic design.

Ring closing metathesis (RCM) has generated a cascade of interest due to the simple and gentle conditions resulting in the formation of cyclic compounds (Figure 3.1.3.).

Figure 3.1.3. General representation of ring closing metathesis.

This new methodology has proven to be important in many difficult bicylic[9]. fused ring closures[10] and macrocylclizations[11] in natural and non-natural product syntheses. The proposed catalytic ring closing metathesis mechanism is in

equilibrium and can be driven to the formation of products by the removal of volatile ethylene gas as depicted in Figure 3.1.4.

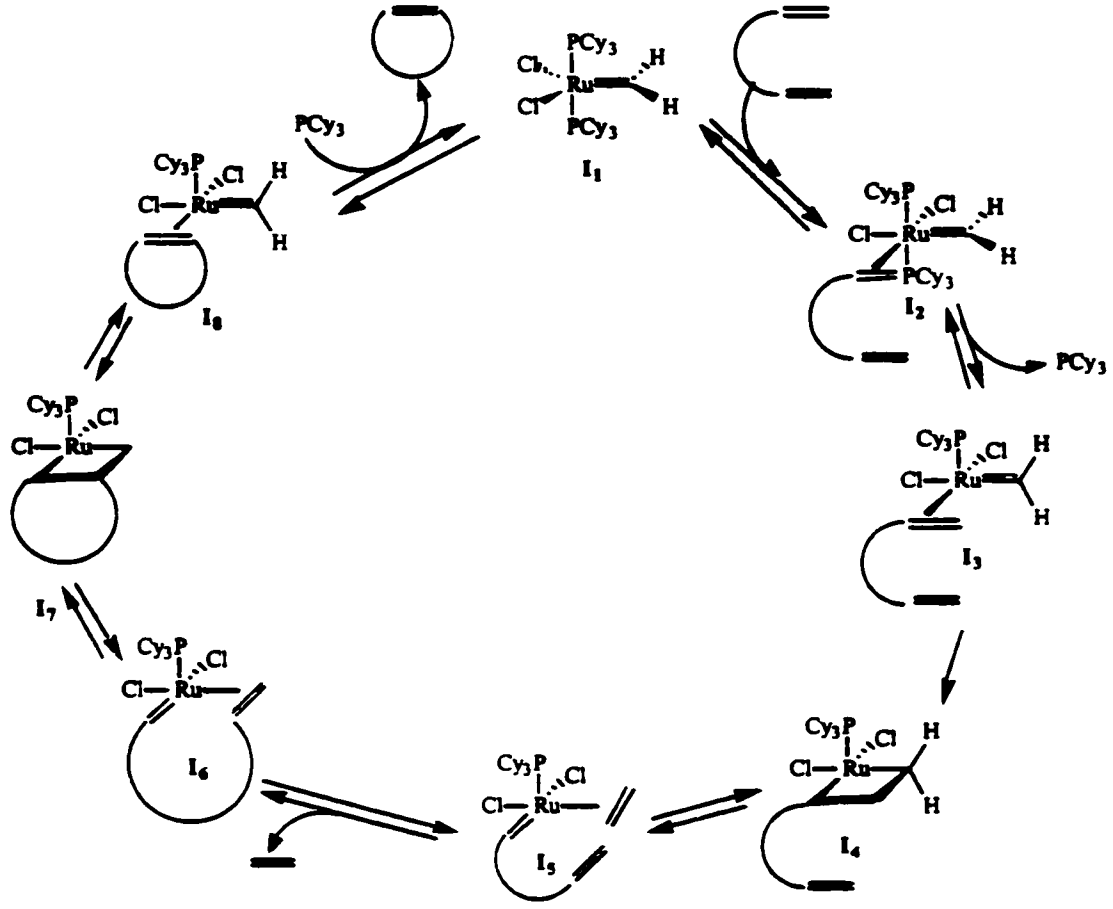

Figure 3.1.4. Proposed ring closing metathesis mechanistic pathway.[12]

The catalyst precursor **2** is converted to the active species after the first cycle. The substrate coordinates to the metal and the resulting strain releases the phosphine ligand. The [2+2] cylcoaddition in the formation of the metallacyclobutane is presumed to be the rate determining step and is followed

by the [2+2] cycloreversion. The second intramolecular alkene coordinates, releasing ethylene gas followed by another [2+2] cycloaddition and cycloreversion. The recoordination of the phosphine ligand allows for the release of the desired cyclic product. The RCM is very stereoselective and generates expected major products under appropriate dilute conditions.

The difference in the activity and performance of the Grubbs' catalysts **2** and **3** are evident in light of the mechanistic pathway. The modified Grubbs' catalyst (**3**) has an electron donating nitrogen ligand that assists in the dissociation of the phosphine ligand in a synergistic effect that increases its activity.[4] A comparison of reactivities of **1-3*** (*backbone of C-N bond is unsaturated) on a D-glucose derivative (Scheme 3.1.1., Table 3.1.1.) highlights the performance of each catalyst.[13]

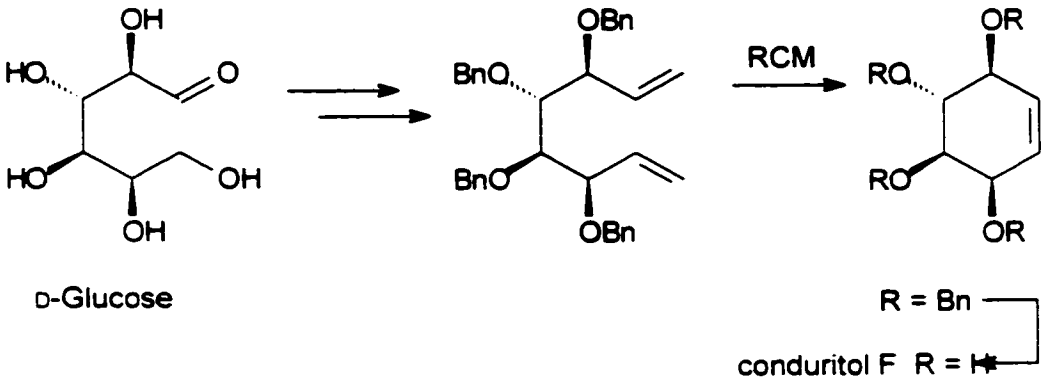

Scheme 3.1.1. RCM of D-glucose derivative using three different metal carbenes.

Table 3.1.1. Comparison of metal catalyst RCM reactivity.

Catalyst	Reaction Time [h]	Yield [%]
1	1	92
2	60	32
3	2	89

It is evident that the slightly modified version of **3** (previous studies show slight increase of activity of **3** (saturated N-ring) over that of the modified **3** (unsaturated N-ring))[14] illustrates tremendous increase in reactivity engendered by the nitrogen ligands and is an extremely attractive alternative to the limited functional group acceptance and sensitivity of Schrock's catalyst.

An interesting example of RCM in carbohydrate chemistry was used in the key step for the construction of the macrocycle in the formal synthesis of the complex natural product Tricolorin A by Fürstner *et al.*[15]

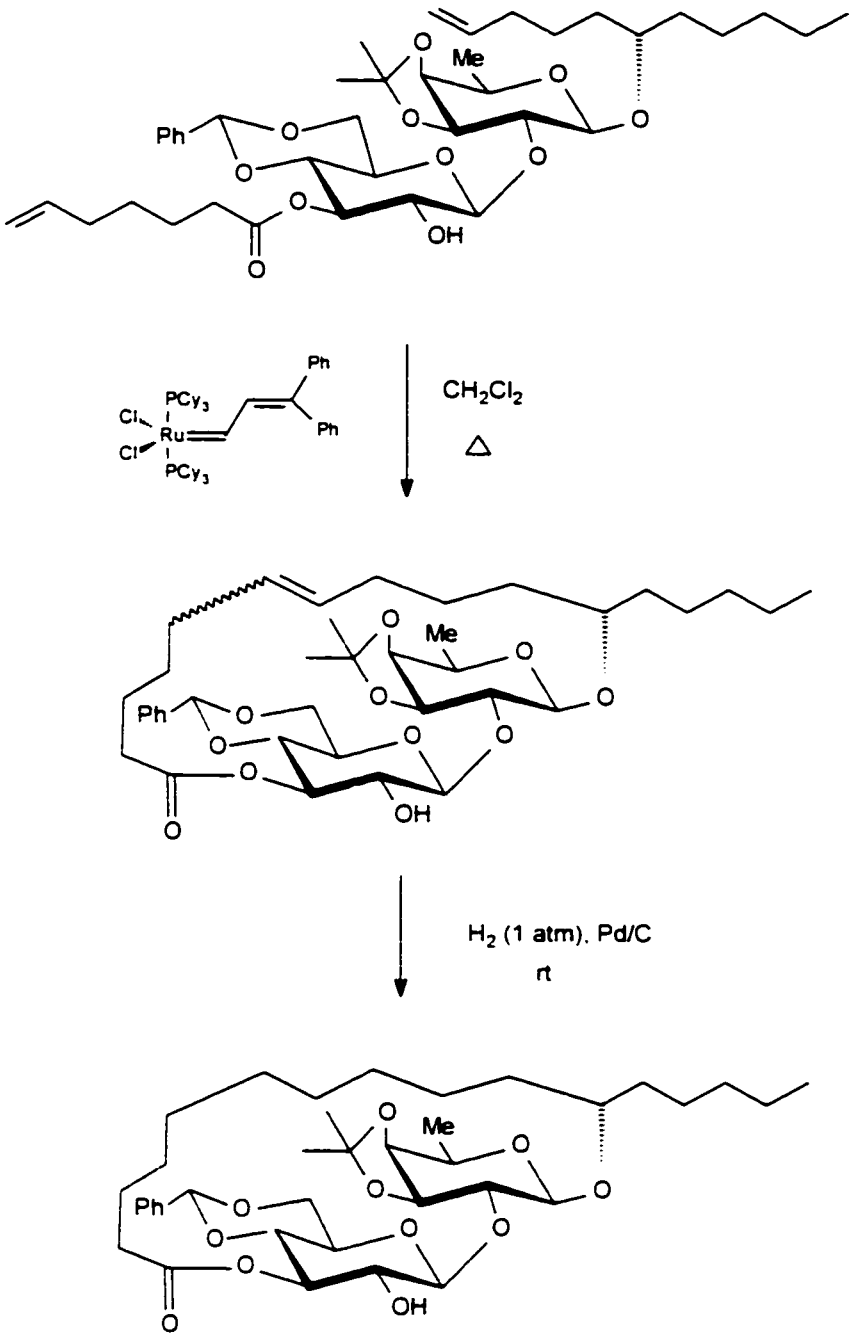

Scheme 3.1.2. RCM macrocyclization in the synthesis of Tricolorin A.[15]

Tricolorin A has significant cytotoxin properties against breast cancer and cultured P-388 cell lines.[16] This is an excellent example of the compatibility of the Grubbs' catalyst in the presence of free hydroxyl groups and of the performance and selectivity witnessed by the 19-membered ring formation achieved in two steps with 77% yield (E/Z mixture).

Ring opening metathesis polymerization (ROMP) is driven by the release of ring strain of the starting cyclic olefin (Figure 3.1.5.). The mechanism is the reverse of RCM (Figure 3.1.4.).

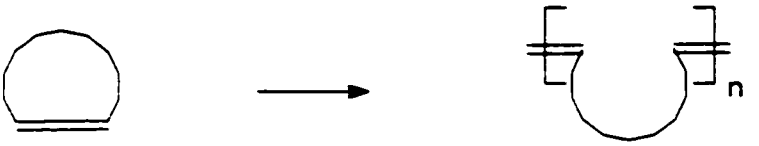

Figure 3.1.5. General representation of ring opening metathesis polymerization.

ROMP has the potential to be very useful in organic synthesis, however, this reaction is restricted by poor chemo-, regio-, and stereoselectivity.[16] A practical application of ROMP is in the area of polymer chemistry. The metal carbene reacts with a series of cyclic alkenes resulting in an unsaturated backbone that can directly incorporate monomer functionality.[1] An added feature of ROMP is the possible elongation of the polymer faster than termination. This yields a living polymer that could be employed in the syntheses of oligomers.

An interesting example of ROMP in carbohydrate chemistry involves the formation of 'sugar-coated' polymers using norbene-based polymers resulting in

water-soluble polymers.[17] Also, Kiesling *et al.*[18] have used a ROMP reaction to create a carbohydrate polymer capable of blocking cell agglutination (Scheme 3.1.3.).

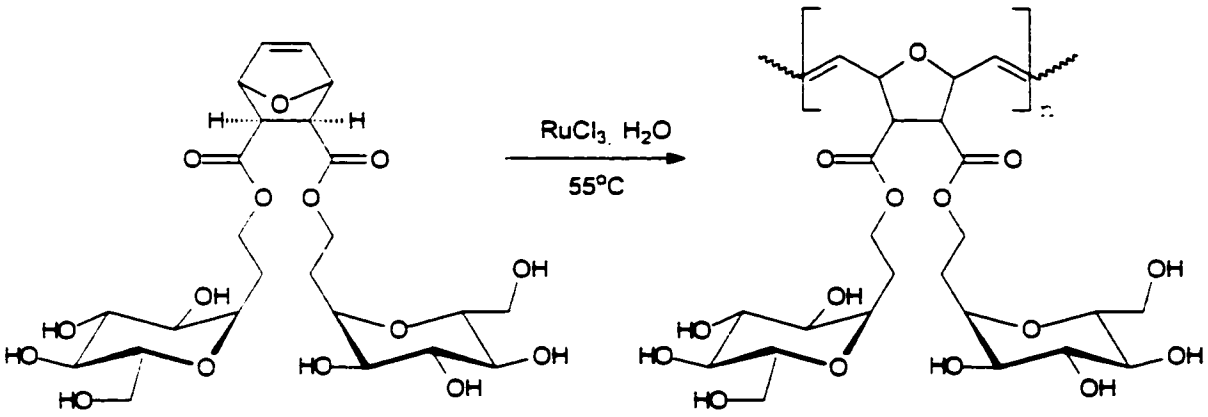

Scheme 3.1.3. Construction of polyvalent sugars using ROMP.

This result has medicinal applications such as biological multivalency studies, regulation of cell adhesion and immobilization of specific cell types.[16]

The entropically challenged cross metathesis (CM) has a wider scope than the ROMP but more limitations than the RCM. Cross metathesis is the formation of a double bond from two different olefin substrates (Figure 3.1.6.). The mechanism of CM is similar to that of RCM (Figure 3.1.1.).

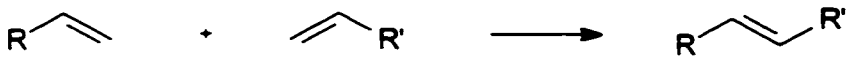

Figure 3.1.6. General representation of cross metathesis.

The limitations of CM arise from poor selectivity and low yields due to possible formation of the two undesired homodimers. However, proper choice of substrates can minimize homodimerization and maximize yields as sterically hindered terminal alkenes do not undergo self-metathesis.[19] Recent advances in metal carbene catalysts have renewed interest in CM. Grubbs *et al.*[20] have generated unhindered terminal alkenes with internal disubstituted alkenes in good selectivity and high yields. Crowe *et al.*[21] have also achieved selectivity by modifying terminal alkenes with conjugated π systems such as acrolein to functionalize terminal alkenes. Although CM is limited in some respects, the mild conditions make it a useful alternative to the Wittig reaction. In addition, the scope of this reaction is still increasing to include metathesis of tri-substituted alkenes with the emergence of the second generation, designer catalysts.[22]

An interesting application of CM in carbohydrate chemistry is the head to tail condensation of two different saccharides to produce pseudodisaccharides (Scheme 3.1.4.).[23]

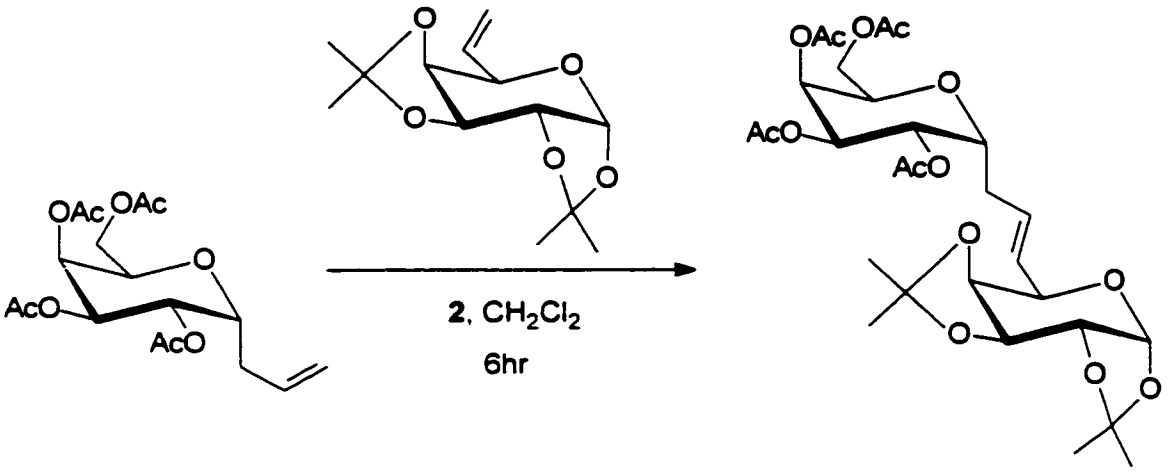

Scheme 3.1.4. Example of pseudodisaccharides produced by cross metathesis.[23]

These simple glycomimetics are strong applicants for drug design due to the enzyme-resistant nature of C-linked sugars. Roy *et al.*[24] have been able to use self-metathesis in the presence of free hydroxyl groups with O- and C-linked glycosides to form homodimers. This provides an easier pathway to carbohydrate drug design as the intermolecular metathesis and the metal carbene catalyst are tolerable to unprotected sugars eliminating the usual protection/deprotection steps of most carbohydrate syntheses.

Sequential metathesis has elevated retrosynthetic design to minimize the number of synthetic steps while maximizing molecular complexity. These domino reactions can quickly and easily form target molecules since all the bond transformations are sequential and take place in a one-pot synthesis. Plumet *et al.*[25] have devised a unique and novel synthetic route to the synthesis of 7-oxanorbornene derivatives using a metathesis domino reaction (Scheme 3.1.5.).

The bicyclic alkynyl starting material is treated with Grubbs' catalyst **2** in the presence of allyl acetate resulting in ROM of the bicyclic ring. Then CM of the allyl acetate with the metal carbene centre followed by RCM of the free allyl and alkyne all under the same reaction conditions, without any additional reagent, yield the desired product.

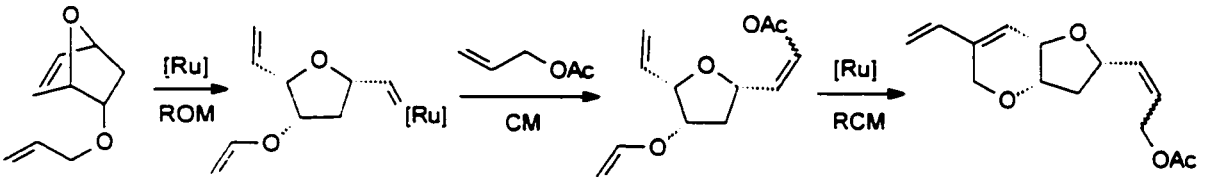

Scheme 3.1.5. Sequential ring opening, cross metathesis and ring closing metathesis in the synthesis of 7-oxanorbornene derivatives.[25]

This highly orchestrated domino approach has tremendous potential to produce extremely elegant syntheses of past, present and future synthetic targets.

3.2. Results and Discussion

3.2.1. Introduction

As discussed earlier, olefin metathesis is a powerful synthetic tool. In the past decade, there has been an incredible amount of work examining and evaluating the scope of this reaction as evident from the many publications and reviews referenced in section 3.1.1. The excitement of this exploding field of

synthesis triggered an interest in the use of metal carbenes in the synthesis of C-linked SLe^x mimetics. It was hypothesized that olefin metathesis could be a novel approach to define the structure of SLe^x mimetics by incorporating a double bond to introduce structural rigidity in the molecule in lieu of the proline ring. This would create an opportunity to couple long alkyl chains to the peptide backbone or carbohydrate portion using olefin metathesis on various alkenyl alkyl chains. The addition of lipophatic groups is known to increase the binding affinity of SLe^x to the selectins (section 1.5.3.).[26] This alkene precursor would also be capable of coupling with different series of simple peptide and peptoid chains to construct mimetics in a convergent approach. The stability, commercial availability and most importantly functional group tolerance of the ruthenium carbene catalysts make Grubbs' reagent an ideal candidate to use in this model study.

3.2.2. Strategies

The use of Grubbs' catalyst has recently extended to the synthesis of SLe^x mimetics. While this work was in progress, Wong *et al.*[27] have constructed a SLe^x mimetic template with a terminal alkene to participate in CM with alkenyl aromatics to determine their added effects on binding affinities to E- and P-selectins (Scheme 3.1.6.). This study prompted the thought of utilizing metal carbene chemistry as the key reaction to create a novel synthetic pathway to form glycomimetics.

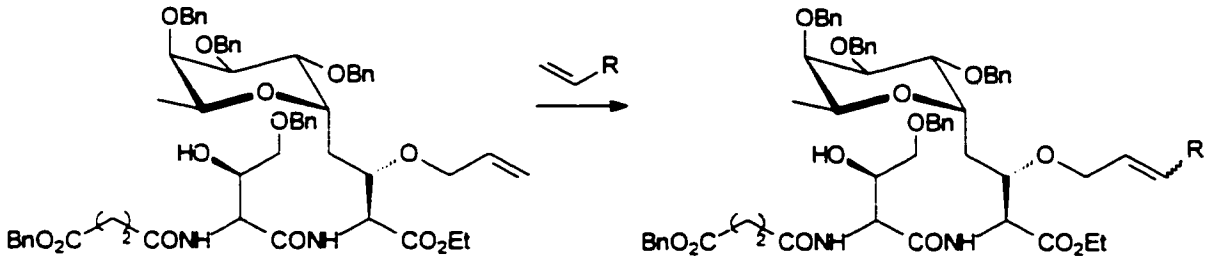

Scheme 3.1.6. Cross metathesis of SLe^x mimetic template with C-aryl alkenes.[27]

Our main objective was to enhance and simplify the structure of the bulky tetrasaccharides by constructing glycomimetics while utilizing the unique chemistry of olefin metathesis. These mimetics needed to be more stable, smaller and have higher binding affinities of SLe^x. As described earlier (section 1.1.4.), we decided to keep fucose and simplify the remaining saccharide linkages by replacing them with a peptide/peptoid chain having the same important hydroxyl and carboxylate functional groups. It was proposed that similar to the previous approach of Chapter 2, the glycomimetic could be synthesized using a convergent approach. We already had in hand different peptoid chains that could be coupled to a carboxylic acid chain extending from the C-fucoside. However, it was necessary to construct the sugar derivative portion of the compound to include some group that would decrease the flexibility of the branch as proline had in the previous studies. Olefin metathesis was used to introduce a double bond on the carbohydrate branch that would replace proline in providing rigidity to the molecule (Scheme 3.1.7.).

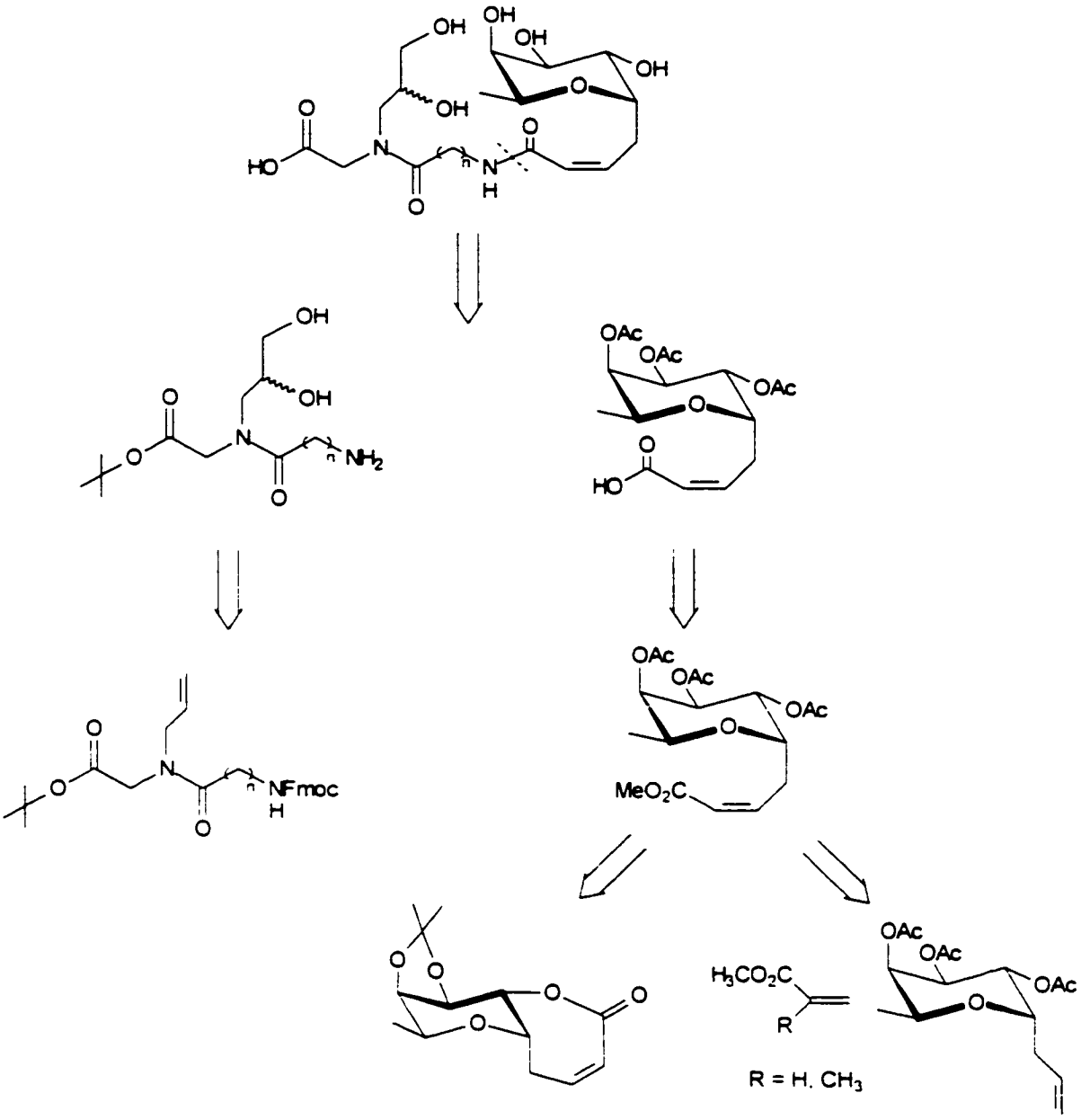

Scheme 3.1.7. Retrosynthetic design of SLe^x mimetic incorporating olefin metathesis.

It was hypothesized that a *cis* π bond would afford the best opportunity to define the shape of the glycomimetic at the junction and increase the potential for H-bonding causing the molecule to adopt a hair pin structure similar to that of the bound conformation of SLe^x.

3.2.3. Olefin metathesis using Grubbs' catalyst (2).

Initially Grubbs' catalyst was first used in the Roy's research group to investigate the scope of the catalyst on carbohydrates that varied in protecting groups, O-/C-linkages, and it's tolerance to unprotected sugars in the synthesis of homodimers.[16] Homodimers are useful biological molecules that mimic larger glycomimetics/glycodendrimers but are small enough to pass easily through the cell membrane. Moreover, ligand-induced dimerization activates polypeptide growth factors that in turn transduce their signals into the cell for growth, differentiation, migration or apoptosis.[28]

Previously synthesized 3-(2, 3, 4-tri-*O*-acetyl-α-L-fucopyranosyl)propene (**I**) was ideal for this study. Self-metathesis of 3-(2, 3, 4-tri-*O*-acetyl-α,β-L-fucopyranosyl)propene with 10 mol% of **2** in a concentrated solution of dichloromethane and refluxed at 40°C proceeded to completion in 12 hours. Purification by silica gel column chromatography gave the homodimer product **4** in 95% yield as a mixture of isomers in the ratio of 3:1 (E/Z) (Scheme 3.1.8.).

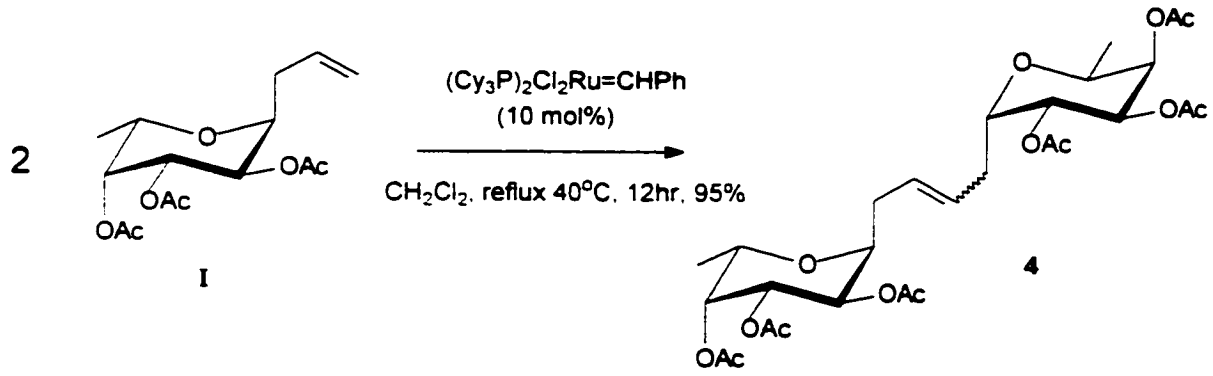

Scheme 3.1.8. Synthesis of allyl 2, 3, 4-tri-C-acetyl-α-L-fucopyranoside homodimer.

NMR confirmed the structure of the product (disappearance of the methylene protons (H-9)) and the presence of geometric isomers. The ratio of *cis* to *trans* was determined using ^{1}H NMR and the γ-effect[29] of ^{13}C NMR. This confirmed that the *trans* isomer was the major product. The compatibility of the self metathesis of 3-(2, 3, 4-tri-*O*-acetyl-α-L-fucopyranosyl)propene with Grubbs' catalyst (**2**) encouraged the idea of a ring closing metathesis of a derivative of 3-(2, 3, 4-tri-*O*-acetyl-α-L-fucopyranosyl)propene in order to guarantee a *cis* alkene. This had not been previously attempted in the construction of SLe^{x} mimetics.

The 3-(2, 3, 4-tri-*O*-acetyl-α-L-fucopyranosyl)propene was determined not to be a suitable starting material for the starting point of this new idea. We required a starting allyl α-L-C-fucopyranoside that was protected at C-3 and C-4, but unprotected at C-2 in order to add an acryloyl group for RCM. The appropriate starting material was 3-(2, 3, 4-tri-*O*-hydroxyl-α-L-fucopyranosyl)propene (**II**) (Scheme 2.1.3.). The 3 and 4 positions in compound

II were protected as an acetonide. This was accomplished by dissolving **II** in dry acetone with 2,2-dimethoxypropane and acidic resin under N_2 atmosphere at room temperature. After 5 hours the reaction was complete and the product was purified by silica gel column chromatography producing **5** in 95% yield (Scheme 3.1.9.).

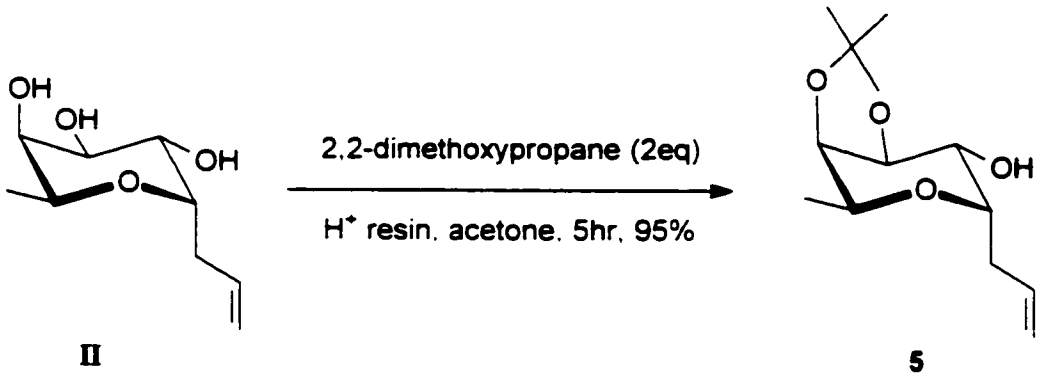

II **5**

Scheme 3.1.9. Synthesis of O-3, O-4 protected allyl C-α-L-fucopyranoside.

The structure of the molecule was confirmed by ^1H NMR that showed an allylic group between δ 5 ppm and δ 6 ppm, hydroxyl at δ 2.23 ppm and two additional methyl groups at δ 1.47 ppm and δ 1.31 ppm. Combination of the ^{13}C NMR and DEPT confirmed the presence of a quaternary carbon of the acetonide. The molecular ion was confirmed by FAB-MS (m/z=229.1 (29%)).

The next step in the sequence was to add a functionalized alkene to the C-2 position of the fucopyranoside derivative. Subsequent ring closure would force the double bond to adopt the less favourable *cis* configuration that was desired for the SLe^x glycomimetic. Acryloyl chloride was chosen as the alkene since it would form a lactone upon RCM that could be attacked by a nucleophile

and hydrolyzed to yield a carboxylic acid for future peptide couplings. Triethylamine and starting material **5** were dissolved in dichloromethane and brought to 0°C. Acryloyl chloride was added dropwise over 20 minutes. The reaction was complete after 1 hour. Purification by extraction and column chromatography yielded **6** in 81% yield (Scheme 3.1.10.).

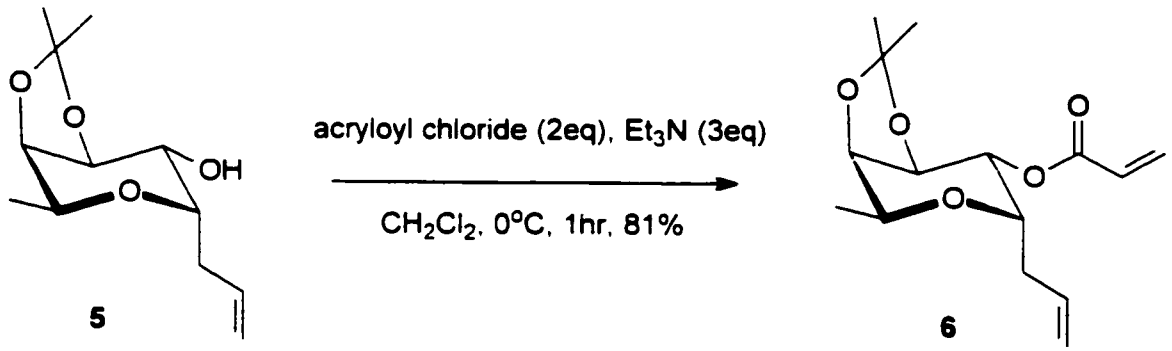

Scheme 3.1.10. Synthesis of RCM precursor **6**.

The structure of **6** was confirmed by NMR. The proton spectrum showed two terminal alkene protons within the range of δ 5.02-6.42 ppm and H-2 had a downfield shift of δ 1.2 ppm confirming the addition of the acryloyl moiety. The carbon spectrum had a carbonyl peak at δ 164.87 ppm ascribed to the ester carbon. The presence of the molecular ion was confirmed by mass spectrometry (CI-MS, m/z=238 (46%)).

The fucoside derivative **6** was dissolved in dry dichloromethane with 10 mol% of Grubbs' catalyst (**2**) and refluxed at 40°C overnight. Column

chromatography afforded dimer **7** in 45% yield (Scheme 3.1.11.). No evidence of the desired monomeric compound was found.

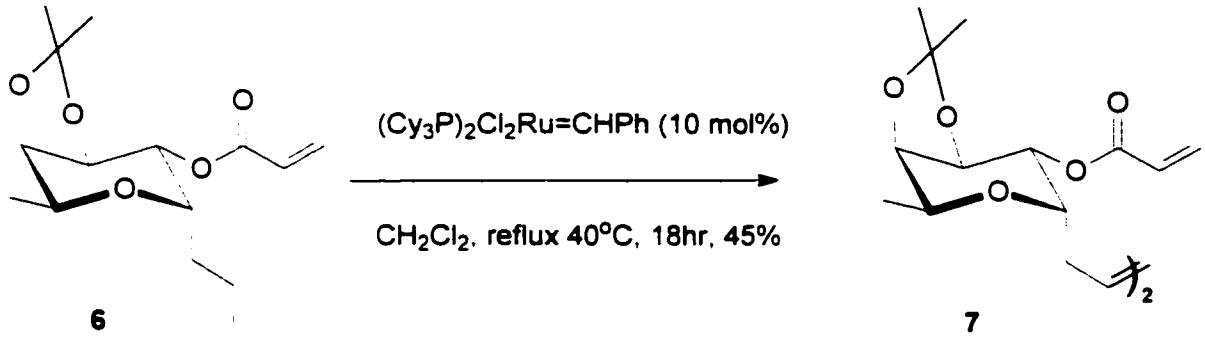

Scheme 3.1.11. Attempted RCM of **6** using Grubbs' catalyst **2** resulting in dimer **7**.

The dimer structure of the product was evident by H^1 NMR analysis. It showed the presence of two terminal double bond protons at δ 5.86 ppm and the mass spectrum did not show the presence of the expected molecular ion. Upon further analysis it was determined that only the homodimer was formed in the ratio of 7:6 (E/Z). This was a disappointing result but not completely unexpected as the Grubbs' catalyst (**2**) was known to be less reactive towards electron poor alkenes such as the one in **6**. The experiment was an exploration into the reactivity of the catalyst and provided valuable information for future reference.

3.2.4. Olefin metathesis using modified Grubbs' catalyst (3)

Introduction, later that year, of a new, more reactive Grubbs' catalyst (**3**) renewed interest in the original concept of RCM as a synthetic route to form a *cis*

double bond in the SLe^x mimetics. The modified Grubbs' catalyst was reported to be just as stable and tolerable to functional groups as the parent compound but more reactive with electron poor and sterically hindered alkenes.

To study the activity of the modified Grubbs' catalyst we experimented with the same starting material, 3-(2, 3, 4-tri-*O*-acetyl-α-L-fucopyranosyl)propene (**I**) and two different conjugate alkenes that could later be reacted with a peptide/peptoid chain. One alkene was electron poor while the other alkene was both electron poor and sterically hindered.

The first alkene used was the electron poor methyl acrylate (excess) that was dissolved with compound **I** and 5 mol% of **3** in dry dichloromethane and refluxed at 45°C for six hours. TLC showed only one spot for the mixture of *cis* and *trans* isomers of the resultant product. However, these isomers were separable using silica gel column chromatography to afford **8a** and **8b** (9:1/E:Z) (Scheme 3.1.12.).

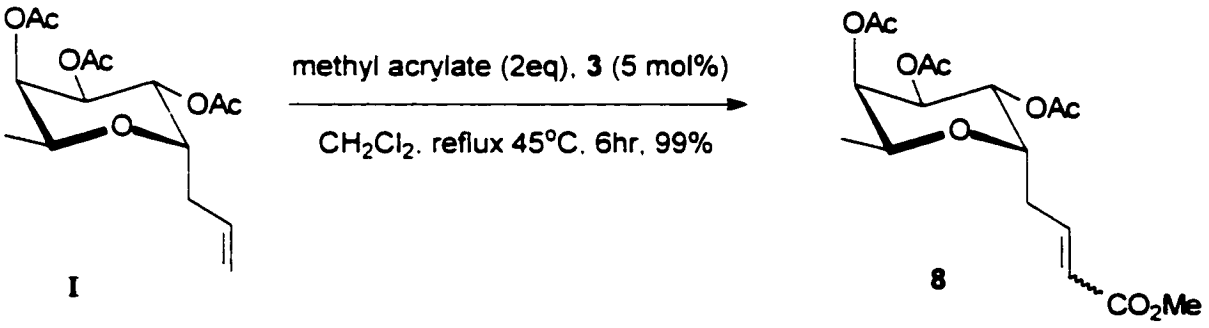

I 8

Scheme 3.1.12. Reaction of modified Grubbs' metal carbene **3** with electron poor alkene to form **8a**, **8b**.

The major product was determined to be the *trans* isomer using the proton coupling constant (J = 15.6 Hz). The ^{1}H NMR also confirmed that the structure of both isomers had two alkenyl protons and the presence of an additional deshielded methyl group at δ 3.71 ppm. The ^{13}C NMR confirmed the presence of the methyl ester from the carbonyl peak at δ 166.5 ppm and the deshielded methyl peak at δ 51.5 ppm. Electron spray ionization showed the presence of the molecular ion for both geometric isomers.

This was an expected and yet encouraging result even though the major isomer was *trans*. At least it was possible to separate the *cis*-double bond and use this substrate to synthesize the desired mimetics. The *trans*-double bond could also be used to examine the affect of the different isomers on the binding affinity of the glycomimetics. Thus, from one reaction, two possible substrates were separated and characterized for future study.

It was now established that the modified Grubbs' catalyst **3** was capable of reacting with electron poor alkenes. Thus another challenging feature was added to the alkene. Methyl methacrylate was the choice for a sterically hindered, electron poor alkene. Excess acrylate was dissolved with compound **I** and 5 mol%. of the modified Grubbs' reagent (**3**). The reaction refluxed overnight at 45°C and the TLC plate showed one major spot and two minor spots. The one minor spot was determined to be the dimer and the other was unreacted starting material. Unlike the previous reaction, it was not surprising that this reaction proceeded slower and was unable to consume all the starting material. The extra feature of steric hindrance would account for the slightly poorer results.

Purification by silica gel chromatography gave only the *trans* product **9** in 86% yield (Scheme 3.1.13.).

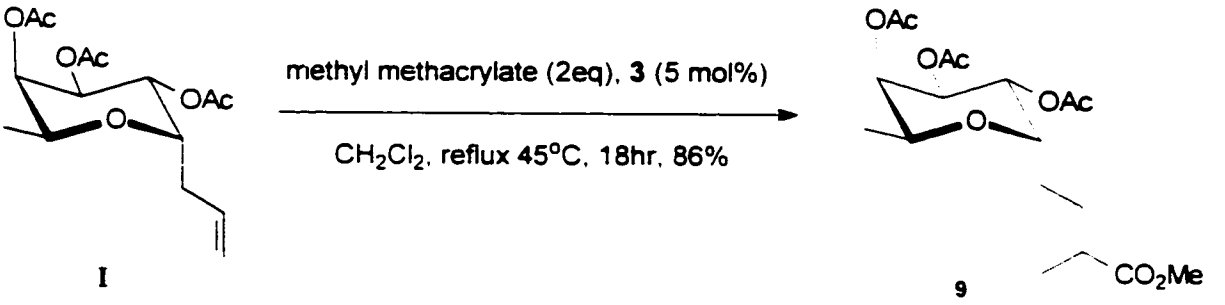

I 9

Scheme 3.1.13. CM of modified Grubbs' catalyst with electron poor and sterically hindered alkene to yield **9**.

The ^{1}H NMR of **9** was similar to that of **8** except for an additional methyl group doublet at δ 1.83 ppm and one less alkenyl proton. ^{13}C NMR showed the carbon peak of the methyl at δ 12.7 ppm. Due to lack of another akenyl proton to determine coupling constants. it was necessary to perform a NOSEY and nOe difference experiment. Both experiments showed through-space interactions between the alkene methyl group and H-7, providing evidence that the *trans* double bond had been formed. The presence of the molecular ion was confirmed by ESI mass spectrometry.

Although this reaction yielded only the less desirable *trans* double bond, it was an excellent example of the increased reactivity of the modified Grubbs' catalyst **3** in comparison to what was known of the parent compound. It has also been difficult to achieve stereoselectivity with cross metathesis and this reaction is one of a few examples that can produce only one isomer. The *trans* product

would also be a possible additional candidate for studying SLe^x mimetics as it has an extra methyl group that could positively or negatively affect the binding affinity of the glycomimetic.

The previous results were very promising and gave us extra incentive to try the RCM of **6** with the less restrictive and more reactive modified Grubbs' catalyst **3**. The starting material **6** was dissolved in dilute dry dichloromethane with 5 mol% of **3** and refluxed at 45°C for four hours. The solvent was diluted to encourage intramolecular ring closing metathesis and discourage intermolecular cross metathesis. TLC analysis showed one major spot and two minor spots. The minor spots were the dimer and remaining starting material. The product was purified with column chromatography and gave **10** in 62% yield (Scheme 3.1.14.).

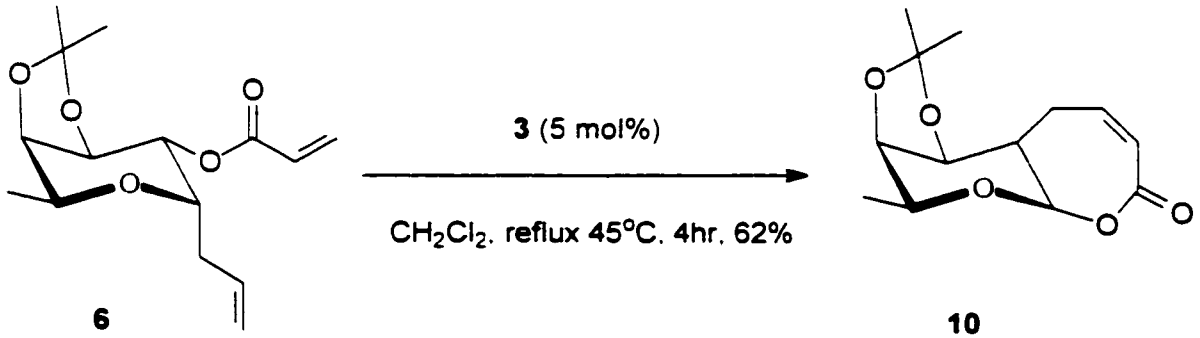

6 **10**

Scheme 3.1.14. RCM of **6** with modified Grubbs' catalyst **3** to form **10**.

The structure of **10** was confirmed by NMR by the presence of two alkene protons and ESI-mass spectrometry confirmed the presence of the molecular ion.

Finally, we obtained the ring which could be attacked by a nucleophile and hydrolyzed to form a carboxylic acid. The carboxylic could then be coupled to many different peptide and peptoid chains to produce a library of SLe^x mimetics. Unfortunately, due to time constraints we had to stop at the RCM that formed the desirable *cis*-double bond. However, this partial synthesis can be used to continue the quest to find a superior alternative for the poorly binding, short lived, anti-inflammatory sialyl $Lewis^x$.

3.3. Conclusions

It is clear that the metal carbene catalysts have had a tremendous impact on modern synthetic chemistry. The ruthenium catalysts of Grubbs have proven to be reliable, effective and easy to use on a multitude of various functional groups. The effect of this incredible tool is still under development and the scope of this reaction has yet to be realized. This is evident from the research presented in this thesis. The introduction of the modified Grubbs' catalyst enabled us to solve the ring closing metathesis problem creating a novel synthetic pathway to the desired target mimetics, effectively making possible a past impossible reaction. The modified Grubbs' reagent proved to be capable of reacting with sterically hindered and electron poor alkenes. This improved activity provided a possible simple route to form a difficult, functionalized *cis*-double bond. This could be an important precursor in the formation of future potent glycomimetic, anti-inflammatory agents.

3.4. Experimental Methods

Olefin Metathesis in the Synthesis of SLe^x Mimetics

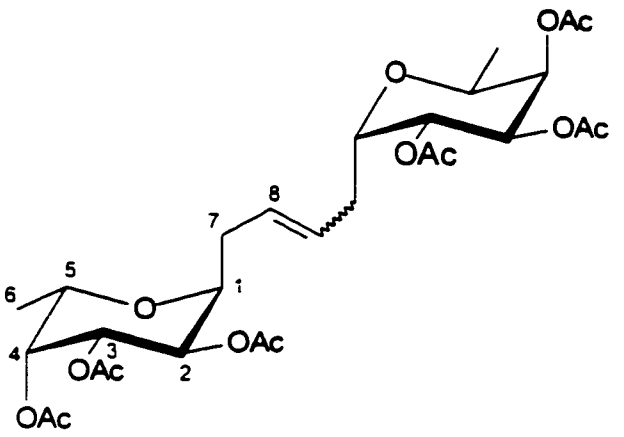

Allyl 2, 3, 4-tri-*O*-acetyl-C-α-L-fucopryranoside homodimer (4)

Grubbs' catalyst **2** (8 mg, 10 mol%) was added to a solution of compound **I** (104 mg, 0.331 mmol) dissolved in dry dichloromethane (0.5 mL). The purple reaction mixture was heated under reflux (40°C) and the solution turned black over 1 hr. The reaction was judged complete by TLC (hexane/ethyl acetate 4/6) after an additional 11 hours. The solution was concentrated under reduced pressure and the residue was purified by silica gel column chromatography using 5% gradient increases of ethyl acetate (5% - 40%) with hexanes to give homodimer **4** as a clear oil having an E/Z of 5:2 (95% yield); ^{1}H NMR ($CDCl_3$, 500 MHz): δ (ppm) 5.48 (t, 2H, H-8' *cis*, J = 4.6 Hz), 5.45 (t, 2H, H-8' *trans*, J = 3.7 Hz), 5.27-5.18 (m, 4H, H-2, H-4), 5.15 (dd, 2H, H-3, $J_{2,3}$ = 9.9 Hz, $J_{3,4}$ = 3.4 Hz), 4.18 (m, 2H, H-1), 3.91 (m, 2H, H-5), 2.55 (m, 2H, H-7), 2.25 (m, 2H, H-7), 2.10, 2.02, 1.97 (3s, 18H, $COCH_3$), 1.11 (2d, 6H, H-6, $J_{5,6}$ = 6.4 Hz) ^{13}C NMR

($CDCl_3$, 125.7 MHz): δ (ppm) 170.0-170.5 (C=O), 128.2 (C-8' *trans*), 126.9 (C-8' *cis*), 29.3 (C-7 *trans*), 24.5 (C-1' *cis*), 15.9 (C-6); FAB-MS calcd. for $C_{28}H_{40}O_{14}$: 600.2; found 601.2 (M+1).

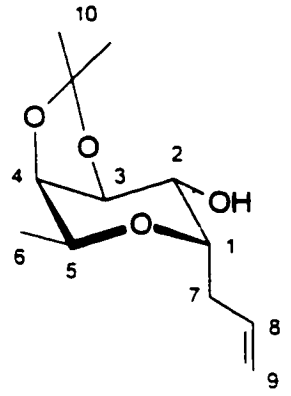

Compound 5[30]

Compound **II** (100 mg, 531 mmol) and 2,2-dimethoxypropane (0.13 mL, 1.06 mol) were dissolved in acetone (1 mL). H^+ resin (330 mg) was added and the reaction mixture stirred under N_2 atmosphere. TLC analysis (ethyl acetate/hexane 2/1) showed that the reaction was complete after 5 hours. The reaction mixture was suction filtered, concentrated and purified by silica gel column chromatography using ethyl acetate/hexane 3/10 as an eluent to give compound **5** (95% yield); $[\alpha]_D^{23}$ = -88.8° (c = 0.74, $CHCl_3$); ^1H NMR ($CDCl_3$, 500 MHz): δ (ppm) 5.82 (m, 1H, H-8), 5.12 (m, 1H, H-9), 5.05 (m, 1H, H-9'), 4.20 (dd,1H, H-3, $J_{2,3}$ = 3.6 Hz, $J_{3,4}$ = 7.1 Hz), 4.09 (dd, 1H, H-4, $J_{3,4}$ = 7.2 Hz, $J_{4,5}$ = 2.0 Hz), 4.07 (dd, 1H, H-5, $J_{4,5}$ = 1.9 Hz, $J_{5,6}$ = 6.5 Hz), 3.98 (dx3, 1H, H-1, $J_{1,2}$ = 2.8 Hz, $J_{1,7}$ = 7.2 Hz), 3.75 (bs, 1H, H-2), 2.34 (dx3, 2H, H-7, $J_{1,7}$ = 7.2 Hz, $^2J_{7,7'}$ = 1.3

Hz), 2.23 (bs, 1H, OH), 1.47 (s, 3H, H-10), 1.31 (s, 3H, H-10'), 1.24 (d,3H, H-6, $J_{5,6}$ = 6.5 Hz); ^{13}C NMR ($CDCl_3$, 125.7 MHz): δ (ppm) 134.5 (C-8), 117.3 (C-9), 109.1 (quaternary-C), 75.3 (C-4), 75.0 (C-3), 70.8 (C-1), 69.1 (C-2), 65.2 (C-5), 34.7 (C-7), 30.0 (C-10), 24.6 (C-10'), 17.6 (C-6); FAB-MS, m/z = 229.1 (29%), $[M+1]^+$ calcd for $C_{12}H_{21}O_4$.

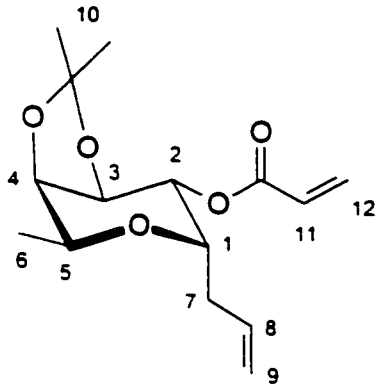

Compound 6

Compound **5** (328 mg, 1.44 mmol) was dissolved in dry dichloromethane (10 mL) at 0°C under a stream of N_2 gas. Triethylamine (0.60 mL, 4.32 mmol) was slowly added followed by addition of acryloyl chloride (0.23 mL, 2.89 mmol) via a dropping funnel over 20 minutes. The reaction was judged complete by TLC (hexane/ethyl acetate 2/1) after 1 hour. The reaction mixture was washed with water (100 mL x 1). Aqueous layers were extracted with dichloromethane (100 mL x 3). The organic extracts were combined and dried over $NaSO_4$. The solvent was removed under reduced pressure and the concentrate was purified by column chromatography on silica gel with 5% ethyl acetate/hexanes as eluent to yield **6** as a clear, colourless oil (81% yield); $[\alpha]_D^{23}$ = -71.5° (c = 1.17, $CHCl_3$);

^{1}H NMR ($CDCl_3$, 500 MHz): δ (ppm) 6.42 (dd, 1H, H-12, $J_{11,12trans}$ = 17.3 Hz, $^2J_{12,12'}$ = 1.3), 6.11 (dd, 1H, H-11, $J_{11,12cis}$ = 10.4 Hz, $J_{11,12trans}$ = 17.3 Hz), 5.86 (dd, 1H, H-12, $J_{11,12cis}$ = 10.4 Hz, $^2J_{12,12'}$ = 1.3 Hz), 5.77 (m, 1H, H-8), 5.02 (m, 3H, H-2, H-9), 4.25 (dd, 1H, H-3, $J_{2,3}$ = 3.3 Hz, $J_{3,4}$ = 7.3 Hz), 4.14 (dx3, 1H, H-1, $J_{1,2}$ = 2.9 Hz, $J_{1,7}$ = 7.3 Hz), 4.09 (dd, 1H, H-4, $J_{3,4}$ = 7.3 Hz, $J_{4,5}$=1.8 Hz), 4.02 (dq, 1H, H-5, $J_{4,5}$ = 1.3 Hz, $J_{5,6}$ = 6.5 Hz), 2.32 (m, 1H, H-7), 2.19 (m, 1H, H-7'), 1.49 (s, 3H, H-10), 1.30 (s, 3H, H-10'), 1.27 (d, 3H, H-6, $J_{5,6}$ = 6.5 Hz); ^{13}C NMR ($CDCl_3$, 125.7 MHz): δ (ppm) 164.9 (C=O), 133.6 (C-8), 131.7 (C-12), 127.9 (C-11), 117.5 (C-9), 109.6 (quaternary-C), 75.2 (C-4), 72.3 (C-3), 69.9 (C-2), 69.7 (C-1), 65.5 (C-5), 35.3 (C-7), 26.7 (C-10), 24.5 (C-10'), 17.7 (C-6); CI-MS, m/z = 283 (46%), $[M+1]^+$ calcd for $C_{15}H_{23}O_5$.

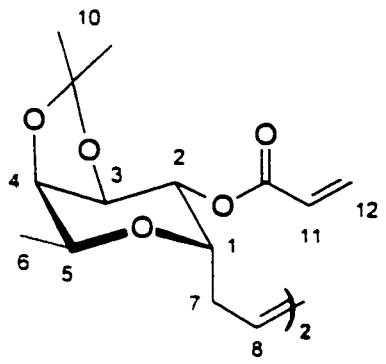

Compound 7

Grubbs' catalyst **2** (8.8 mg, 10 mol%) was added to a solution of **6** (30 mg, 0.106 mmol) dissolved in dry dichloromethane (30 mL). The purple reaction mixture refluxed at 40°C and after 18 hours was judged complete by TLC (hexane/ethyl acetate 2/1). The solvent was removed under vacuo and the

concentrate was purified by silica gel column chromatography using ethyl acetate/hexane 1/2 as eluent to give compound **7** as an off-white, clear oil having an E/Z ratio of 7/6 (45% yield); ^{1}H NMR ($CDCl_3$, 500 MHz): δ (ppm) 6.41 (dd, 1H, H-11, $J_{10,11trans}$ = 17.3 Hz, $^{2}J_{11,11'}$ = 1.3 Hz), 6.11 (dd, 1H, H-10, $J_{10,11cis}$ = 10.5 Hz, $J_{10,11trans}$ = 17.4 Hz), 5.86 (dd, 1H, H-11, $J_{10,11cis}$ = 10.5 Hz, $^{2}J_{11,11'}$ = 1.3 Hz), 5.45, 5.39 (mx2, 1H, H-8 *cis*, H-8 *trans*), 5.01, 4.99 (mx2, 1H, H-2 *cis*, H-2 *trans*, $J_{2,3}$ = 3.2 Hz), 4.24 (dd, 1H, H-3, $J_{2,3}$ = 3.2 Hz, $J_{3,4}$ = 7.2 Hz), 4.09 (m, 2H, H-1, H-4), 4.00 (m, 1H, H-5), 2.24 (bm, 2H, H-7), 1.50, 1.49 (sx2, 3H, H-10 *trans*, H-9 *cis*), 1.31 (s, 3H, H-9'), 1.27 (d, 3H, H-6, $J_{5,6}$ = 6.5 Hz); ^{13}C NMR ($CDCl_3$, 125.7 MHz): δ (ppm) 164.82 (C=O), 131.66, 131.51 (C-11), 128.12, 126.76 (C-8), 127.91, 127.88 (C-10), 109.61, 109.6 (quaternary-C), 75.2, 75.2 (C-4), 72.4, 72.3 (C-3), 70.0, 69.7 (C-1), 70.0, 69.9 (C-2), 65.5, 65.4 (C-5), 33.9, 29.6 (C-7), 26.7, 26.7 (C-9), 24.6, 24.5 (C-9'), 17.6, 17.6 (C-6).

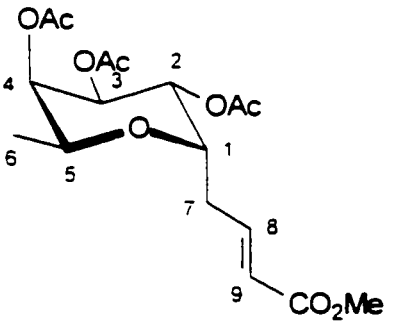

a

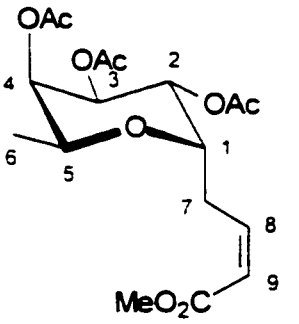

b

Compound 8a,b

Compound **I** (50.0 mg, 0.159 mmol) and methyl acrylate (30 μL, 0.318 mmol) were dissolved in dry dichloromethane (2 mL). Grubbs' catalyst **3** (6.7 mg, 5 mol%) was added and the solution refluxed at 45°C. TLC analysis (hexane/ethyl acetate 2/1) showed that the reaction was complete after 6 hours. The solution was concentrated under reduced pressure and the residue was purified by silica gel column chromatography starting with 10% ethyl acetate/hexanes and using 5% increasing gradients to 20% ethyl acetate/hexanes. The product obtained was a clear, colourless oil having an E/Z ratio of 9:1 (99% yield). The geometric isomers were separated by silica gel column chromatography. *Trans* compound **8a**: $[\alpha]_D^{23}$ = -79.3° (c = 0.55, $CHCl_3$); ^1H NMR ($CDCl_3$, 500 MHz): δ (ppm) 6.90 (m, 1H, H-8), 5.91 (dd, 1H, H-9, $J_{8,9}$ = 15.6 Hz, $^4J_{7,9}$ = 1.2 Hz), 5.30 (dd, 1H, H-2, $J_{1,2}$ = 5.6 Hz, $J_{2,3}$ = 9.9 Hz), 5.25 (m, 1H, H-4), 5.18 (dd, 1H, H-3, $J_{2,3}$ = 9.9 Hz, $J_{3,4}$ = 3.4 Hz), 4.32 (m, 1H, H-1), 3.93 (dq, 1H, H-5, $J_{4,5}$ = 2.7 Hz, $J_{5,6}$ = 6.4 Hz), 3.71 (s, 3H, CO_2Me), 2.63 (m, 1H, H-7), 2.43 (m, 1H, H-7'), 2.13, 2.03, 1.99 (3s, 9H, $COCH_3$), 1.13 (d, 3H, H-6, $J_{5,6}$ = 6.4 Hz); ^{13}C NMR ($CDCl_3$, 125.7 MHz): δ (ppm) 170.5, 170.1, 169.8 ($\underline{C}OCH_3$), 166.5 ($\underline{C}O_2Me$), 144.2 (C-8), 123.4 (C-9), 71.4 (C-1), 70.4 (C-4), 68.4 (C-3), 68.0 (C-2), 66.1 (C-5), 51.5 ($CO_2\underline{Me}$), 29.2 (C-7), 20.7, 20.7, 20.7 ($CO\underline{C}H_3$), 15.9 (C-6); *Cis* compound **8b**: $[\alpha]_D^{23}$ = -71.2° (c = 0.30, $CHCl_3$); ^1H NMR ($CDCl_3$, 500 MHz): δ (ppm) 6.23 (ddd, 1H, H-8, $J_{7,8}$ = 11.5 Hz, $J_{7,8}$ = 6.5 Hz, $J_{8,9}$ = 9.9 Hz), 5.89 (ddd, 1H, H-9, $J_{8,9}$ = 9.9 Hz, $^4J_{7,9}$ = 1.7 Hz, $^4J_{7,9}$ = 1.6 Hz), 5.32 (dd, 1H, H-2, $J_{1,2}$ = 5.9 Hz, $J_{2,3}$ = 10.2 Hz), 5.26 (dd, 1H, H-4, $J_{3,4}$ = 3.4 Hz, $J_{4,5}$ = 1.6 Hz), 5.22 (dd, 1H,

H-3, $J_{2,3}$ = 10.3 Hz, $J_{3,4}$ = 3.4 Hz), 4.33 (m, 1H, H-1, $J_{1,2}$ = 5.6 Hz), 4.01 (dq, 1H, H-5, $J_{4,5}$ = 1.4 Hz, $J_{5,6}$ = 6.4 Hz), 3.70 (s, 3H, CO_2Me), 3.32 (m, 1H, H-7), 2.76 (mx2, 1H, H-7', $^2J_{7,7'}$ = 16.2 Hz), 2.13, 2.05, 1.98 (s, 9H, $COCH_3$), 1.09 (d, 3H, H-6, $J_{5,6}$ = 6.4 Hz); ^{13}C NMR ($CDCl_3$, 125.7 MHz): δ (ppm) 170.6 ($\underline{C}OCH_3$), 170.0 ($\underline{C}OCH_3$x2), 166.6 ($\underline{C}O_2Me$), 145.4 (C-8), 121.4 (C-9), 72.6 (C-1), 70.8 (C-4), 68.5 (C-3), 69.1 (C-2), 65.8 (C-5), 51.2 ($CO_2\underline{Me}$), 25.5 (C-7), 20.8, 20.7, 20.7 ($CO\underline{C}H_3$), 16.1 (C-6); ESI-MS, m/z = 373.0 (8%), $[M+1]^+$ calcd for $C_{17}H_{25}O_9$.

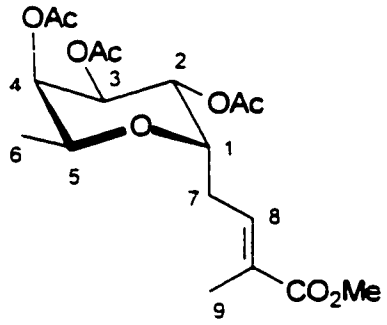

Compound 9

Compound **I** (50.0 mg, 0.159 mmol) and methyl methacrylate (34 μL, 0.318 mmol) were dissolved in dry dichloromethane (2 mL). Grubbs' catalyst **3** (6.7 mg, 5 mol%) was added and the solution refluxed at 45°C. After 18 hours the reaction was stopped as TLC analysis (hexane/ethyl acetate 2/1) showed that the reaction was no longer progressing. The solution was concentrated under reduced pressure and the residue was purified by silica gel column chromatography starting with 10% ethyl acetate/hexanes and using 5% increasing gradients to 20% ethyl acetate/hexanes. Only the *trans* product

formed under these conditions as a clear, colourless oil (86% yield); $[\alpha]_D^{23}$ = -90.3° (c = 2.66, $CHCl_3$); ^1H NMR ($CDCl_3$, 500 MHz): δ (ppm) 6.90 (m, 1H, H-8, $J_{8,9}$ = 1.4 Hz), 5.30 (dd, 1H, H-2, $J_{1,2}$ = 5.6 Hz, $J_{2,3}$ = 9.9 Hz), 5.24 (dd, 1H, H-4, $J_{3,4}$ = 3.4 Hz, $J_{4,5}$ = 2.0 Hz), 5.20 (dd, 1H, H-3, $J_{2,3}$ = 9.9 Hz, $J_{3,4}$ = 3.4 Hz), 4.29 (m, 1H, H-1, $J_{1,2}$ = 5.4 Hz), 3.92 (dq, 1H, H-5, $J_{4,5}$ = 1.9 Hz, $J_{5,6}$ = 6.4 Hz), 3.71 (s, 3H, CO_2Me), 2.56 (m, 1H, H-7), 2.41 (m, 1H, H-7'), 2.12, 2.02, 1.99 (3s, 9H, $COCH_3$), 1.83 (d, 3H, H-9, $J_{8,9}$ = 1.3 Hz), 1.12 (d, 3H, H-6, $J_{5,6}$ = 6.4 Hz); ^{13}C NMR ($CDCl_3$, 125.7 MHz): δ (ppm) 170.5, 170.1, 169.8, 166.5 (C=O), 137.1 (C-8), 129.6 (quaternary-C), 71.8 (C-1), 70.4 (C-4), 68.4 (C-3), 68.1 (C-2), 66.2 (C-5), 51.8 ($CO_2\underline{Me}$), 26.1 (C-7), 20.7 ($CO\underline{C}H_3$ x2), 20.7 ($CO\underline{C}H_3$), 15.9 (C-6), 12.7 (C-9); ESI-MS, m/z = 387.1 (37%), $[M+1]^+$ calcd for $C_{18}H_{27}O_9$.

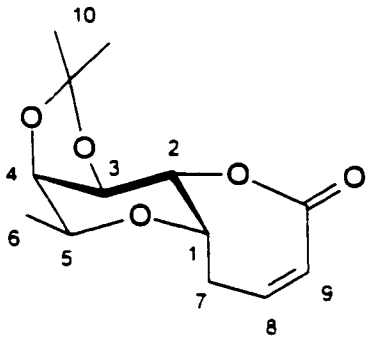

Compound 10

Grubbs' catalyst **3** (4.5 mg, 5 mol%) was added to a solution of **6** (30 mg, 0.106 mmol) dissolved in dry dichloromethane (30 mL). The purple reaction mixture refluxed at 45°C and after 4 hours was judged complete by TLC (hexane/ethyl acetate 2/1). The solvent was removed under vacuo and the

concentrate was purified by silica gel column chromatography using 10% ethyl acetate/hexane as eluent to give the white solid compound **10** (62% yield); ^{1}H NMR ($CDCl_3$, 500 MHz): δ (ppm) 6.52 (ddd, 1H, H-8, $J_{7,8}$ = 6.0 Hz, $J_{7,8}$ = 7.4, $J_{8,9}$ = 11.0 Hz), 5.98 (dd, 1H, H-9, $J_{8,9}$ = 11.1 Hz, $^{4}J_{7,9}$ = 1.5 Hz), 4.63 (dd, 1H, H-3, $J_{2,3}$ = 3.0 Hz, $J_{3,4}$ = 7.6 Hz), 4.57 (dd, 1H, H-2, $J_{1,2}$ = 4.4 Hz, $J_{2,3}$ = 3.0 Hz), 4.44 (ddd, 1H, H-1, $J_{1,2}$ = 4.5 Hz, $J_{1,7}$ = 8.0 Hz, $J_{1,7'}$ = 12.5 Hz), 4.14 (dd, 1H, H-4, $J_{3,4}$ = 7.6 Hz, $J_{4,5}$ = 1.6 Hz), 4.00 (dq, 1H, H-5, $J_{4,5}$ = 1.6 Hz, $J_{5,6}$ = 6.5 Hz), 2.60 (m, 2H, H-7, $J_{1,7}$ = 7.8 Hz, $J_{7,8}$ = 6.3 Hz, $^{2}J_{7,7'}$ = 16.0 Hz, $^{4}J_{7,9}$ = 1.5 Hz), 1.46 (s, 3H, H-10), 1.35 (s, 3H, H-10'), 1.20 (d, 3H, H-6, $J_{5,6}$=6.5 Hz); ^{13}C NMR ($CDCl_3$, 125.7 MHz): δ (ppm) 168.3 (C=O), 140.2 (C-8), 124.4 (C-9), 110.2 (quaternary-C), 74.2 (C-4), 73.3 (C-2), 72.6 (C-3), 71.5 (C-1), 66.4 (C-5), 31.9 (C-7), 26.2 (C-10), 24.8 (C-10'), 16.6 (C-6); ESI-MS, m/z = 255.0 (2%), $[M+1]^{+}$ calcd for $C_{13}H_{19}O_5$.

References

(1) Trnka, T. M.; Grubbs, R. H. *Acc. Chem. Res.* **2001**, 34, 18.

(2) Blechert, S. *Pure Appl. Chem.* **1999**, 71, 1393.

(3) Schrock, R. R.; Murdzek, J. S.; Bazan, G. C.; Robbins, J.; Dimare, M.; O'Regan, M. *J. Am. Chem. Soc.* **1990**, 112, 3875.

(4) Fürstner, A. *Angew. Chem. Int. Ed.* **2000**, 39, 3012.

(5) Lynn, D. M.; Mohr, B.; Grubbs, R. H. *J. Am. Chem. Soc.* **1998**, 120, 1627.

(6) Nguyen, S. T.; Grubbs, R. H.; Ziller, J. W.; *J. Am. Chem. Soc.* **1993**, 115, 9858.

(7) Scholl, M.; Ding, S.; Lee, C. W.; Grubbs, R. H. *Org. Lett.* **1999**, 1, 953.

(8) Bielawski, C. W.; Grubbs, R. H. *Angew. Chem. Int. Ed.* **2000**, 39, 2903.

(9) Kim, S. H.; Zuercher, W. J.; Bowden, N. B.; Grubbs, R. H. *J. Org. Chem.* **1996**, 61, 1073.

(10) Morehead, A.; Grubbs, R. H. *Chem. Commun.* **1998**, 275.

(11) Nicolaou, K. C.; He, Y.; Vourloumis, D.; Valberg, H.; Roschangar, F.; Sarabia, F.; Ninkovic, S.; Yang, Z.; Trujilo, J. I. *J. Am. Chem. Soc.* **1997**, 119, 7960.

(12) Jørgensen, M.; Hadwiger, P.; Madsen, R.; Stütz, A. E.; Wrodnigg, T. M. *Curr. Org. Chem.* **2000**, 4, 565.

(13) Ackerman, L.; El Tom, D.; Fürstner, A. *Tetrahedron* **2000**, 56, 2195.

(14) Scholl, M.; Ding, S.; Lee, C. W.; Grubbs, R. H. *Org. Lett.* **1999**, 1, 953.

(15) Fürstner, A.; Muller, T. *J. Org. Chem.* **1998**, 63, 424.

(16) Roy. R.; Das, S. K. *Chem. Commun.* **2000**, 519.

(17) Nomura, K.; Schrock, R. R. *Macromolecules* **1996**, 29, 540.

(18) Mortell, K. H.; Gingras, M.; Kiessling, L. L. *J. Am. Chem. Soc.* **1994**, 116, 12 053.

(19) Brummer, O.; Ruckert, A.; Blechert, S. *Chem. Eur. J.* **1997**, 3, 441.

(20) Blackwell, H. E.; O'Leary, D. J.; Chatterjee, A. K.; Washenfelder, R. A.; Bussmann, D. A.; Grubbs, R. H. *J. Am. Chem. Soc.* **2000**, 122, 58.

(21) Crowe, W. E.; Goldberg, D. R. *J. Am. Chem. Soc.* **1995**, 117, 5162.
(22) Chatterjee, A. K.; Grubbs, R. H. *Org. Lett.* **1999**, 1, 1751.

(23) Roy, R.; Dominque, R.; Das, S. K. *J. Org. Chem.* **1999**, 64, 5408.

(24) Das, S. K.; Dominque, R.; Smith, C.; Nahra, J.; Roy, R. *Carbohydr. Lett.* **1999**, 3, 361.

(25) Arjona, O.; Csaky, A. G.; Murcia, M. C.; Plumet, J. *Tetrahedron Lett.* **2000**, 41, 9777.

(26) Woltering, T. J.; Weiz-Schmidt, G.; Wong, C. H. *Tetrahedron Lett.* **1996**, 37, 9033.

(27) Huwe, C. M.; Woltering, T. J.; Jiricek, J.; Weiz-Schmidt, Wong, C. H. *Bioorg. Med. Chem.* **1999**, 7, 773.

(28) Heldin, C. H. *Cell* **1995**, 80, 213.

(29) Dominque, R.; Das, S. K.; Roy, R. *Chem. Comm.* **1998**, 2437

(30) Greene, T. W.; Wuts, P. M. In *Protective Groups in Organic Synthesis*, 3rd Ed; John Wiley & Sons, Inc.: Toronto, 1999, p. 207.

Claims to Original Research

(1) Novel convergent approaches towards the synthesis of C-linked sialyl Lewis^x glycomimetics.

(2) This is the first report of the syntheses of C-linked fucosyl peptoid sialyl Lewis^x mimetics

(3) Application of molecular modelling in the determination and design of novel glycomimetics

(4) Determination of Gibb's free energy for of *cis* and *trans* proline amide rotamers through variable temperature NMR analysis.

(5) Determination of energy of activation for the interconversion of rotamers in novel glycopeptoids

(6) First report of self-metathesis synthesis of a fucosyl homodimer using Grubbs' catalyst.

(7) Application of new generation Grubbs' catalyst in a highly stereoselective cross metathesis in the synthesis of glycomimetic precursors.

(8) First report of ring closing metathesis using the new generation Grubbs' catalyst on a carbohydrate substrate.

Publications and Conference Proceedings

S. Das, R. Dominque, C. Smith, J. Nahra and R. Roy. "Novel Carbohydrate Homodimers by Olefin Metathesis Reactions of Alkenyl Glycosides." *Carbohydr. Lett.*, **1999**, 3, 361.

C. Smith, G. Piizzi, B. Schmor and R. Roy. "Solution and Solid-Phase Synthesis of Glycopeptide and Glycopeptoid Mimetics of Sialyl-Lewis-X." *9th Quebec-Ontario Minisymposium of Bioorganic Chemistry*, St. Catherines, Ontario, Canada, October 31, **1998**.